

AD702691

The Effect of Microstructure on the Stress-Corrosion Susceptibility of an Al-Zn-Mg Alloy

by  
A. J. DeArdo, Jr. and R. D. Townsend\*

Metallurgy & Materials Science  
Carnegie-Mellon University  
Pittsburgh, Pennsylvania 15213

METALS RESEARCH LABORATORY  
CARNEGIE INSTITUTE OF TECHNOLOGY  
Carnegie Mellon University



PITTSBURGH, PENNSYLVANIA

Reproduced by the  
**CLEARINGHOUSE**  
for Federal Scientific & Technical  
Information Springfield Va 22151

D D C  
REPRODUCED  
MAR 31 1970  
RECEIVED

This document has been approved  
for public release and sale; its  
distribution is unlimited.

**BEST  
AVAILABLE COPY**

The Effect of Microstructure on the Stress-  
Corrosion Susceptibility of an Al-Zn-Mg  
Alloy

by

A. J. DeArdo, Jr. and R. D. Townsend\*

Metallurgy & Materials Science  
Carnegie-Mellon University  
Pittsburgh, Pennsylvania 15213

February 1970

(To be submitted in part for publication)

\* Presently at: Central Electric Generating Board Research Laboratories,  
Leatherhead, Surry, England

This research was supported by the Advanced Research Project Agency,  
Order #378, Department of Defense under Nonr-760(31).  
Distribution of this document is unlimited and reproduction in whole or  
in part is permitted for any purpose of the U. S. Government.

This document has been approved  
for public release and sale; its  
distribution is unlimited.

## TABLE OF CONTENTS

	<u>Page Number</u>
Acknowledgments .....	i
List of Tables .....	ii
List of Figures .....	iii
Abstract .....	v
INTRODUCTION .....	1
LITERATURE REVIEW .....	4
2.1 Physical Metallurgy of Al-Zn-Mg Alloys	4
.1 Precipitates	4
.2 Microstructures	6
2.2 Stress-Corrosion of Al-Zn-Mg Alloys	19
.1 Variables Affecting Stress-Corrosion Susceptibility	19
.2 Theories of Stress-Corrosion Cracking	21
EXPERIMENTAL PROCEDURE .....	30
3.1 Material	30
3.2 Heat Treatments	30
3.3 Obtaining the Microstructures Necessary for the Stress-Corrosion Investigation.	31
3.4 Equipment and Techniques Used in Experiments	34
.1 Transmission Electron Microscopy	34
.2 Tensile Testing	35
.3 Hardness Testing	35
.4 Scanning Electron Microscopy	36
.5 Optical Microscopy	36
3.5 Experiments Used in Investigation	36
.1 Determination of Stress-Corrosion Susceptibility	36
.2 Effect of Stress on the Corrosion Propensity of Grain Boundaries.	38
.3 Deformation Study	39
.4 Fractography	40
.5 Correlation of Rate of Work Hardening with Susceptibility to Stress-Corrosion.	40
RESULTS AND INTERPRETATIONS .....	41
4.1 The Microstructures Chosen for the Stress-Corrosion Investigation.	41
4.2 Stress-Corrosion Behavior	46
.1 Constant-Load Tests	46
.2 Constant-Deflection Tests	48
4.3 Effect of Stress on the Corrosion Propensity of Grain Boundaries.	49
4.4 Deformation Study	51

Table of Contents (Cont'd)

	<u>Page Number</u>
4.5 Fractography	54
4.6 Correlation of Rate of Work Hardening with Susceptibility.	57
DISCUSSION.....	59
5.1 P.F.Z. Hypothesis in the Stress-Corrosion Cracking of Al-Zn-Mg Alloys.	
5.2 Grain Boundary Precipitate Hypothesis in the Stress-Corrosion Cracking of Al-Zn-Mg Alloys.	62
5.3 Matrix Precipitate Hypothesis in the Stress-Corrosion Cracking of Al-Zn-Mg Alloys.	64
5.4 Effect of Matrix Precipitate on Deformation	65
5.5 Electrochemical Conditions at Grain Boundaries	75
5.6 Effect of Matrix Precipitate on the Stress-Corrosion Susceptibility of Al-Zn-Mg Alloys.	78
.1 Initiation of Stress-Corrosion Cracks	83
.2 Propagation of Stress-Corrosion Cracks	85
SUMMARY AND CONCLUSIONS.....	88
BIBLIOGRAPHY.....	90

---

### Acknowledgments

The author wishes to express his sincere appreciation to his thesis advisor, Professor R. D. Townsend, for his invaluable guidance and assistance given during the course of this investigation. Sincere thanks is also extended to Professors H. W. Paxton, H. R. Piehler, R. W. Dunlap, T. L. Davis, L. F. Vassamillet and J. R. Low and Drs. W. Leo, C. D. Statham, D. Moon and J. Defilippi for many enlightening discussions. Messrs. W. Poing T. Nuhfer, P. Bucci and T. Kinne provided laboratory assistance, Mr. G. Biddle and his co-workers provided all of the machine shop work used in the investigation, Mr. R. Miller made many drawings and Mr. Francis J. Samuels typed the draft and final manuscript. These people are all gratefully acknowledged by the author.

The author acknowledges with thanks the receipt of fellowship support from N.D.E.A. and the National Steel Company. This research was supported by the Advanced Research Projects Agency of the Department of Defense.

This thesis is dedicated to the author's wife, Margie, for her sacrifice, patience, encouragement and understanding during the course of this investigation.

List of Tables

<u>Table No.</u>	<u>Title</u>	<u>Page No.</u>
I	Characteristics of Microstructures Used in Stress-Corrosion Investigation.	45
II	Stress-Corrosion Behavior of Microstructures Tested Under Constant-Load Conditions.	47
III	Stress-Corrosion Behavior of Microstructures Tested Under Constant-Deflection Conditions.	50
IV	Correlation of Tangent Modulus (T) and Stress-Corrosion Susceptibility for Microstructures Investigated.	58

List of Figures

<u>Figure No.</u>	<u>Caption</u>	<u>Following Page No.</u>
1.	A comparison of the vacancy concentration profiles and associated P.F.Z. widths for various solution treatment, quenching and aging conditions.	16
2.	Effects of stress level and composition on stress-corrosion susceptibility.	21
3.	Effect of aging time on hardness, and on stress-corrosion life for a high-purity Al-5.5% Zn - 2.5% Mg alloy.	24
4.	Heat treatments used in investigation.	32
5.	Specimen configuration used in determining mechanical and stress-corrosion properties.	35
6.	Specimen mounted in copper cylinder for scanning electron fractographic investigation.	36
7.	Schematic representation of apparatus employed in constant-load stress-corrosion testing.	37
8.	Effect of aging at 180°C on the hardness measured at room temperature.	42
9.	Yield stress (0.2% offset) versus final aging time at 180°C. Microstructures chosen for stress-corrosion investigation are shown by arrows.	42
10.	Percent elongation to failure versus final aging time at 180°C.	42
11.	Transmission electron micrographs of microstructures used in stress-corrosion investigation.	43
12.	Optical micrographs showing corrosion occurring on electropolished surface of structure 2 - underaged after a 30 minute exposure.	51

List of Figures (Cont'd)

<u>Figure No.</u>	<u>Caption</u>	<u>Following Page No.</u>
13.	Transmission electron micrographs illustrating heterogeneous nature of dislocation distribution resulting from a 2% macroscopic strain.	51
14.	Transmission electron micrographs showing variations in dislocation-matrix precipitate interaction in microstructures used in stress-corrosion investigation.	51
15.	Optical micrograph illustrating the deformation accompanying a stress-corrosion crack in structure 2 - underaged.	54
16.	Optical micrograph illustrating the deformation accompanying a stress-corrosion crack in structure 2 - overaged.	54
17.	Schematic representation of fracture surface appearance.	55
18.	Scanning electron micrographs of stress-corrosion fracture surface of structure 2 - underaged.	55
19.	Stress concentrations at slip band-grain boundary intersections in MgO bicrystal.	79
20.	Broad slip band in NaCl deformed at room temperature.	79
21.	Microcracks at slip bands blocked by grain boundary in MgO bicrystal.	80
22.	Transmitted light micrograph illustrating initiation of cracks in polycrystalline silver chloride deformed in an aggressive environment.	81

CARNEGIE-MELLON UNIVERSITY

Effect of Microstructure on the Stress-Corrosion  
Susceptibility of an Al-Zn-Mg Alloy

Anthony J. DeArdo, Jr.

Abstract

The effect of microstructure on the susceptibility of a high purity Al-6.8% Zn - 2.3% Mg alloy to stress-corrosion cracking in an aqueous salt solution (3.5 wt % NaCl) has been studied. The results of testing a series of specimens having controlled microstructures and the same yield strength of 40,000 psi indicate that the susceptibility to stress-corrosion is controlled by the type, size and spacing of the matrix precipitate through the effect on these precipitates on the deformation process. Although the width of the precipitate free zone appears to have no effect on susceptibility, the grain boundary precipitate seems to influence susceptibility in certain cases. Supporting evidence for these observations has been obtained by light and electron microscopic examinations of deformed specimens and by fractographic studies. A model is proposed which explains many experimental observations.

## Introduction

Alloys of the Al-Zn-Mg type possess high yield and tensile strengths, however, the full strength potential of these alloys has not yet been realized because they suffer from a very high degree of stress-corrosion susceptibility. It is unfortunate, but true, that the maximum degree of susceptibility occurs in those microstructures which exhibit the highest yield strengths. With these facts in mind, it is understandable that the stress-corrosion problem has received much attention especially in the last few decades when technology has demanded materials with increasingly higher tensile properties.

Stress-corrosion in Al-Zn-Mg alloys is a rather peculiar phenomenon in that it is a cracking process which requires a susceptible alloy, a certain type of microstructure, a tensile stress and exposure to particular types of environment. Despite intensive research over the last few decades, the mechanism of stress-corrosion cracking in Al-Zn-Mg alloys remains obscure. In particular, the role of microstructure in controlling this phenomenon has been the subject of wide controversy. Because failure both in air and in aqueous environments generally proceeds along an intergranular path, many investigators have focussed their attention on the precipitate distribution in the region of the grain boundaries. This region displays three prominent features: (1) the equilibrium precipitates lying along the grain boundary, (2) a precipitate free zone (P.F.Z.) and (3) precipitates in the grain interior. All

three features can show considerable variations depending on the heat treatment to which the alloys subjected. By careful selection of the heat treatment, each of these features may be independently controlled to a greater or lesser extent. However, it is extremely difficult except under severely limited conditions to produce a given variation in one feature without a concomitant change in the other two. This fact has not always been realized and is in part responsible for the lack of agreement on the role of microstructure during stress-corrosion cracking.

Several authors<sup>(1-4)</sup> have postulated that the presence of P.F.Z.'s has a deleterious effect on the stress-corrosion resistance of these alloys. The main contention of these investigators is that the P.F.Z.'s act as mechanically weak paths through the material in which deformation processes such as slip are most likely to occur and that the preferential nature of this deformation ultimately leads to crack initiation. Thomas and Nutting<sup>(1)</sup> while subscribing to this general view have further suggested that maximum susceptibility will result when the equilibrium precipitates along the grain boundary are continuous thus preventing slip from one grain to another and concentrating the slip within the P.F.Z.

In contrast, other authors<sup>(5,6)</sup> consider that the presence of a P.F.Z. has no effect on the stress-corrosion resistance, but that, in fact, this phenomenon is controlled by deformation processes occurring within the grain interior which in turn is controlled by the type, size and distribution of precipitates within the matrix.

The purposes of the present investigation were to identify which of the microstructural features control susceptibility and to determine how this control was effected. To achieve these goals, a study was conducted to determine the stress-corrosion properties of an Al-Zn-Mg alloy in which both the P.F.Z. width and the matrix precipitate present in the microstructure were varied under controlled conditions.

## Literature Review

### 2.1 Physical Metallurgy of Al-Zn-Mg Alloys

#### 2.1.1 Precipitates

It has been well established that there can be two equilibrium precipitates in the Al-Zn-Mg system depending upon the composition of the solid solution and the temperature of decomposition<sup>(7)</sup>.

If the alloy is fairly concentrated and the temperature of decomposition is high (above 190°C) the T phase  $(\text{AlZn})_{49}\text{Mg}_{32}$  will be in equilibrium with the solid solution<sup>(7-9)</sup>. This phase has a cubic structure with  $a = 14.16$ <sup>(10,11)</sup> and an orientation relationship with the matrix of:

$$(100)_T \parallel (112)_{\text{Al}}, \quad (001)_T \parallel (1\bar{1}0)_{\text{Al}} \quad (8,12).$$

The more commonly observed equilibrium precipitate observed in this system is  $\text{MgZn}_2$  which is referred to as  $\eta$ . This phase is in equilibrium with the solid solution in dilute alloys when the aging temperature is relatively low. The  $\eta$  phase is believed to be hexagonal in structure. There is some slight disagreement regarding the lattice parameters of  $\eta$ . The following parameters have been previously reported:  $a = 5.15\text{\AA}$ ,  $c = 8.48\text{\AA}$ <sup>(13)</sup>;  $a = 5.21\text{\AA}$ ,  $c = 8.60\text{\AA}$ <sup>(14)</sup>;  $a = 5.23\text{\AA}$ ,  $c = 8.57\text{\AA}$ <sup>(15)</sup> and  $a = 5.17\text{\AA}$ ,  $c = 8.50\text{\AA}$ <sup>(16)</sup>. Reported orientation relationships of the  $\eta$  phase with the matrix are:

Orientation A	$(10.0)_\eta \parallel (100)_{\text{Al}},$	$(00.1)_\eta \parallel (011)_{\text{Al}} \quad (12)$
Orientation B	$(10.0)_\eta \parallel (110)_{\text{Al}},$	$(00.1)_\eta \parallel (1\bar{1}1)_{\text{Al}} \quad (12)$
Orientation C	$(10.0)_\eta \parallel (121)_{\text{Al}},$	$(00.1)_\eta \parallel (111)_{\text{Al}} \quad (12)$
Orientation D	$(10.0)_\eta \parallel (1\bar{1}0)_{\text{Al}},$	$(00.1)_\eta \parallel (110)_{\text{Al}} \quad (8)$

Thackery<sup>(17)</sup> has recently found other orientation relationships between  $\eta$  and the matrix. They are listed below:

Orientation 1	$(1\bar{2}.0)_\eta$	$\parallel$	$(1\bar{1}.1)_{Al}$	,	$(00.1)_\eta$	$\parallel$	$(110)_{Al}$
Orientation 2	$(1\bar{2}.0)_\eta$	$\parallel$	$(1\bar{1}1)_{Al}$	,	$(30.2)_\eta$	$\parallel$	$(110)_{Al}$
Orientation 3	$(1\bar{2}.0)_\eta$	$\parallel$	$(1\bar{1}1)_{Al}$	,	$(20.1)_\eta$	$\parallel$	$(121)_{Al}$
Orientation 4	$(1\bar{2}.0)_\eta$	$\parallel$	$(1\bar{1}1)_{Al}$	,	$(10.4)_\eta$	$\parallel$	$(110)_{Al}$
Orientation 5	$(00.1)_\eta$	$\parallel$	$(1\bar{1}1)_{Al}$	,	$(10.0)_\eta$	$\parallel$	$(110)_{Al}$
Orientation 6	$(10.0)_\eta$	$\parallel$	$(100)_{Al}$	,	$(00.1)_\eta$	$\parallel$	$(011)_{Al}$

Precipitates of the first four orientations were reportedly lath shaped lying on the  $\{111\}_{Al}$  with their longitudinal axes lying within  $25^\circ$  of  $\langle 110 \rangle_{Al}$ . Precipitates of orientation 5 were either hexagonal or rounded platelets, lying on  $\{111\}_{Al}$  with the basal plane of the  $\eta$  parallel to  $\{111\}_{Al}$ . Precipitates of orientation 6 formed as elongated eight-sided platelets on  $\{100\}_{Al}$ . No evidence of the previously reported orientations C and D was found.

Another result of Thackery's work was the confirmation of the existence of a recently reported phase<sup>(18)</sup> which has been labeled X phase. This phase appeared to have a hexagonal structure with  $a = 2.67\text{\AA}$  and  $c = 4.90\text{\AA}$ . Cornish and Day<sup>(19)</sup> have also recently reported finding X phase.

There are two metastable phases in this system. The first,  $\eta'$ , forms during aging at intermediate and low temperatures. This phase is also hexagonal with lattice parameters  $a = 4.96\text{\AA}$  and  $c = 8.68\text{\AA}$ <sup>(13,20)</sup>. Thomas and Nutting<sup>(1)</sup> have shown that this phase nucleates on  $\{111\}_{Al}$  and this result is in accord with previous X-ray results of other workers<sup>(12,13,21)</sup>. There is

evidence that thin plates of  $\eta'$  are coherent with the matrix<sup>(1,8,22)</sup> in the  $\{111\}_{Al}$ . Thackery could not confirm the existence of  $\eta'$  from the results of his work. Guinier-Preston (G.P.) zones represent the other transition phase in this system. Transmission microscopy and X-ray studies have shown that the G.P. zones are spherical, ordered and coherent with the matrix<sup>(1,12,23-25)</sup>. There is some controversy over the habit plane of the G.P. zones. Graf<sup>(21)</sup> and others<sup>(12)</sup> show that the  $\{100\}_{Al}$  seems to be the habit plane while Mondolfo et al.<sup>(13)</sup> present evidence that it might be the  $\{111\}_{Al}$ . Graf<sup>(24)</sup> has noted that the size of the zones appeared to depend on the Mg content of the alloy.

#### 2.1.2 Microstructures

The Al-Zn-Mg system can exhibit many different microstructures depending on the alloy composition and the heat treatment employed. This review will pertain to ternary compositions in the range of 4 to 8 w/o Zn and less than 4 w/o Mg.

It has become evident recently<sup>(26)</sup> from a study of directly quenched specimens that there is a change in the mechanism of precipitate nucleation below a certain temperature. This has been labeled the G.P. zone solvus temperature,  $T_{G.P.}$ , and denotes the upper temperature limit of this metastable phase. Specimens quenched and aged above  $T_{G.P.}$  showed microstructures typical of heterogeneous nucleation while specimens quenched to and aged below  $T_{G.P.}$  showed microstructures typical of homogeneous nucleation. Lorimer and Nicholson<sup>(26)</sup> have noted that there was a refinement of the precipitate

distribution of the order of  $10^3$  when lowering the quenching and aging temperature  $10^\circ\text{C}$ . (This temperature decrement traversed  $T_{\text{G.P.}}$ )

It is possible to characterize, in principle, the microstructures observed in Al-Zn-Mg on the basis of the type of heat treatment employed:

Type I: Microstructures generated by quenching to a temperature above  $T_{\text{G.P.}}$  and aging at that temperature.

Type II: Microstructures generated by quenching to a temperature below  $T_{\text{G.P.}}$  and aging at that temperature.

Type III: Microstructures generated by quenching to a temperature below but aging above  $T_{\text{G.P.}}$ .

#### Type I Microstructure

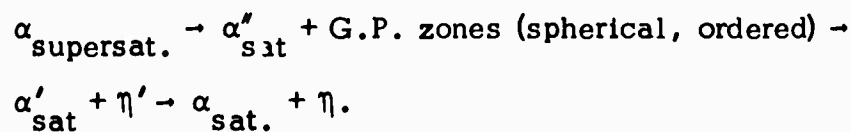
The first type of microstructure (Type I) has not been extensively studied since it is not of practical value. It is clear that the nucleation of precipitates in this type of microstructure is heterogeneous in nature. At very high aging temperatures,  $T$  or  $\eta$ , depending on the composition, are precipitated at grain boundaries and dislocations<sup>(26)</sup>. At lower temperatures, ( $T_\eta > T > T_{\text{G.P.}}$ , where  $T_\eta$  is the  $\eta$  solvus temperature) lath type precipitates typical of  $\eta$  or  $\eta'$  are found<sup>(26)</sup>. It is not clear whether these precipitates are  $\eta'$  or  $\eta$  (possibly forming from  $\eta'$ ).

There is evidence supporting a sequence of precipitates ( $\alpha_{\text{supersat.}} \rightarrow \alpha'_{\text{sat}} + T' \rightarrow \alpha_{\text{sat}} + T$ ) during high temperature aging<sup>(9,21)</sup> but these observations were made on microstructures of type III and so the question of whether a sequence of precipitates would obtain in the absence of G.P. zones remains unanswered.

Type I microstructures can be summarized as containing few large, incoherent and widely spaced precipitates which have been nucleated in a heterogeneous manner.

### Type II Microstructure

The second type of microstructure has received much attention because it is this microstructure which achieves the high strength characteristic of Al-Zn-Mg alloys. As the time of aging below  $T_{G.P.}$  increases, a series of precipitates appears:



The formation of G.P. zones has been studied extensively in Al alloys. This research has been stimulated by both academic and practical (viz. mechanical property) considerations.

In contrast to the large amount of work done on the formation of G.P. zones in binary Al alloys, viz. Al-Zn, Al-Ag and Al-Cu, relatively little work has been done in Al-Zn-Mg. This is probably due to the problems involved in analyzing the diffusion in the ternary alloy. Panseri and Federighi have investigated the kinetics of G.P. zone formation in Al-10% Zn<sup>(27)</sup> and Al-10% Zn - 0.1% Mg<sup>(28)</sup> alloys. Since the two alloys exhibited qualitatively similar kinetic behavior, much of the fundamental work done on the binary alloys would appear to apply to Al-Zn-Mg. Previous work performed on the binary alloys Al-Zn<sup>(27)</sup>, Al-Ag<sup>(29,30)</sup> and Al-Cu<sup>(31,32)</sup> has shown that in each case the low temperature,

isothermal decomposition of the solid solution is accompanied by the formation of clusters. These clusters or G.P. zones are very small and are the cause of the unexpected increase in resistivity which has been noted during the initial stages of aging<sup>(33)</sup>. The G.P. zones initially form and grow at very high rates and the shape of the transformation curves indicates that there is no activation barrier to the formation of these zones<sup>(33)</sup>.

There is much experimental evidence indicating the very important effect of vacancy concentration on the kinetics of clustering. De Sorbo et al.<sup>(31)</sup> have shown that specimens of Al-Cu which had been quenched directly to and aged at 0°C had a much higher rate of cluster formation than did specimens which had the quench interrupted at 200°C. Cold work introduced prior to aging at 0°C was shown to increase the clustering rate of specimens having had an interrupted quench but did not affect the clustering rate of directly quenched specimens. These observations were explained on the basis of the vacancy concentrations present in the specimens<sup>(31)</sup>. In directly quenched specimens, most of the vacancies in equilibrium at the solution temperature are retained during the quench and hence a large excess of vacancies is available to assist the diffusional clustering process. When the quench is interrupted at 200°C, however, vacancies are annihilated at grain boundaries and dislocations, fewer vacancies are retained and the rate of clustering is consequently reduced. The cold work introduced prior to aging in specimens having had an interrupted quench supposedly increased the vacancy concentration (point defect generation by dislocations) and this allowed the clustering rate to increase. Cold work was not expected to aid the kinetics of clustering in directly quenched specimens since these

specimens were already supersaturated with vacancies.

The kinetics of clustering in Al-Cu have been shown to be extremely rapid necessitating a diffusion coefficient approximately  $10^7$  greater than the coefficient obtained by the extrapolation of high temperature data<sup>(32)</sup>. This inconsistency led to the excess vacancy theory originally proposed by Zener<sup>(34)</sup> and has subsequently been developed by Federighi<sup>(35)</sup> and DeSorbo<sup>(31)</sup> et al. to explain most of the experimental facts concerning the kinetics of clustering.

The excess vacancy theory uses

$$D_{\text{Cu}} = A \exp\left(-\frac{E_m}{kT_A}\right) \exp\left(-\frac{E_F}{kT_S}\right)$$

to explain the high clustering rate instead of the usual

$$D_{\text{Cu}} = A \exp\left(-\frac{E_m + E_F}{kT_A}\right)$$

where

$D_{\text{Cu}}$  = diffusion coefficient of Cu in Al

A = a constant

$E_m$  = activation energy for vacancy migration

$E_F$  = activation energy for vacancy formation

$T_A$  = aging temperature

$T_S$  = solution temperature.

The addition of small amounts of Mg to an Al-10% Zn alloy has been shown by Panseri and Federighi<sup>(28)</sup> to have perceptible effects on the kinetics of clustering. Their results show that Mg not only lowers but also seems to

stabilize the kinetics of clustering, viz. reduces the effects of varying the solution and aging temperature.

Panseri and Federighi<sup>(28)</sup> conclude that there is a strong binding energy between Mg and vacancies ( $\sim 0.5$  eV) so that practically all vacancies are coupled to Mg atoms. They also note that the Mg - vacancy couples are quite mobile at room temperature.

Polmear<sup>(36)</sup> has investigated the low temperature aging behavior of Al-Zn-Mg alloys. His results show that hardness was strongly dependent upon the Mg content of his material. He found, for example, that after identical aging treatments an Al-Zn alloy showed an increase of 19 V.P.N. over the quenched value while the same alloy containing 0.08% Mg showed an increase of 55 V.P.N. over the quenched value. Polmear has determined the C-curve behavior of his ternary alloys and indicates that the intersections of his C-curves are related to metastable equilibrium lines. This implies that each phase initially precipitated during a sequence of isochronal aging treatments should have its own C-curve. Polmear showed that there can be one of two phases initially present depending on the aging temperature. G.P. zones represent the low temperature phase while the phase initially present at higher temperatures is probably  $\eta'$ . He also determined the compositional dependence of  $T_{G.P.}$  which increased linearly with Zn content at constant Mg content. At very low Mg contents (0.08% Mg), only G.P. zones were present and this is understandable since the  $\alpha'$  (fcc) phase in Al-Zn only appears at temperatures ( $\sim 275^\circ\text{C}$ <sup>(33)</sup>) higher than the highest temperature used by Polmear. The results of Polmear<sup>(36)</sup> and Panseri

and Federighi<sup>(28)</sup> are compatible since the latter authors showed that Mg retarded the kinetics of clustering in Al-Zn and Polmear showed that the incubation time for Al-8% Zn was much shorter than that for the ternary.

Townsend and Osiecki<sup>(37)</sup> have investigated the kinetics of G.P. zone formation in an Al-7% Zn-1% Mg alloy using a technique similar to that of Polmear<sup>(36)</sup>. Their experiments consisted of determining C-curves for the decomposition of the solid solution for both direct quenching and interrupted quenching conditions. Their results strongly indicate that below the nose of the C-curve the initial vacancy concentration has no effect on initial zone formation. Above the nose of the curve, however, the initial formation of G.P. zones was strongly dependent on initial vacancy concentration. These results indicate that perhaps the dependency of the initial clustering rate on the vacancy concentration in Al-Cu suggests that the aging temperatures used in the Al-Cu investigation were above the nose of the Al-Cu C-curve.

One final comment is deemed necessary concerning the technique used to determine C-curves. This technique first used by Hardy<sup>(38)</sup> is based on measuring the incubation time of aging using hardness determinations. Although the results of this technique are undoubtedly valuable, one must keep in mind that the incubation time is a function of the sensitivity of the hardness test. Stated another way, G.P. zones grow from the time of decomposition of the solid

solution but the hardness is affected only when the zones reach some critical size. This incubation period is therefore not the start of clustering but the time to reach a certain, detectable size of clusters.

Lorimer and Nicholson<sup>(39)</sup> have shown that, in principle, G.P. zones can sometime act as nuclei for  $\eta'$  during isothermal aging. They show that at any aging temperature  $T_a$ , the G.P. zones of size greater than the critical nucleus size of  $\eta'$  at  $T_a$  ( $d_c^{T_a}$ ) can act as nuclei for  $\eta'$ . There is little doubt that this concept closely approximates the truth although there are no direct experimental observations supporting it in type II microstructures. As will be shown later, however, this concept of G.P. zones acting as  $\eta'$  nuclei has been indirectly confirmed in the type III and should therefore also apply in the case of type II microstructures. There has been little if any work done in varying the type II microstructures although, in principle, some work in the area of increasing the maximum strength at a given aging temperature could be accomplished.

The  $\eta' \rightarrow \eta$  transition takes place at very long aging times and is characterized by the loss of coherency of the semicoherent  $\eta'$  as well as a change in lattice parameter<sup>(13)</sup>. Little additional information is available since this transformation has not been extensively studied. It would appear likely that the  $\eta$  would nucleate from the  $\eta'$  or perhaps  $\eta'$  is simply an underdeveloped form of  $\eta$ .

The region of the microstructure near the grain boundary is interesting since there is a zone free of precipitate adjacent to the grain boundary. There

are two explanations of the existence of the precipitate free zone (P.F.Z.) depending on the details of the heat treatment. The P.F.Z. occurring in type II microstructures has been shown to result principally from solute denudation<sup>(19, 26)</sup> while the P.F.Z. in type III microstructures is mainly due to vacancy depletion<sup>(8, 19, 26)</sup>. The P.F.Z. in type II microstructures is due to the competitive growth of grain boundary precipitates and G.P. zones. These P.F.Z. are on the order of  $200\text{\AA}$  and this figure is probably determined by the vacancy concentration gradient (and its effect on diffusion of solute to the grain boundary) in the region of the grain boundary.

### Type III Microstructure

The third type of microstructure (where  $T_{\text{quench}} < T_{\text{G.P.}} < T_{\text{age}}$ ) has received the most study in recent years. Hirano and Takagi<sup>(9)</sup> have studied the precipitation in an 8 w/o Zn - 4 w/o Mg alloy over a range of aging temperatures and have found that above  $230^{\circ}\text{C}$  only the T phase (as well as  $\alpha$ ) exists. In the range of  $200^{\circ}\text{C}$  to  $230^{\circ}\text{C}$ , they found the sequence



This confirms the results of earlier X-ray experiments of Graf<sup>(21)</sup>. Below  $200^{\circ}\text{C}$  they found the sequence



The only direct observation of this T phase was made by Embury and Nicholson<sup>(8)</sup> who have shown that the T phase nucleates heterogeneously at grain boundaries and dislocations. Graf<sup>(24)</sup> reports that below  $300^{\circ}\text{C}$  the T phase is not precipitated directly but is preceded by  $\eta$ .

The current state of knowledge concerning the formation of precipitates in type III microstructures is mainly due to Nicholson and his colleagues Embury<sup>(8, 40)</sup> and Lorimer<sup>(26, 39)</sup>. Their work was initiated by the fact that the dispersion of matrix precipitate could be neither adequately predicted nor explained by the application of classical metallurgy principles. It was noted that solute supersaturation arguments previously considered to be the controlling factor in precipitate distribution<sup>(41, 42)</sup> could not explain many experimental observations. In particular, they mentioned that supersaturation arguments can not explain: (1) the presence of P.F.Z.s which occur adjacent to grain boundaries; (2) microstructures having different degrees of precipitate dispersion although decomposing under similar solute supersaturations and (3) quenching rates, time spent at room temperature before aging, the rate of heating to the aging temperature and the presence of trace elements all affecting the precipitate dispersion although none of these appreciably affect the solute supersaturation.

Lorimer and Nicholson<sup>(39)</sup> have proposed a model that does explain this anomalous behavior. In effect, they say that not only is there a sequence of precipitates but also that  $\eta'$  can nucleate on certain G.P. zones which exceed a minimum size. Their model postulates that upon quenching to a temperature  $T_b$  below the  $T_{G.P.}$ , G.P. zones form from the solid solution, the size distribution of which depends upon  $T_b$  and the time at  $T_b$ . Upon upquenching above  $T_{G.P.}$  to  $T_a$ , those G.P. zones having reached a size greater than  $d_c^a$ , related to the critical nucleus size of  $\eta'$  at  $T_a$ , will act as nuclei for  $\eta'$ . It may be concluded from this investigation that the larger the G.P. zones before upquenching,

the finer the distribution of  $\eta'$  (more G.P. zones exceed  $d_c^{T_a}$  therefore more nuclei). It should be clear that any factor which varies the G.P. zone size distribution would also necessarily vary the  $\eta'$  distribution. The quenching rate affects the G.P. zone distribution by its effect on the vacancy concentration while variations in the heating rate would allow the sizes of zones to vary. Trace elements can affect the precipitation process by either stabilizing the solute atom/vacancy clusters<sup>(8)</sup> thereby preventing a loss of vacancies to grain boundaries or by changing  $T_{G.P.}$ <sup>(26)</sup>.

One of the most important results of the work of Lorimer and Nicholson<sup>(26, 39)</sup> was that they showed that the dispersion of matrix precipitate can be controlled by controlling the size distribution of G.P. zones. In general, the larger the G. P. zones grown below  $T_{G.P.}$  the finer the distribution of  $\eta'$  upon upquenching to  $T_a (> T_{G.P.})$ .

Embury and Nicholson<sup>(8)</sup> as well as Taylor<sup>(43)</sup> have shown that the formation of a P.F.Z. in a type III microstructure is caused by a vacancy rather than a solute depletion at the grain boundaries as previously postulated<sup>(44)</sup>. Embury and Nicholson<sup>(8)</sup> say that the high supersaturation of vacancies of solution treated and quenched material would be first reduced at the strongest vacancy sinks viz. grain boundaries and dislocations. The vacancy concentration in the bulk of the grains would retain a supersaturation of vacancies anchored by the Mg atoms. Figure 1 schematically illustrates their postulated vacancy profiles under different solution treating and quenching conditions. They

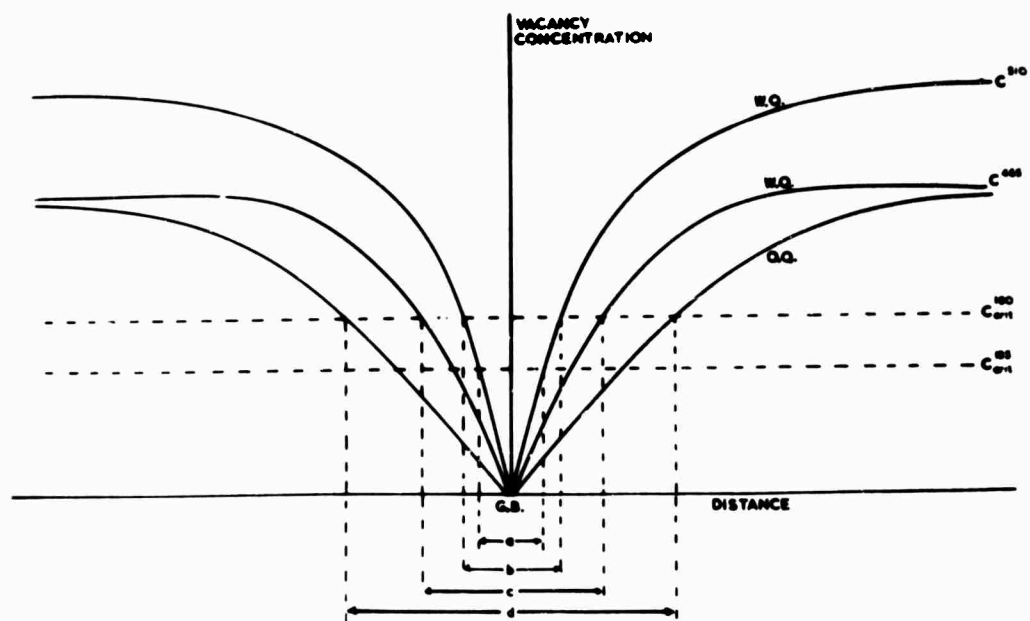


Figure 1. A comparison of the vacancy concentration profiles for various solution treatment, quenching and aging conditions. The P.F.Z. widths depicted are (a) solution at 510°C, water quench, age at 135°C, (b) solution at 510°C, water quench, age at 180°C, (c) solution at 465°C, water quench, age at 180°C and (d) solution at 465°C, oil quench, age at 180°C. (8)

suggest that specimens given a low quench rate would have more vacancies diffusing to the grain boundaries causing lower vacancy concentrations in the immediate vicinity of the boundaries than specimens given faster quenches. Upon aging at some elevated temperature, Embury and Nicholson assume that a critical vacancy concentration (permitting the formation of G.P. zones of the critical size) is necessary for the nucleation of the matrix precipitate and the combination of this critical vacancy concentration and the above mentioned vacancy concentration gradient leads to the formation of the P.F.Z. as indicated in Figure 1. There is some experimental evidence indicating that the P.F.Z. can be attributed to vacancy concentrations. Both the P.F.Z. and the size and distribution of matrix precipitate are strongly dependent upon quenching rate<sup>(8)</sup>. Slower quenches result in both wider P.F.Z.s and larger, more widely spaced precipitates than faster quenches. These observations might be explained by considering the expected differences in vacancy concentrations.

The addition of certain trace elements such as Ag to Al-Zn-Mg alloys has created a finer distribution of matrix precipitate and nearly eliminated the P.F.Z.<sup>(45,46)</sup>. Nicholson<sup>(47)</sup> has suggested that this could be caused by the Ag acting to stabilize the vacancy profile and preventing a large vacancy flow to the grain boundaries. Embury and Nicholson<sup>(8)</sup> present other experimental observations that strongly support the hypothesis that the P.F.Z. is caused by vacancy rather than solute depletion. For example, a microstructure containing a P.F.Z. formed by aging at 180°C was reaged at 135°C. They<sup>(8)</sup> found that the

second age had caused precipitation within the original P.F.Z. and this new P.F.Z. was identical to that formed in material aged only at 135°C. The width of the P.F.Z. was shown to be independent of aging time although the grain boundary precipitate had coarsened with aging time. The P.F.Z. width was also shown to be dependent on the solution treating temperature (initial vacancy concentration).

Several other workers have found results similar to those of Embury and Nicholson regarding the effects of solution temperature<sup>(43,48)</sup> and quenching rate<sup>(19,49)</sup> on both the P.F.Z. width and the dispersion of matrix precipitate.

Cornish and Day<sup>(19)</sup> have recently studied the precipitation occurring in the vicinity of grain boundaries in an Al-Zn-Mg alloy and their results substantiated the claims of Nicholson et al. It seems well established that P.F.Z.s in type II microstructures are due to both a solute and vacancy depletion while in type III they are due to a vacancy depletion in the grain boundary region. There is evidence that grain boundaries can act as vacancy sinks. Previous work with pure aluminum that has been solution treated, quenched and aged has shown that voids<sup>(50)</sup> and dislocation loops of both the faulted<sup>(51)</sup> (Frank) and prismatic types<sup>(51,52)</sup> can form as a result of a supersaturation of vacancies. The type of defect that forms appeared to depend on the solution treating temperature, quenching rate and aging temperature. One result of this work<sup>(50-52)</sup> that is pertinent to this present discussion is the fact that there were regions free of these defects, viz. voids and loops, in the vicinity of both grain

boundaries and dislocations. These observations have been explained on the basis that since grain boundaries and dislocations are potent vacancy sinks, the vacancy supersaturation in regions adjacent to grain boundaries and dislocations would be reduced and these regions would not be expected to contain voids and dislocation loops.

## 2.2 Stress-Corrosion of Al-Zn-Mg Alloys

### 2.2.1 Variables Affecting Susceptibility

The Al-Zn-Mg system has been a source of much frustration to metallurgists for nearly 50 years. This frustration exists because the same microstructures that have exhibited high yield and tensile strengths have also been extremely susceptible to stress-corrosion cracking.

This disturbing situation was first documented by Rosenhain et al.<sup>(53)</sup> in 1921 when they showed that certain Al-Zn-Mg alloys possessed both high strength and high susceptibility to stress-corrosion. Sanders and Mussner<sup>(54)</sup> later showed that corrosion was a significant factor in the cracking of Al-Zn-Mg alloys under an enduring load.

In the nearly 50 years since this initial work was reported, there has been an intensive effort made on the part of many workers to understand and thereby possibly eliminate the problem of stress-corrosion in Al-Zn-Mg alloys.

Most of the historical research was concerned with determining what factors influenced stress-corrosion and in order to gain insight into the phenomenon, variables such as composition, phases present, trace elements, stress

level, grain size and testing temperature were examined. One of the few non-controversial conclusions that has been reached as a result of this work was a workable definition of stress-corrosion of aluminum alloys, viz. that stress-corrosion is a cracking process requiring a susceptible alloy, specific microstructures, a sustained tensile stress and exposure to a particular environment<sup>(55)</sup>.

In the first attempts to understand the phenomenon, investigators tried to establish a correlation between susceptibility and alloy composition. Hansen et al.<sup>(56,57)</sup> found that dilute alloys with less than 6% (Zn + Mg) were resistant to stress-corrosion after a wide variety of heat treatments. They also found that higher alloying (including Mn) resulted in extreme susceptibility unless aging was performed either at room temperature or above 100°C. The tendency for increased susceptibility with increased alloying was substantiated by Siebel and Vosskühler<sup>(58,59)</sup> who again noted that aging above 125°C resulted in low susceptibility. These authors also showed that Cu, Mn and Cr in small amounts led to a decrease in susceptibility. Chadwick et al.<sup>(60)</sup> have studied the stress-corrosion behavior of a series of ternary compositions and found no correlation between susceptibility and the equilibrium phase field in which the composition existed although they did find the general trend that susceptibility increased with alloy content. Later work in stress-corrosion has dealt with the effect of trace elements on the susceptibility of Al-Zn-Mg alloys of compositions based on commercial alloys. The element receiving the most

attention is Ag. Polmear<sup>(45,61)</sup> and later Elkington and Turner<sup>(62)</sup> have shown that small amounts of Ag (~ 0.3%) not only increased the mechanical properties of Al-Zn-Mg alloys but also slightly decreased the susceptibility to stress-corrosion. Chadwick et al.<sup>(60)</sup> have also shown that while individual additions of Cu, Mn and Cr in small amounts did not appear to increase stress-corrosion resistance, Cu when added with Cr or with Cr and Mn did appear to reduce susceptibility. The results of Chadwick et al.<sup>(60)</sup> were compatible with those due to earlier work of Dix<sup>(63)</sup>.

The effect of stress level on susceptibility has been investigated by Chadwick et al.<sup>(60)</sup>. A portion of their results is shown in Figure 2 which reveals the effect of composition as well as stress level on susceptibility. These authors have also shown that when a commercially pure base rather than pure base material is used, a grain refinement is achieved. This fine grain material was less susceptible to stress-corrosion than was coarse grained.

The temperature of stress-corrosion testing has been shown to be a very important variable. Wasserman<sup>(64)</sup> observed that for each 10° increase in temperature in the range 10°-70°C, the time to failure is shortened by more than a factor of 10. Gruhl<sup>(65)</sup> later confirmed this observation by reporting that in the same temperature range a 1° increase in temperature reduced the life of specimens by about 5%.

### 2.2.2 Theories of Stress-Corrosion Cracking in Al-Zn-Mg Alloys

Several theories have been proposed concerning the stress-corrosion of

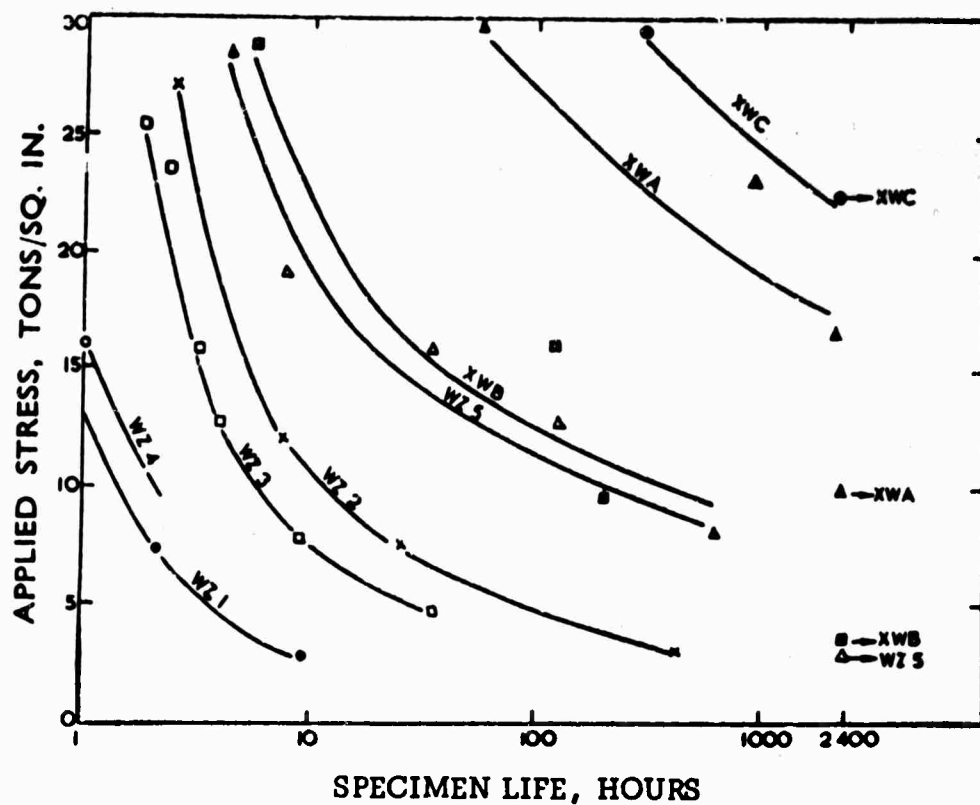


Figure 2. Effects of stress level and composition on stress-corrosion susceptibility<sup>(60)</sup>.

Compositions (w/o)

<u>Alloy</u>	<u>Zn</u>	<u>Mg</u>	<u>Cu</u>	<u>Mn</u>	<u>Cr</u>	<u>Fe</u>	<u>Si</u>
WZ1	7.34	2.23	-	-	-	0.01	.01
WZ2	7.31	2.38	0.29	-	-	0.01	.015
WZ3	7.41	2.23	0.13	-	-	-	-
WZ4	7.13	2.17	-	0.28	-	0.015	.02
WZ5	7.15	2.06	-	-	0.23	0.02	.05
XWA	7.27	2.37	1.38	-	-	0.005	.03
XWB	7.04	2.33	1.32	0.27	-	-	-
XWC	7.05	2.30	1.40	0.28	-	0.02	.04

Heat Treatment: 460°C, 30 min., WQ to RT, aged 18 hrs. at 125°C.  
 Stress-Corrosion Test: Specimens sprayed three times daily with 3% NaCl solution.

Al-Zn-Mg alloys. The first was a general theory presented by Mears et al.<sup>(66)</sup>. Their theory, basically electrochemical in nature, states that corrosion occurs along localized paths (grain boundaries) producing fissures. A stress concentration is created at the root of these fissures which magnifies the component of stress normal to the path. This stress concentration increases as the fissure grows or if the radius of the fissure tip decreases. When this stress concentration reaches a sufficient level, the fissures open further exposing unfiled metal to the environment and an accelerated rate of attack would then be expected until protective films are reformed. The fissure continues to grow under the action of corrosion. An increased rate of penetration occurs because of the mutually accelerating effects of stress and corrosion. Dix<sup>(63)</sup> later applied this general theory to the stress-corrosion of Al-Zn-Mg alloys. He noted that the precipitates in this system were anodic to the surrounding material and that the zones adjacent to grain boundaries would be expected to be cathodes since they were denuded of solute<sup>(67)</sup>. The anodic path was therefore depicted as being the grain boundaries containing small precipitates adjacent to a large cathode (Dix's depleted zone). The mechanism of crack growth was presented as the sequential process of mechanical tearing of the denuded zone followed by dissolution of other grain boundary precipitates. Dix<sup>(63)</sup> suggested that susceptibility would decrease if precipitation along crystallographic surfaces could be prevented.

Another predominately electrochemical theory has been proposed by

McEvily et al. <sup>(3,68)</sup>. These authors state that stress-corrosion will occur in materials when the combination of stress and environment produce a situation where a film forms which protects against general corrosion but which is not mechanically strong enough to prevent localized rupture under the influence of stress. This model uses the P.F.Z. as the active path for stress-corrosion. These authors, as well as Thomas <sup>(69)</sup>, note that cold work prior to aging reduces susceptibility by jogging the grain boundary (partial recrystallization) and eliminating the P.F.Z. <sup>(3,68)</sup>. McEvily et al. <sup>(68)</sup> have shown that in the absence of stress, the grain boundaries are cathodic to the grain interiors (specimen at  $-0.84V \cdot S.C.E.$ ) while in the presence of stress the boundaries are anodic. They also note that the environment (halide ions) can aid stress-corrosion by being incorporated into the oxide thereby weakening it and also by interfering in the repair process of ruptured oxide. The crack growth mechanism is a two stage process: (a) the formation followed by the rupturing of oxide film at the crack tip and (b) the plastic deformation of the ductile substrate and the arrest of the crack by plastic blunting. Once the crack has stopped, the film reforms and then is fractured due to creep in the P.F.Z. These authors think that most of the crack advance would occur during the blunting process. McEvily et al. <sup>(3,68)</sup> present fractographs showing striations on the fracture surface. These authors claim that this is direct evidence of a two-stage cracking process where the striations are the locations of the arrest of the advancing crack.

Although the electrochemical theory of Dix et al. <sup>(63,66)</sup> and the film

rupture theory of McEvily et al.<sup>(3,68)</sup> are important contributions in the study of the stress-corrosion of Al-Zn-Mg alloys, they do not begin to explain all of the observations in this area. Probably the most important failure of these theories is that they can not adequately explain the well documented effect of microstructure in stress-corrosion. For example, Mickle<sup>(70)</sup> and Pugh<sup>(71)</sup> have shown that any one alloy can exhibit a wide variety of stress-corrosion behavior depending on what particular microstructure is being tested. This relationship between susceptibility and microstructure is shown in Figure 3.

Most current theories of stress-corrosion deal with the role of microstructure in the stress-corrosion of Al-Zn-Mg alloys. It is interesting to note that the quest for the understanding of the role of microstructure in stress-corrosion began simultaneously with the acceptance of modern transmission electron microscopy as a tool of metallurgical research. Since stress-corrosion cracks advance along intergranular paths<sup>(63,72)</sup> in Al-Zn-Mg alloys, most investigators have focussed their attention in the regions near the grain boundaries. These regions have been shown<sup>(1,8,19)</sup> to exhibit three distinct features: (1) the grain boundary and grain boundary precipitates, (2) the P.F.Z. adjacent to the boundary and (3) the precipitate in the matrix.

At the present time each of these microstructural features is held responsible for stress-corrosion by different groups of investigators. The first group, the advocates of the P.F.Z., imply that susceptibility is due to the presence per se. of the P.F.Z.<sup>(1,2,4)</sup>. Other investigators<sup>(3,68)</sup> have implied that the

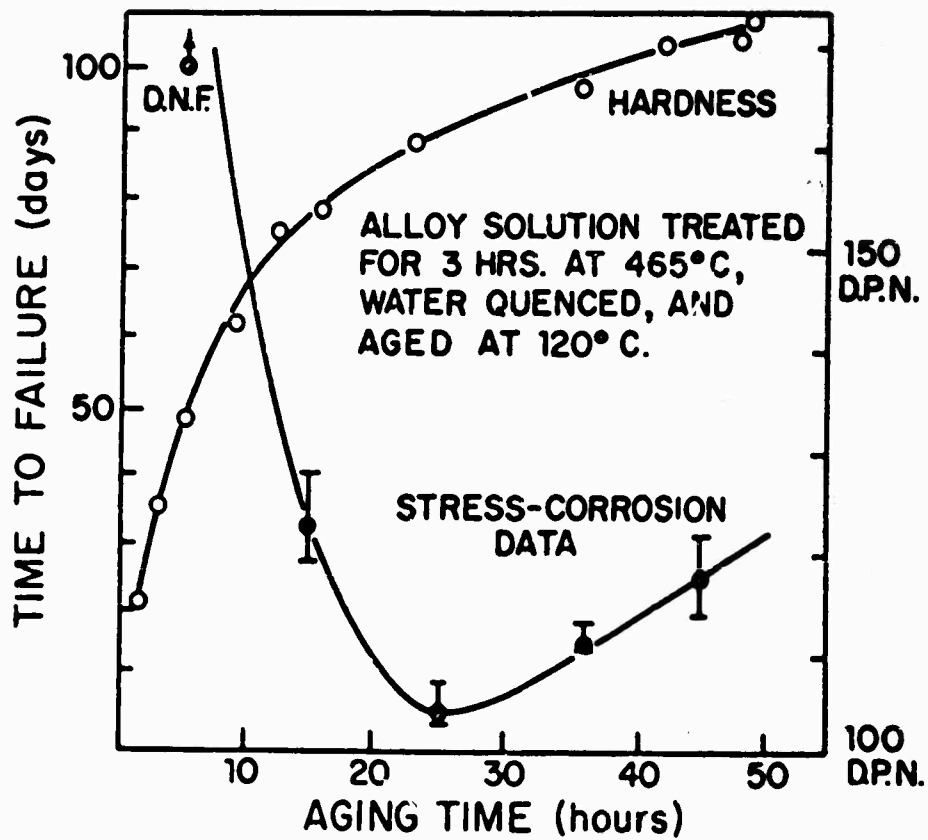


Figure 3. Effect of aging time on hardness, and on stress-corrosion life for a high-purity Al-5.5% Zn - 2.5% Mg alloy. (71)

P.F.Z. would affect cracking rates but would not in itself cause susceptibility. The advocates of the P.F.Z. base their theory on two main assumptions: (1) that there is preferential plastic flow in the P.F.Z. and (2) that deformed material is anodic to undeformed material. Although the first assumption is questionable, there is some evidence that the second might be true<sup>(73,74)</sup>. Thomas and Nutting<sup>(1)</sup> and later Pugh and Jones<sup>(2)</sup> proposed similar models relating the P.F.Z. to susceptibility. These models suggest that due to the difference in strength between the P.F.Z. and the matrix, preferential plastic flow would be expected in the P.F.Z. Since this deformed P.F.Z. is anodic to the matrix, dissolution of the P.F.Z. would occur producing stress concentration effects which would cause further plastic flow and the process would continue. It was assumed<sup>(2)</sup> that the electrochemical stage was most important because the mechanical stage (which depends on the difference in strength between the P.F.Z. and the matrix) could not explain the observations presented in Figure 3. The results of recent work have been considered by Sedricks et al.<sup>(4)</sup> to show that a reduction in the P.F.Z. width results in an increase in susceptibility. They note that these results indicate that a dissolution model is likely since a decrease in what they consider to be the anodic area has led to an increase in susceptibility. Sedricks et al.<sup>(4)</sup> suggest that the role of stress is to make the P.F.Z. anodic to the grain interior.

Another group of investigators, viz. Jacobs<sup>(75)</sup> and Kent<sup>(76)</sup>, suggest that the grain boundary precipitates are responsible for stress-corrosion susceptibility. Actually, the model proposed by Thomas and Nutting<sup>(1)</sup> might also be

classified with this group since they<sup>(1)</sup> suggest that at maximum hardness (and according to them simultaneous maximum susceptibility) the grain boundaries are covered with a film-like precipitate which inhibits slip transfer across the boundaries. Although Kent<sup>(76)</sup> does not propose a model, he did note that an increase in the size and spacing of grain boundary precipitate correlated with a decrease in susceptibility. The model due to Jacobs<sup>(75)</sup> was propounded to explain the difference in susceptibility of a commercial 7075 alloy in the T6 (maximum hardness and very susceptible) and the T73 (overaged and not susceptible) conditions. Jacobs<sup>(75)</sup> noted that the T6 treatment retained dislocations from the quench while the T73 treatment did not. In previous work, Jacobs<sup>(77)</sup> found that in the absence of stress, the corrosion behavior of the two treatments was identical. In both cases (T6 and T73), the process consisted of the dissolution of grain boundary precipitates. In Jacobs' model<sup>(75)</sup> the initiation stage is identical for each microstructure, viz. the dissolution of grain boundary precipitate at a free surface. This pit would cause a stress concentration which in the case of T6, with the dislocations present, would be sufficient to fracture the grain boundary precipitate-matrix interface but in T73 would only cause plastic flow. The propagation of the crack in T73 postulated by Jacobs is similar to that proposed by Pugh and Jones<sup>(2)</sup>, viz. the cycle of deformation accelerated corrosion, causing a stress concentration, causing deformation accelerated corrosion. Jacobs<sup>(75)</sup> notes that T73, having a higher dislocation mobility, would be more efficient at blunting a propagating crack. He also

notes that since the T6 structure had a lower dislocation mobility, it would be less efficient (than T73) in blunting a crack and the crack formed at the precipitate would then be able to run along the boundary until it impinged on the next precipitate. This process would then repeat until final fracture occurred.

Jacobs assumes that the propagation of the crack between the precipitates is deformation assisted corrosion and therefore would be the slow step in the cycle.

It seems that the cracking rate in model would depend on the size and spacing of the grain boundary precipitates and that the findings of Kent<sup>(76)</sup> are therefore compatible with this model.

The third group of investigators disregard the effects of the P.F.Z. as well as the grain boundary precipitate noting that there is a strong correlation between susceptibility and deformation substructure. This group feels that the size, type and distribution of matrix precipitate actually controls susceptibility through its effect on deformation processes. Gruhl et al.<sup>(78,79)</sup> have reported that the highest susceptibility occurs when an Al-Zn-Mg alloy is hardened by G.P. zones. Speidel<sup>(6)</sup> and Holl<sup>(5)</sup> have shown a strong correlation between susceptibility and deformation substructure. In general, their results indicate that microstructures exhibiting localized slip after deformation are susceptible to stress corrosion while unsusceptible microstructure show a more homogeneous type substructure. They have also shown by direct observation that there is no preferential slip in the P.F.Z.. This fact appears to invalidate the P.F.Z. theory since preferential slip in the P.F.Z. is a basic tenet of that theory.

Speidel<sup>(6,80)</sup> has proposed a model to explain how the susceptibility of an alloy depends upon the microstructure (Figure 3). This model assumes that the effective stress which pushes dislocations against the grain boundary is

$$\tau_e = \tau_a - \tau_o$$

where  $\tau_a$  is the applied shear stress and  $\tau_o$  is the friction stress.  $\tau_o$  is considered to consist of four terms

$$\tau_e = \tau_a - (\tau_G + \tau_S + \tau_{SS} + \tau_p)$$

where

$\tau_G$  = stress due to elastic interactions with other dislocations

$\tau_S$  = stress due to intersection of dislocations

$\tau_{SS}$  = stress due to solid solution hardening

$\tau_p$  = stress due to precipitation hardening.

Speidel<sup>(6,80)</sup> notes that dislocations can shear G.P. zones thereby lowering  $\tau_p$  and raising  $\tau_e$ . He states that  $\tau_p$  will increase in the underaged condition as the aging time increases to maximum hardness. The stress concentration  $n\tau_e$  ( $n$  is the number of dislocations in the pile up) at the head of the pile-up would therefore be expected to increase as the time of aging increases up to maximum hardness. Speidel explains the decrease in susceptibility with larger aging times by suggesting that at these times there is an increasing volume fraction of particles that cannot be sheared and this would lead to lower stress at the grain boundaries. Speidel notes that the role of microstructure in stress-corrosion is to vary the stress concentration at the intersections of slip bands

and grain boundaries by varying  $\tau_p$ .

In summary, the literature has revealed many important results concerning the relationship between microstructure and susceptibility of Al-Zn-Mg alloys to stress-corrosion cracking. It is clear that a controversy exists as to the exact role of microstructure in stress-corrosion. While it appears disturbing that there is such little agreement among the various authors, the controversy is easily understood. The lack of agreement arises mainly because of the relationship among the metallurgical features of the microstructures that have recently been investigated. Most of this recent work has dealt with the effect of changes in one of the microstructural features (viz. P.F.Z., grain boundary and matrix precipitates) on susceptibility while neither controlling nor accounting for the concomitant changes in the other features. Although the situation appears hopeless, superficially at least, the work done by Nicholson et al. (8,26,39,40) has provided insight into the relationship between the P.F.Z. and the matrix precipitate. Using this relationship and simultaneously accounting for variations in grain boundary precipitates, it seemed as if a series of microstructures could be generated that might, after stress-corrosion testing, resolve the controversy in the literature.

## Experimental Procedure

### 3.1 Material

The composition of the alloy used in this investigation was Al-6.8 wt % Zn-2.3 wt % Mg with less than 0.01 wt % Si, Fe, Cu, Mn, Cr, Ni and Ti. This material was purchased from the Aluminum Company of America in the form of 0.040 inch thick sheet. A portion of this sheet was subsequently further reduced to 0.010 inch thick sheet.

### 3.2 Heat Treatments

All high temperature heat treatments (viz. pre-solution and solution treatments) were performed in air using a resistance wound, vertical furnace. The temperature in this furnace was controlled to within  $\pm 5^{\circ}\text{C}$  and the constant-temperature zone was long enough to completely enclose the specimens.

There has been little work done in determining the various important temperatures in this system. Nevertheless, it was possible to estimate the critical temperatures of this alloy from the literature. The solidus temperature for this composition is approximately  $370^{\circ}\text{C}$ <sup>(9,81)</sup> while the  $\eta$  solvus is approximately  $250^{\circ}\text{C}$ <sup>(9)</sup> and the G.P. zone solvus is approximately  $170^{\circ}\text{C}$ <sup>(9,26,36)</sup>.

All specimens were given a pre-solution treatment consisting of 30 minutes at  $430^{\circ}\text{C}$ , followed by 1 hour at  $530^{\circ}\text{C}$ , followed by air cooling to room temperature. This treatment was deemed necessary to ensure a uniform grain size, some degree of homogenization and complete recrystallization in the material. This last aspect was considered important since Holl<sup>(82)</sup> has demonstrated that

large variations in precipitate distribution can be obtained in specimens having different degrees of recrystallization prior to aging.

The solution treatment given all specimens consisted of holding the specimens for one hour at 465°C, followed by an oil quench to room temperature.

Temperature controlled silicone oil baths were used for all aging treatments except those at 100°C when boiling water was used.

The temperature of the oil baths was maintained to within  $\pm 1^\circ\text{C}$  of the desired aging temperature.

The heat treatments employed in this investigation resulted in a mean grain diameter of approximately 0.5mm.

### 3.3 Obtaining the Microstructures Necessary for the Stress-Corrosion Investigation

It was apparent from the literature that a wide variety of microstructures (type III) could be obtained through heat treating. It also seemed possible to generate an ideal series of microstructures which, after being tested for stress-corrosion susceptibility, would establish which microstructural feature (viz. P.F.Z., grain boundary or matrix precipitate) controls the phenomenon. These results might also be expected to resolve the controversy in the literature. This ideal series of microstructures would have to have the following qualifications:

(A) Two microstructures with the same P.F.Z. width and grain boundary precipitate but having different matrix precipitate.

(B) Two microstructures with the same grain boundary and matrix precipitate but having different P.F.Z. widths.

(C) Two microstructures with the same P.F.Z. width and matrix precipitate but having different grain boundary precipitate.

Unfortunately, it does not seem possible to satisfy all three conditions with one alloy. While conditions (A) and (B) perhaps could be satisfied with one alloy, it would not seem possible to fulfill condition (C) with one composition since the solute necessary to effect a change in the grain boundary precipitate would necessarily come from the matrix and thereby violate the constraints of condition (C). However, all three conditions might be satisfied by more than one alloy.

It was decided that heat treatments should be developed to approximate conditions (A) and (B) and although the grain boundary precipitates would be allowed to vary, they could be observed and taken into account in the analysis.

The heat treatments designed to vary the width of the P.F.Z.s and the matrix precipitates are shown in Figure 4. These treatments were based on the work of Nicholson and his colleagues Embury<sup>(8,40)</sup> and Lorimer<sup>(26,39)</sup>.

In all three heat treatments, specimens were oil quenched to room temperature and this fairly slow quench was used to establish a large vacancy depleted region adjacent to the grain boundaries. Heat treatment 1 was designed to give a wide P.F.Z. and a relatively coarse distribution (relatively large particles and large interparticle spacings) of matrix precipitates. Specimens were therefore upquenched to  $T_a = 180^\circ\text{C}$  after only 30 seconds at room temperature.

In heat treatment 2, the 1 hour age at  $T_B = 100^\circ\text{C}$  was given to allow time

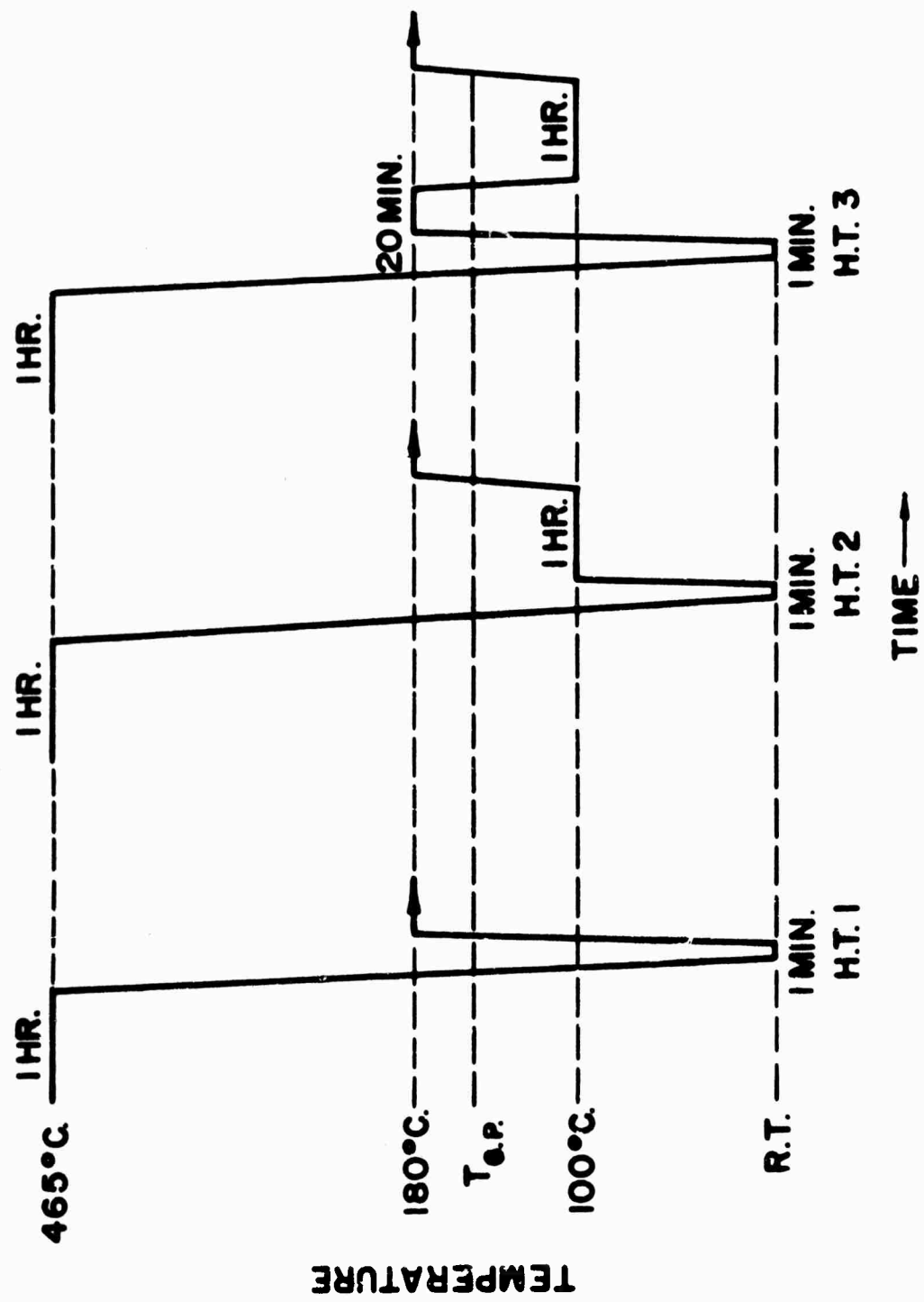


Figure 4. Heat treatments used in investigation.

for the growth of G.P. zones within the vacancy depleted region and also to cause a large number of G.P. zones within the grain interior to achieve a size greater than  $d_c^{180^\circ\text{C}}$ . Consequently, the structure expected on aging at  $180^\circ\text{C}$  would have a narrow P.F.Z. and a fine distribution (relatively small particles and small interparticle spacings) of matrix precipitates.

Heat treatment 3 was an attempt to obtain a narrow P.F.Z. and a distribution of precipitates within the matrix closely resembling that of heat treatment 1. The 30 seconds at room temperature followed by 20 minutes at  $180^\circ\text{C}$  was given to establish a P.F.Z. and a distribution of matrix precipitates characteristic of heat treatment 1. This was followed by a 1 hour age at  $100^\circ\text{C}$  to allow the growth of G.P. zones within the original P.F.Z. so that on upquenching to  $180^\circ\text{C}$ , the P.F.Z. width would be reduced. Additional nucleation of  $\eta'$  within the grain interior was considered unlikely as the  $\eta'$  particles formed during the first 20 minutes at  $180^\circ\text{C}$  would have considerably reduced the solute supersaturation in this region.

The progress of aging at  $180^\circ\text{C}$  of the three heat treatments was followed by means of room temperature hardness and tensile measurements. The microstructures to be used in the stress-corrosion investigation would then be chosen from these aging curves.

### 3.4 Equipment and Techniques Used in Experiments

#### 3.4.1 Transmission Electron Microscopy

Thin foils for transmission electron microscopy were prepared by employing either a "window" technique<sup>(83)</sup> or a jet-polishing technique<sup>(84)</sup>. These electropolishing techniques have been widely used in the last few years and since they are adequately described in the literature, only a brief summary of each will be presented. Both techniques employed an electrolyte of 67% methanol and 33% nitric acid cooled to  $-20^{\circ}\text{C}$ . In both cases a cell potential of 10 volts and a stainless steel cathode were used. The resulting current density was approximately  $7.2 \text{ ma/mm}^2$ . The starting material for the "window" technique was one inch square and 0.01 inches thick. The center area of the square was lightly abraded on both sides and the edges of the specimen were insulated with Microstop. Electropolishing was then initiated and continued until the first hole(s) appeared. The specimen was removed from the electrolyte, washed in methanol, dried and then insulated around the periphery of the hole(s) with Microstop. After repeating this sequence a few times, an area thin enough for transmission of 100 kV electrons would be obtained. This area would then be cut from the specimen, washed in methanol, dried and inserted into the microscope for observation.

Discs of 3.2mm diameter were punched from material to be thinned by jet-polishing. The disc was inserted into a commercial P.V.C. holder and positioned between two jets such that the flow of the electrolyte would impinge on

the area of the specimen not insulated by the holder. The specimen was observed during electropolishing by using a telescope and a high intensity lamp. When a hole formed, electropolishing was discontinued, the specimen holder (and specimen) removed from the cell and the specimen removed from the holder. The specimen was then washed in methanol, dried and ready for observation in the microscope.

The transmission electron microscopy was performed on a Philips E.M. 200 operated at 100 kV. There were two goals to the electron microscopy: (1) the characterization of specimens given specific heat treatments with regard to grain boundary precipitates, the P.F.Z. width and the matrix precipitates and (2) a study of the deformation occurring in specific microstructures, viz. those chosen for stress-corrosion experiments, which had been plastically deformed.

#### 3.4.2 Tensile Testing

The room temperature tensile properties of the various microstructures generated were determined by using an Instron testing machine operated at a cross head speed of 0.02 inches per minute. The specimen configuration used to measure tensile properties is shown in Figure 5.

#### 3.4.3 Hardness Testing

The room temperature hardness of the microstructures investigated was obtained by using a Rockwell 15-T hardness test. The specimens used for hardness determination were one half inch square and 0.040 inches thick.

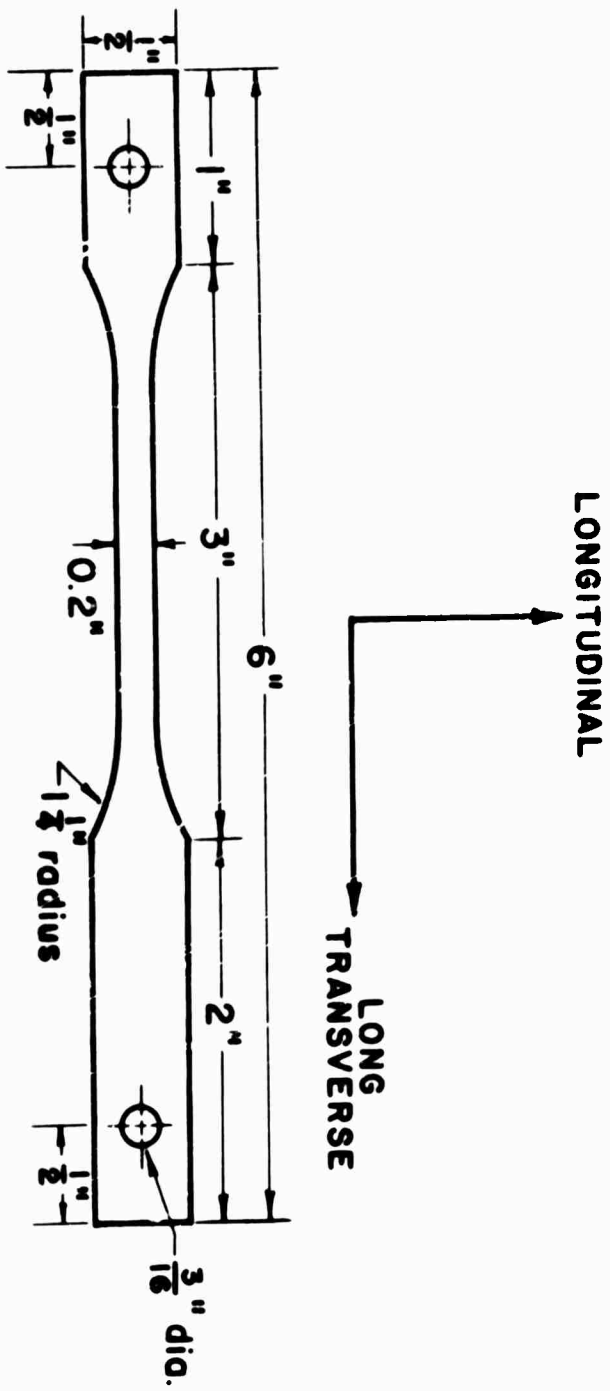


Figure 5. Specimen configuration used in determining mechanical and stress-corrosion properties.

#### 3.4.4 Scanning Electron Microscopy

A JSM-2 scanning electron microscope was used to observe the stress-corrosion fracture surfaces. Specimens whose fracture surfaces were to be observed were sheared 1/4 inch from the surface and mounted in copper cylinders as shown in Figure 6. The specimens were placed under the electron beam at an angle of 45° to the beam. The microscope was operated at 25 kV for this work.

#### 3.4.5 Optical Microscopy

The optical microscopy used in the investigation was performed on either a Zeiss or a Untron metallograph. When high magnification was desired and the specimens were relatively flat (corrosion in absence of stress experiments), the Zeiss metallograph was used. However, when low magnification was needed or when the specimens were not flat (side surface deformation and fractography), the Untron metallograph was employed. Slip step heights were measured using a Normarski interferometer attached to a Reichert metallograph. These step heights (S.S.H.) were calculated using the equation

$$S.S.H. = \frac{\lambda}{2} \cdot \frac{1}{n}$$

where  $\lambda = 0.6\mu$ , the wavelength of yellow light and  $n$  is the ratio of the fringe displacement to the fringe spacing.

### 3.5 Experiments Used in Investigation

#### 3.5.1 Determination of Stress-Corrosion Susceptibility

A 3.5 wt % NaCl solution (pH = 6.5) was the corrosive environment used

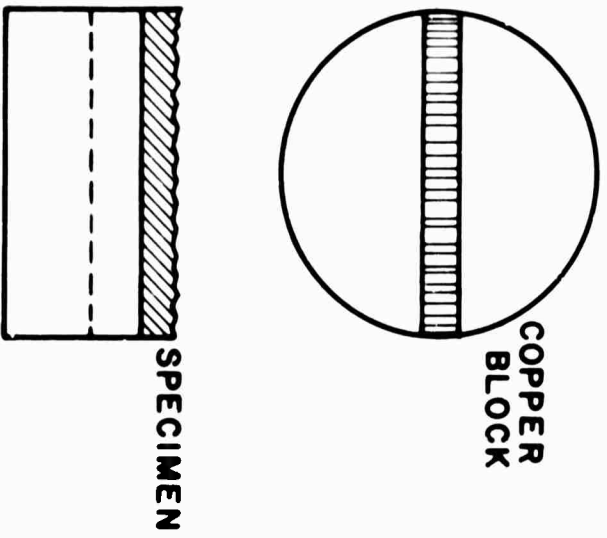


Figure 6. Specimen mounted in copper cylinder for scanning electron fractographic investigation.

in all of the stress-corrosion tests. This solution was maintained at 30°C and flowed past the specimen at approximately 20 cm/min. The specimen configuration used in these tests is shown in Figure 5. The standard specimen preparation procedure included degreasing the heat treated specimens with kerosene followed by a rinse of toluene. The gage lengths of the specimens were then lightly abraded with a paste of Linde "A" (0.3 $\mu$ ) and cotton. Finally, the specimens were insulated with Microstop except for one inch of the gage length. The specimens were then ready for stress-corrosion testing. The stress-corrosion tests were of the continuous immersion type.

There were two methods used to determine the susceptibility of a microstructure to stress-corrosion, viz. the constant-load and constant-deflection (fixed grip) tests. The procedure used in conducting the tests was similar in both cases. A prepared specimen would be inserted into the glass corrosion cell, properly aligned and gripped. A load of 5 pounds was then applied to the specimen and the bottom opening of the cell was sealed with Silastic (Dow Corning Silastic - 892 RTV adhesive/sealant). A small amount of the solution was placed in the cell and when the seal was completed, the circulation of the solution was started. Figure 7 shows, schematically the details of the apparatus employed. When the test was of the constant-load type, the full load would be gently placed on the loading pan, the timer started and the test would proceed until the specimen fractured. See Figure 7 for details. At the moment of fracture, the timer would be stopped by a microswitch in the timer circuit and

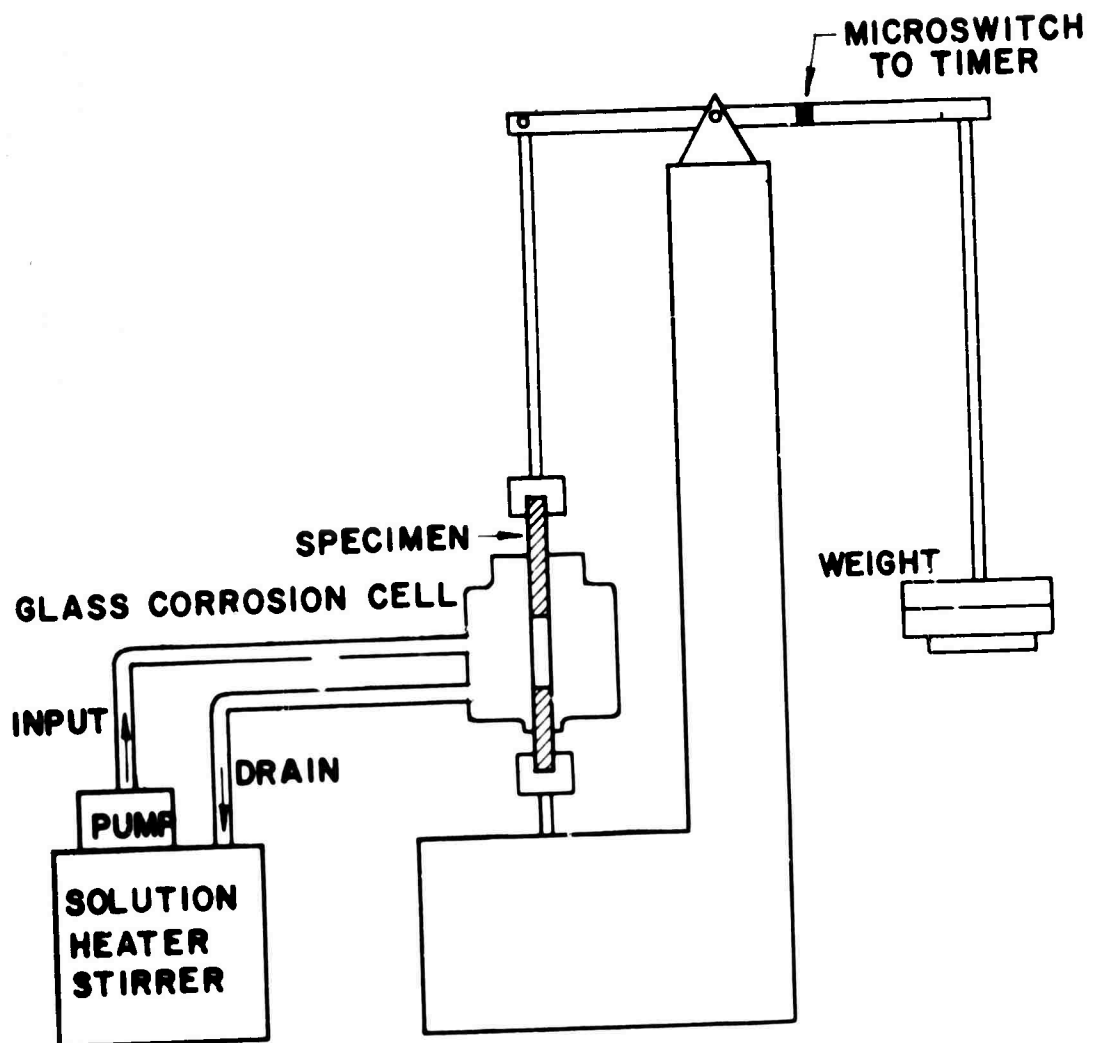


Figure 7. Schematic representation of apparatus employed in constant-load stress-corrosion testing.

the time to failure recorded. The life time of a specimen was considered a measure of the resistance to stress-corrosion.

The constant-deflection experiments were performed on an Instron testing machine. In this test the full load was applied by moving the cross-head down until the proper load was applied. Once this was achieved, the crosshead was stopped and load relaxation on the specimen traced as a function of test time on the Instron recorder. In both types of tests, the full load represented 70% of the 0.2% offset yield stress ( $Y.S. = 40 \text{ ksi.}$ ). It was possible to determine both the time for the initiation of a stress-corrosion crack ( $t_i$ ) as well as the time for the propagation of a sub-critical crack ( $t_p$ ) from the Instron record.

### 3.5.2 Effect of Stress on the Corrosion Propensity of Grain Boundaries

An investigation was performed to assess:

(1) whether or not corrosion in the absence of stress would cause a degradation of tensile properties. This objective was achieved by heat treating specimens to obtain microstructures identical to those tested for stress-corrosion susceptibility, preparing the surfaces and exposing the specimens to the corrosive environment in the absence of stress for times equal to the life of similar specimens as determined in the stress-corrosion study. After a suitable exposure, the specimens (two per microstructure) were removed from the solution, cleaned and tested on the Instron machine.

(2) the effect of stress on the corrosion propensity of grain boundaries. In order to evaluate this situation, specimens were heat treated to

obtain microstructures identical to those used in the stress-corrosion study. These specimens were then electropolished and separated into two groups. One group was placed in the NaCl solution, in the absence of stress, and exposed for times up to ~ 60% of the stress-corrosion life of each particular microstructure. The specimens from the second group were also exposed for the same time periods except under a load representing 70% of the yield stress. After suitable exposures, the specimens were removed from the solution, rinsed with distilled water, dried and examined with an optical microscope.

### 3.5.3 Deformation Study

A deformation study was conducted on microstructures identical to those tested under stress-corrosion conditions. The specimens used in this study were plastically strained on the Instron either 2% or to failure. Blanks (3.2mm diameter) for thin foil preparation were taken from regions either in the center of the gage length or adjacent to the fracture. The thin foils were prepared from these blanks using the jet-polishing technique described earlier. The diffraction conditions necessary for dislocation observation were obtained by employing both the standard Philips single-tilt specimen stage and a double-tilt specimen stage<sup>(85)</sup>.

The deformation accompanying a propagating stress-corrosion crack was also investigated. Specimens, heat treated to the appropriate microstructures, were electropolished and tested in a manner identical to that used for the constant-deflection stress-corrosion test. The test was stopped during the crack

propagation stage and the specimens were removed from the Instron machine, washed with distilled water, dried and observed with an optical microscope. Slip step heights were determined from these specimens.

#### 3.5.4 Fractography

An investigation of the fracture surfaces of specimens that failed by stress-corrosion cracking was performed. Fracture surfaces of specimens heat treated to the various microstructures were examined using both the scanning electron and the optical microscope.

#### 3.5.5 Correlation of Rate of Work Hardening with Susceptibility to Stress-Corrosion

If the matrix precipitate were the most important microstructural feature controlling stress-corrosion, it seemed likely that a correlation should exist between susceptibility and the rate of work hardening. To evaluate this possibility, the tangent modulus<sup>(86)</sup> (T) was extracted from stress-strain curves of microstructures identical to those tested for stress-corrosion susceptibility.

This parameter T was calculated using the following formula:

$$T = \frac{\delta\sigma}{\delta\epsilon} = \frac{\sigma(0.6\%) - \sigma(0.2\%)}{\epsilon(0.6\%) - \epsilon(0.2\%)}$$

where  $\sigma(0.6\%)$ ,  $\sigma(0.2\%)$ ,  $\epsilon(0.6\%)$  and  $\epsilon(0.2\%)$  are the true stresses and strains evaluated at 0.6% and 0.2% plastic elongation. The tangent modulus was evaluated at small plastic strains to enhance the possibility of measuring dislocation-precipitate interaction rather than dislocation-dislocation interaction that might arise at larger strains.

## Results and Interpretations

### 4.1 The Microstructures Chosen for the Stress-Corrosion Investigation

A preliminary transmission electron microscopy investigation of specimens given the three heat treatments with a constant final age of 180°C revealed that the microstructures were very similar to those predicted by the work of Nicholson et al. (8,26,39,40). After a short final aging treatment at 180°C, specimens given heat treatment 1 exhibited a relatively coarse, partially coherent matrix precipitate and a wide P.F.Z. while specimens given heat treatment 2 showed a relatively fine, coherent matrix precipitate and a narrow P.F.Z. Heat treatment 3 resulted in specimens having a narrow P.F.Z. and matrix precipitates very similar to heat treatment 1 at distances approximately  $2\mu$  away from the grain boundaries.

Although a complete analysis of the changes in microstructure with aging time was not performed, the general trend was observed. The only heat treatment that showed reversion was treatment 1. The other two treatments showed an increase in strength during the first stage of final aging at 180°C. In general, as the time of aging increased both the grain boundary and matrix precipitate coarsened. At short aging times, the precipitates of structure 2 were almost completely coherent and lost coherency with the matrix as aging progressed. There was some coherency present even in slightly overaged specimens. The matrix precipitate in structures 1 and 3 meanwhile, were semi-coherent at the earliest stages of aging and gradually lost coherency as aging progressed.

Again there was some evidence of coherency strains in slightly overaged material. In agreement with the observations of other investigators<sup>(8,26,40,48)</sup> the width of the P.F.Z. was independent of aging time.

It was evident from the transmission micrographs that the precipitation in this alloy is extremely complex. If one were to compare a microstructure of the Al-Zn-Mg system to a more conventional microstructure viz. Al-Cu, one would immediately notice from both the light field micrographs and diffraction patterns that the precipitates in Al-Cu have a simple morphology and a simple orientation with the matrix<sup>(33)</sup> while the precipitates in the Al-Zn-Mg alloy exhibited many morphologies and orientations with the matrix.

Although the work of Thackery<sup>(17)</sup> has shown that the  $\eta$  precipitate can have six different orientation relationships with the matrix and that a previously unreported phase was noticed ( $\chi$  - phase), he did not find the transition  $\eta'$  phase present in his study. There was direct evidence of the existence of  $\eta'$  after heat treatment 1. The measured d-spacings and corresponding lattice parameters were nearly identical to those of Mondolfo et al.<sup>(13)</sup> for this  $\eta'$  phase.

The progress of aging at 180°C of specimens given heat treatment 1 was first determined from hardness data (Figure 8). Unfortunately, the hardness response to changes in microstructure with aging time was not very informative.

The changes in tensile properties with final aging time at 180°C are shown for the three heat treatments in Figures 9 and 10. Figure 9 was taken as the true response to aging at 180°C.

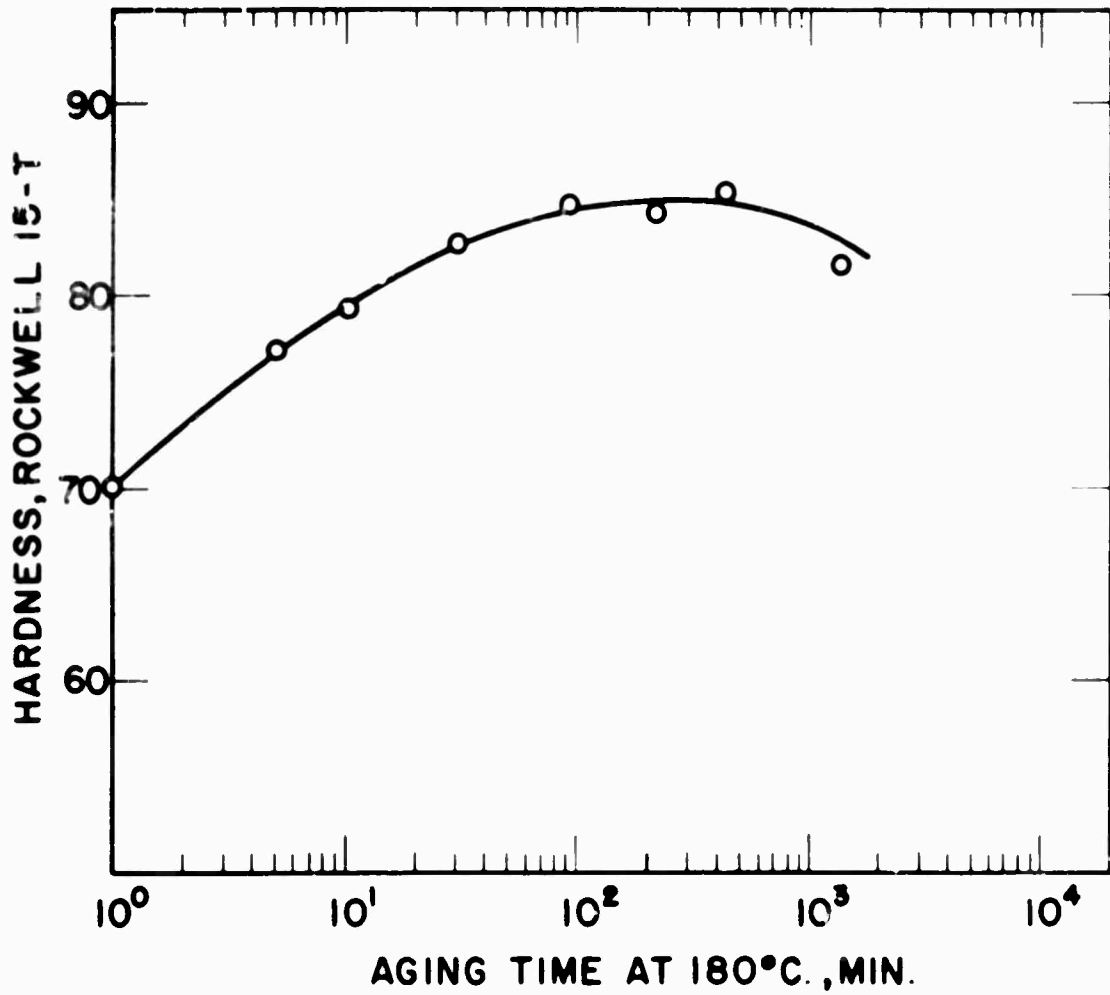


Figure 8. Effect of aging at 180°C on the hardness measured at room temperature. All specimens were solution treated for one hour at 465°C and oil quenched to room temperature prior to aging.

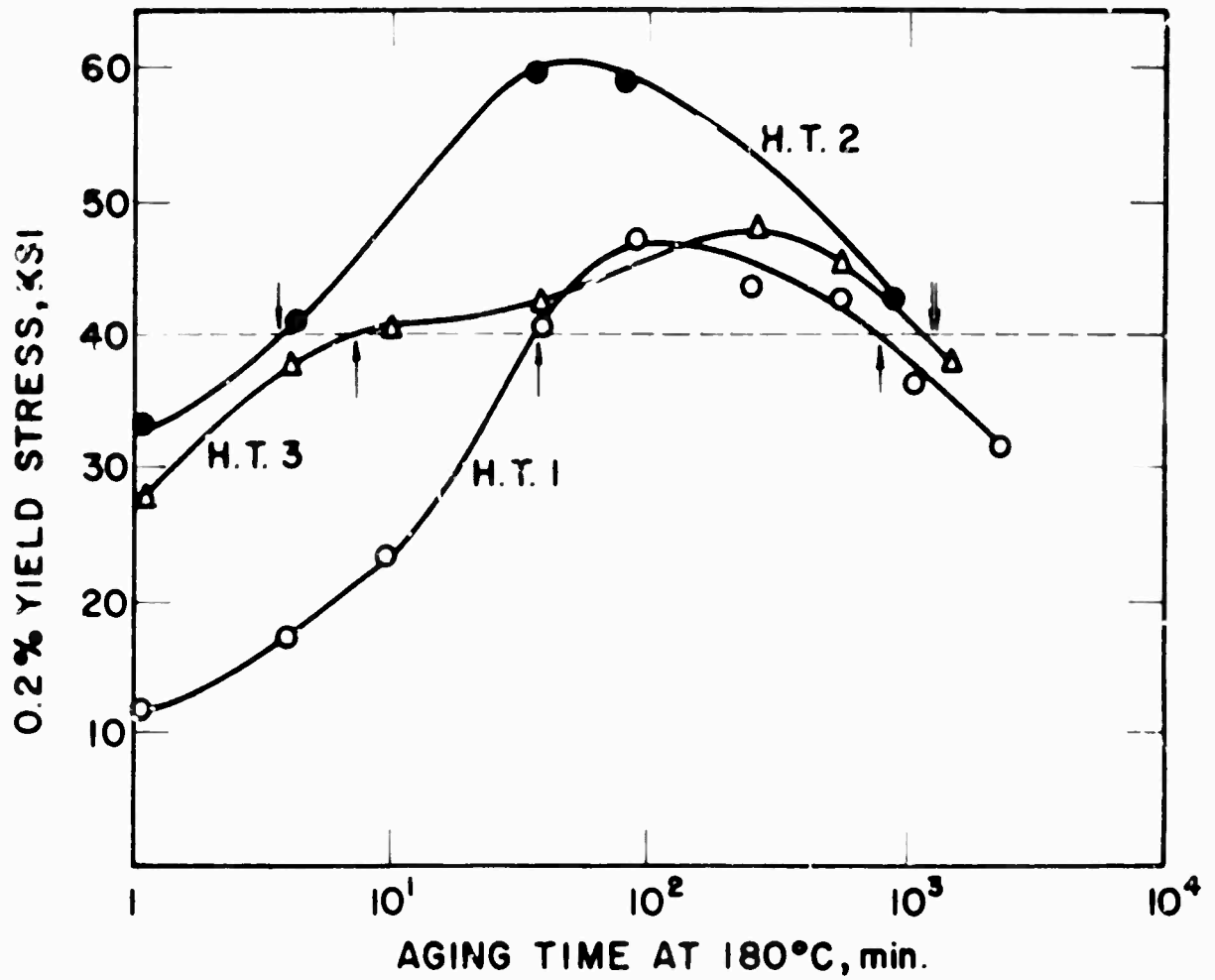


Figure 9. Yield stress (0.2% offset) versus final aging time at 180°C. Microstructures chosen for stress-corrosion investigation are shown by arrows.

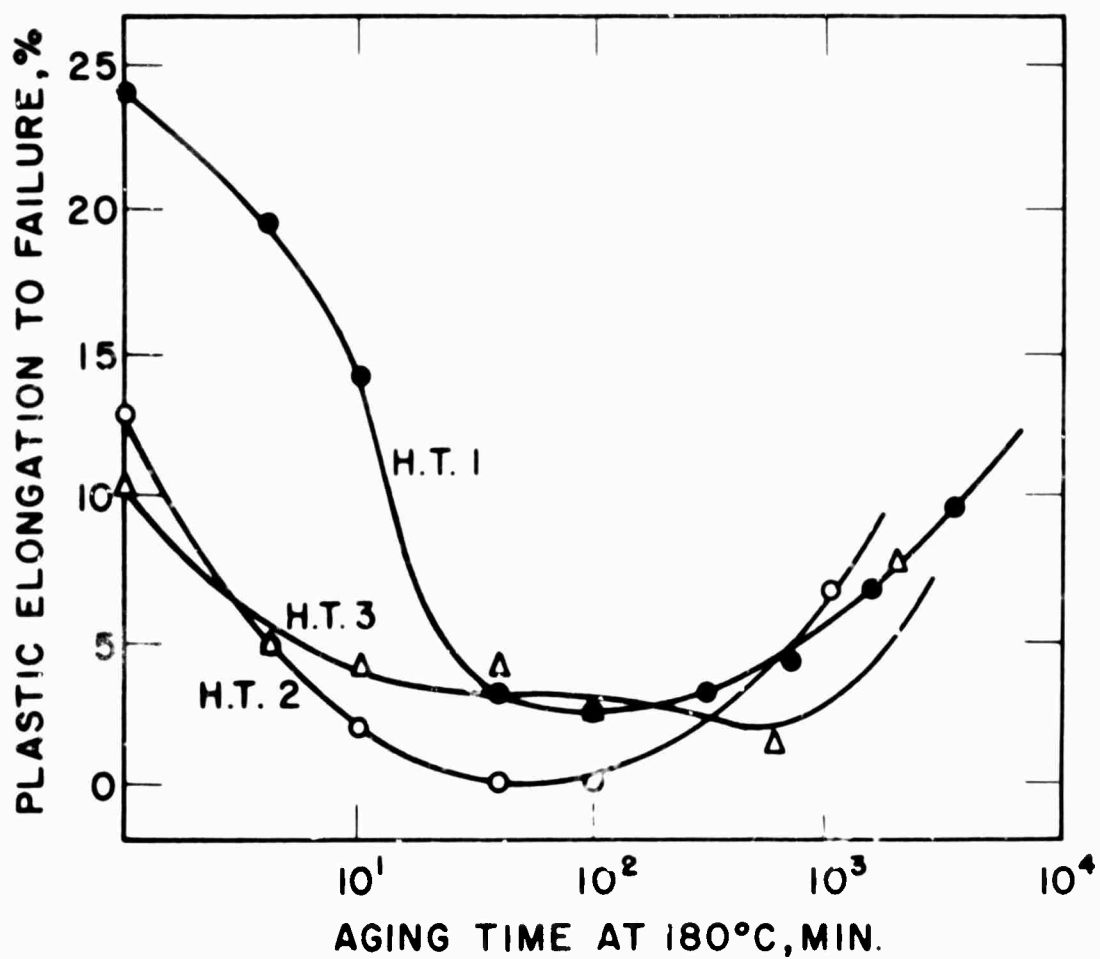
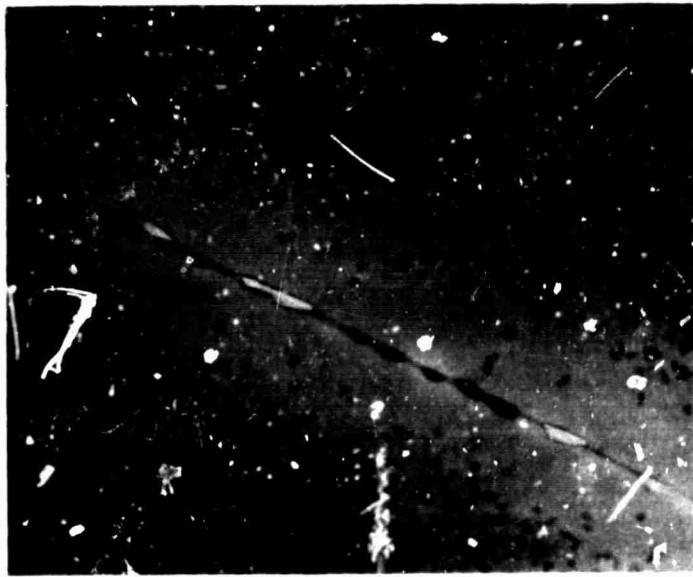


Figure 10. Percent elongation to failure versus final aging time at 180°C.

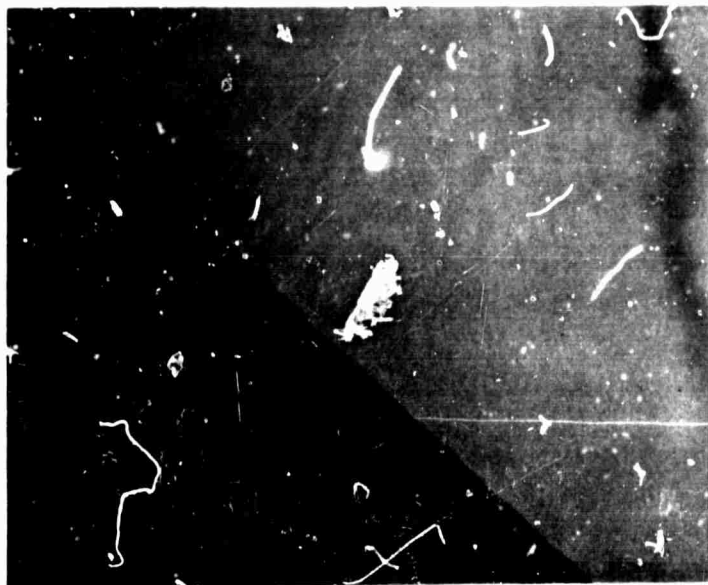
It seems clear that classical age hardening behavior occurs during each heat treatment, indicating a change in the size, shape and degree of coherency of the matrix precipitate with aging time. The highest maximum strength of specimens given heat treatment 2 undoubtedly results from the comparatively fine matrix precipitate present in that structure. The strengths of specimens given heat treatments 1 and 3 are similar, considering the extra 20 minute age initially used in treatment 3, and in the overaged state all three treatments resulted in similar strengths indicating that the strength in this case is apparently independent of initial heat treating conditions.

The microstructures chosen for the stress-corrosion experiments were those that had the common yield stress of 40 ksi. The reasons for choosing these microstructures were to prevent the testing of various microstructures under differing loads and also to permit the testing of six different microstructures with an underaged and an overaged condition for each of the three heat treatments. These microstructures are marked by arrows in Figure 9.

Figure 11 is a series of micrographs taken of specimens subjected to heat treatments identical to those given the stress-corrosion specimens. It should be noted that despite the marked differences in the P.F.Z. width and in matrix precipitate size, type and distribution, all structures had the same yield stress. These observations are in agreement with those of Ryum<sup>(48)</sup> who found that the tensile strength is independent of variations in P.F.Z. width. The hardness of the matrix was the same in each case and this also has been reported in the



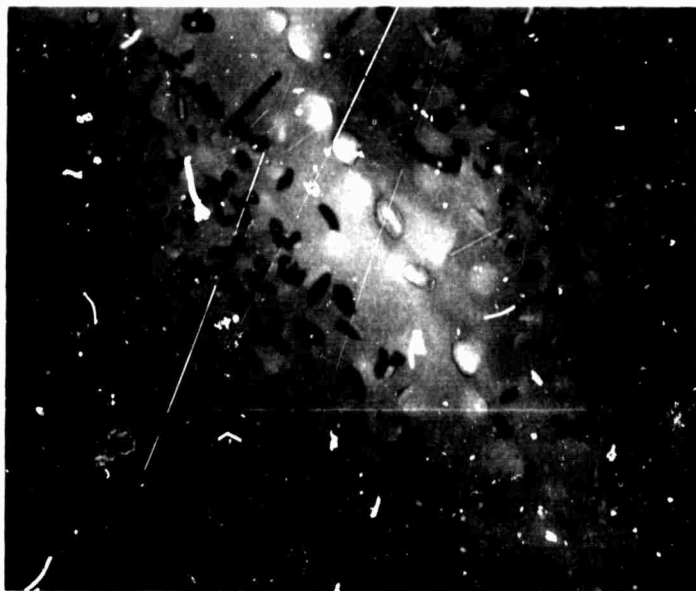
11(a) Heat treatment 1 - underaged X60,000.



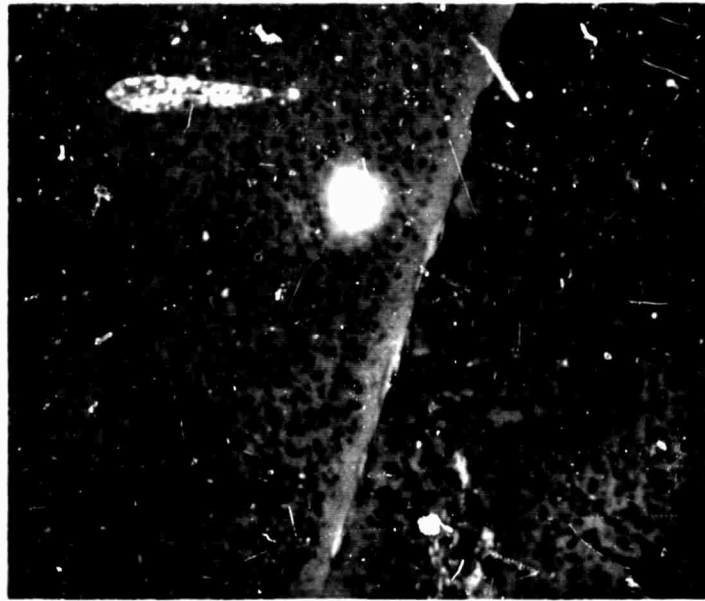
11(b) Heat treatment 2 - underaged X60,000.



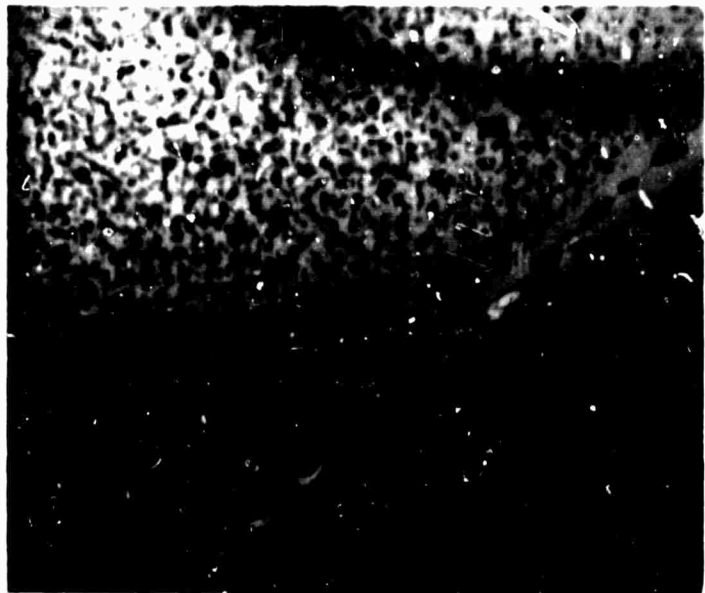
11(c) Heat treatment 3 - underaged X80,000.



11(d) Heat treatment 1 - overaged X60,000.



11(e) Heat treatment 2 - overaged X60,000.



11(f) Heat treatment 3 - overaged X60,000.

**Figure 11.** Transmission electron micrographs of microstructures used in stress-corrosion investigation.

literature<sup>(4)</sup>.

Measurements of the P.F.Z. width, taken as the sum of the precipitate free regions on both sides of the grain boundary are shown in Table I. As mentioned above, the width of the P.F.Z. changed very slightly, if at all, with aging time. This is to be expected since, as explained above, the formation of a P.F.Z. is due to difficulties in the nucleation rather than the growth of the matrix precipitate. Therefore, the only variation expected in the P.F.Z. width on aging above the G.P. zone solvus is a slight increase due to the coarsening of the matrix precipitate<sup>(19)</sup>; this could be the cause of the slight variation noted for heat treatment 2.

The size and spacing of grain boundary precipitates were measured and these results are also shown in Table I. The data compiled in Table I were the averages of at least five different boundaries per microstructure.

An effort was made to measure the sizes and spacings of the matrix precipitate present in the six microstructures. The results are shown in Table I.

These measurements are considered only approximate since: (1) the proper {111} foil orientations could not be normally achieved, (2) a three dimensional distribution was being measured in two dimensions and (3) the nature of the precipitate was very complex with many precipitate morphologies, sizes and orientations present in many of the microstructures.

**TABLE I**

**Characteristics of Microstructures Used  
In Stress-Corrosion Investigation**

<u>MICROSTRUCTURE</u> Heat Treatment	<u>Aged State</u>	<u>P.F.Z.</u> <u>Width</u> ( $\mu$ )	<u>GRAIN BOUNDARY PPT</u> <u>Size*</u> ( $\mu$ )	<u>Spacings</u> ( $\mu$ )	<u>MATRIX PPT</u> <u>Size**</u> ( $\text{\AA}$ )	<u>Spacing**</u> ( $\text{\AA}$ )	<u>0.2% Yield Stress</u> (ksi)
H.T.1	Underaged	0.5	0.065	0.183	130	240	40
H.T.2	Underaged	0.08	0.062	0.184	50	70	40
H.T.3	Underaged	0.1	0.025	0.055	110	210	40
H.T.1	Overaged	0.5	0.119	0.200	260	330	40
H.T.2	Overaged	0.1	0.085	0.237	200	300	40
H.T.3	Overaged	0.1	0.099	0.170	230	300	40

NOTE: \* - The major axis of an ellipsoid in grain boundary.  
 \*\* - Dimensions pertain to non-lath type precipitates.

## 4.2 Stress-Corrosion Behavior

### 4.2.1 Constant-Load Tests

The times to failure,  $t_f$ , shown in Table II are the average of at least eight tests performed on each of the six microstructures. A scatter of approximately  $\pm 25\%$  was observed in the failure times for a particular structure. The following points should be noted:

1. For each heat treatment, the underaged samples failed in times considerably shorter than the overaged samples and yet no change due to overaging was observed in the P.F.Z. widths of heat treatments 1 and 3 and only a slight increase of  $0.02\mu$  was observed for heat treatment 2.
2. In the underaged condition, specimens of heat treatment 3 failed in times only slightly less than those of heat treatment 1 (490 mins. against 540 mins.) although there was a large difference in the widths of the P.F.Z.s.
3. In the underaged condition, specimens of heat treatment 3 failed in much longer times than those of heat treatment 2 and yet there was only  $0.02\mu$  difference in their respective P.F.Z. widths.
4. In the overaged condition, all microstructures had essentially the same susceptibility despite large differences in the P.F.Z. widths.

These results strongly indicate that there is no correlation between the width of the P.F.Z. and susceptibility to stress-corrosion cracking. However, as the matrix precipitate varied with the same grain boundary precipitate size (treatments 1 and 2 - underaged), the susceptibility decreased by an order of

TABLE IIStress-Corrosion Behavior of Microstructures  
Tested Under Constant-Load Conditions

<u>MICROSTRUCTURE</u>		<u>LIFE OF SPECIMENS</u>
<u>Heat Treatment</u>	<u>Aged State</u>	<u><math>t_f</math> (minutes)</u>
H.T.1	Underaged	540
H.T.2	Underaged	48
H.T.3	Underaged	490
H.T.1	Overaged	2470
H.T.2	Overaged	2440
H.T.3	Overaged	2100

magnitude. Furthermore, specimens with smaller grain boundary precipitates seemed to be slightly more susceptible than those with larger precipitates when both had essentially the same matrix precipitate (treatments 1 and 3 - undamaged). The large decrease in susceptibility caused by overaging is also attended by a coarsening of both the grain boundary precipitates as well as the matrix precipitates. It is possible therefore, that the susceptibility to stress-corrosion cracking is controlled by both the matrix and the grain boundary precipitate with the experimental evidence indicating that the matrix precipitate is the more important.

#### 4.2.2 Constant-Deflection Test

Under the conditions of this test, three distinct stages were observed: Stage 1: a short period of rapid load relaxation during which the load decreased from 70% to ~ 67% of the 0.2% proof stress; Stage 2: a long period during which the load decreased at a very slow but constant rate and Stage 3: consisting of accelerated and irregular periods of load relaxation which ultimately terminated in failure. Stress-corrosion cracks were only detected at the beginning of Stage 3 and hence it is considered that the time up to the end of Stage 2 represents the time,  $t_i$ , for the initiation of a stress-corrosion crack and that the duration of Stage 3 is the time  $t_p$ , for crack propagation. Values of  $t_i$  and  $t_p$ , representing the average of at least two tests are given in Table III. It should be noted that the sum of these is greater than  $t_f$  in the constant load test, Table II. This is to be expected because of the load relaxation under constant-deflection conditions.

These results indicate that crack nucleation represents a considerable fraction of the total time to failure. Furthermore, it is apparent that the P.F.Z. width has little effect on the time of initiation or propagation. Both times increase considerably due to overaging and yet both conditions of heat treatment 2 had nearly the same P.F.Z. width.

The discontinuous crack propagation during Stage 3 appeared to be associated with the orientation of the grain boundaries ahead of the running crack. Visual observations revealed that boundaries nearly normal to the tensile axis cracked rapidly in a brittle-like manner while the boundaries which had a smaller normal stress cracked at a much slower rate. The terms rapid and slowly are used only in a comparative sense; the cracking rates in structure 2 - underaged were much faster than for structure 2 - overaged, for example, but the relative effect of boundary orientation was the same in each structure.

#### 4.3 Effect of Stress on the Corrosion Propensity of Grain Boundaries

The results of this experiment indicated that the environmentally induced, catastrophic failure observed in loaded specimens was indeed stress-corrosion rather than simply the mechanical overload of a cross-section reduced through corrosion. Specimens exposed to the NaCl solution in the absence of stress for times equal to their life in the stress-corrosion tests did not suffer a degradation in mechanical properties.

The metallographic observations made on specimens both stressed and unstressed revealed that in all cases there was general pitting in the grain

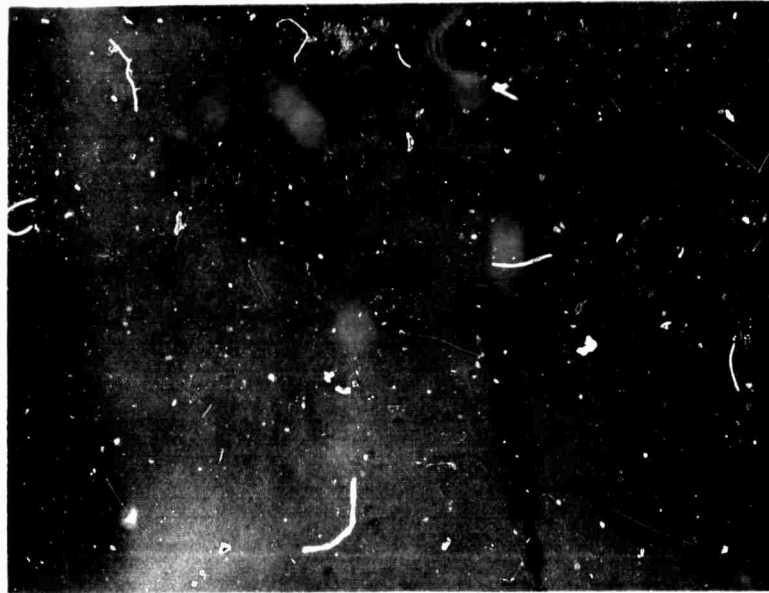
TABLE IIIStress-Corrosion Behavior of Microstructures Tested  
Under Constant-Deflection Conditions

<u>MICROSTRUCTURE</u>		<u>INITIATION TIME</u>	<u>PROPAGATION TIME</u>
<u>Heat Treatment</u>	<u>Aged State</u>	<u>t<sub>i</sub> (minutes)</u>	<u>t<sub>p</sub> (minutes)</u>
H.T.1	Underaged	513	> 227
H.T.2	Underaged	50	> 29
H.T.2	Overaged	1970	> 225

interiors and concentrated pitting in the grain boundary regions. The three underaged microstructures were examined in this investigation and in general, all three showed relatively similar behavior. In the absence of stress, this behavior included light general pitting and a few lightly attacked boundaries after short exposures (relative to the respective failure time) and as the time in solution increased so did the severity of the general pitting as well as the grain boundary attack. A marked change in behavior occurred when this experiment was conducted with the specimen under stress. Again, at short times, there was light general pitting in grain interiors and few grain boundaries attacked. However, in the presence of stress more boundaries were attacked and the attack was more severe. As the time of exposure increased, more boundaries became attacked and the severity of attack increased with time. Figure 12 shows this behavior for microstructure 2 - underaged. Comparing Figures 12a and 12b, one can see that in the former the bottom of the grain boundary "trench" is visible while in the latter it is not. This seems to indicate that the presence of stress leads to a greater depth of grain boundary penetration.

#### 4.4 Deformation Study

Typical transmission electron micrographs of specimens which had been plastically deformed after aging are shown in Figures 13 and 14. It should be noted that there was little difference in dislocation arrangement when the same initial microstructure was strained to either 2% or to failure. The heterogeneous nature of the deformation observed in this alloy (structure 2 - underaged) has



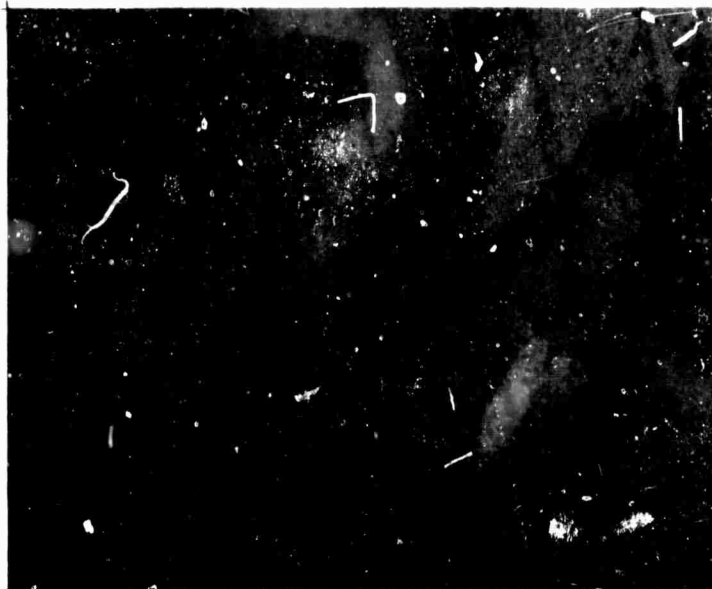
12(a)



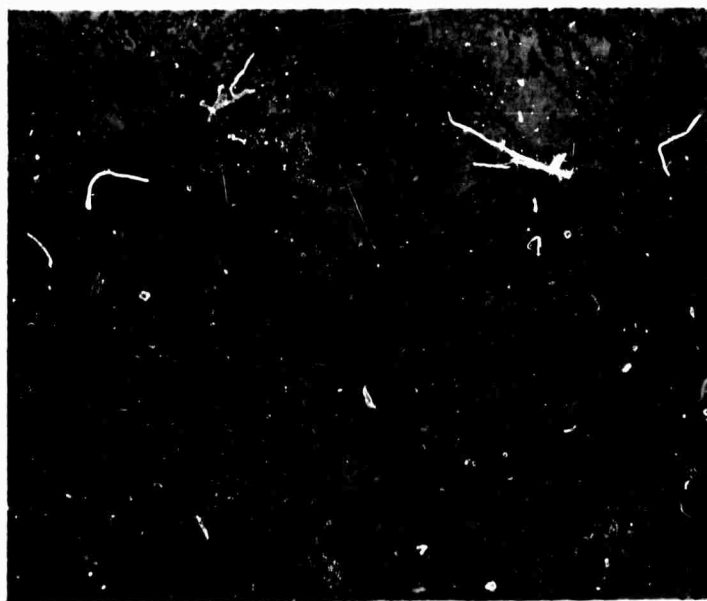
12(b)

Figure 12. Optical micrographs of corrosion occurring on electropolished surface of structure 2 - underaged after a 30 minute exposure. 950X

- (a) In absence of stress.
- (b) Stressed to ~ 70% yield stress.



13(a)

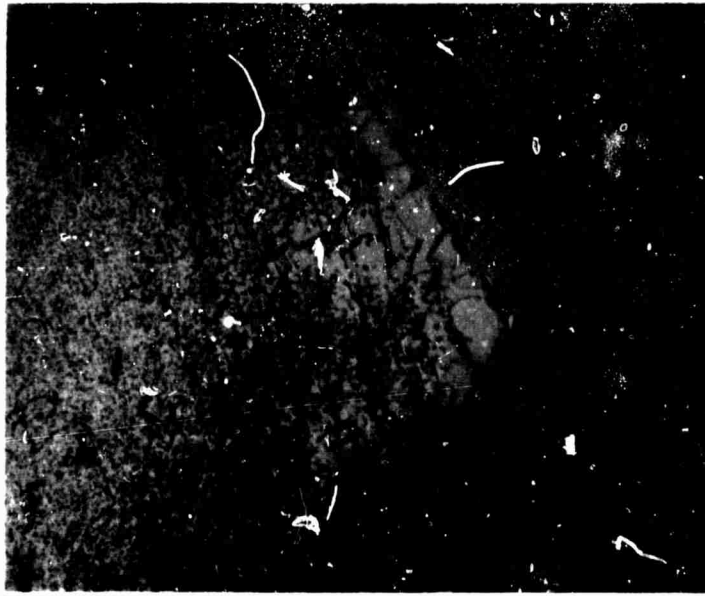


13(b)

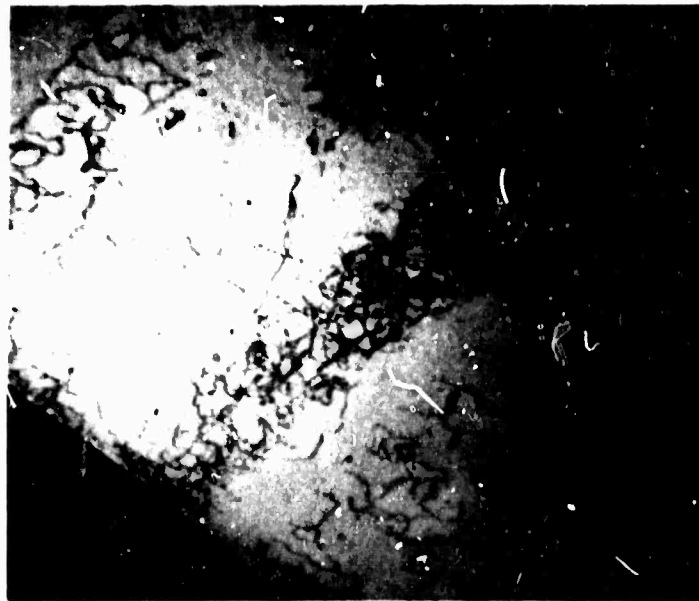
Figure 13. Transmission electron micrographs illustrating heterogeneous nature of dislocation distribution resulting from a 2% macroscopic strain.

(a) Heat treatment 1 - underaged X14,000.

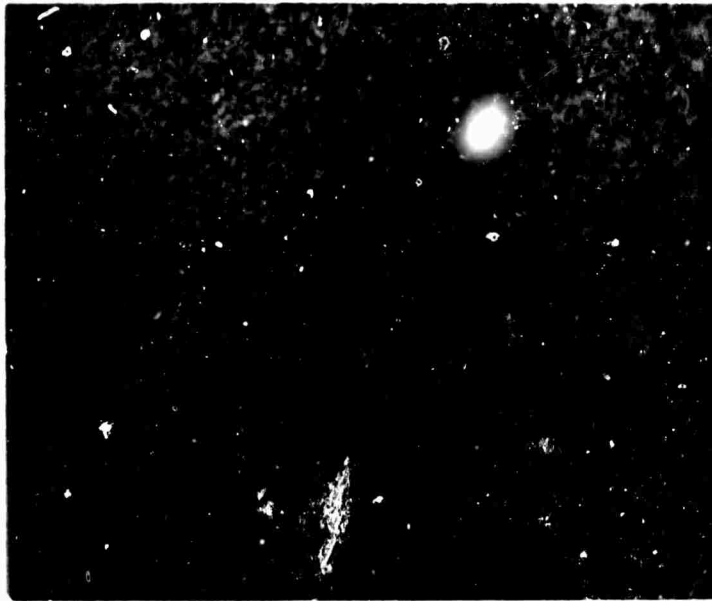
(b) Heat treatment 2 - underaged X22,000.



14(a) Heat treatment 1 - underaged, strained 2%  
X22,000.



14(b) Heat treatment 2 - underaged, strained to  
failure (5%) X22,000.



14(c) Heat treatment 2 - overaged, strained to failure (6%) X40,000.

Figure 14. Transmission electron micrographs showing variations in dislocation-matrix precipitate interaction in microstructures used in stress-corrosion investigation.

been noted frequently in the literature<sup>(5,6,48,87,88)</sup>. Most of the dislocation activity seemed to be confined to a few slip bands (Figure 13). The dislocation density in these bands in structure 2 - underaged was very high ( $\sim 10^{12}$  lines/cm<sup>2</sup>) while regions between the bands had a relatively low density ( $\sim 10^7$  lines/cm<sup>2</sup>).

A close examination of these deformation bands reveals a variation in the dislocation arrangements within these bands which is related to the type, size and spacing of matrix precipitates in the microstructure. It is this variation in dislocation arrangement which correlates strongly with stress-corrosion susceptibility. Figure 14 shows the dislocation arrangement within a deformation band in microstructures which show the three degrees of stress-corrosion susceptibility, viz. extremely susceptible (structure 2 - underaged), moderately susceptible (structure 1 - underaged) and relatively unsusceptible (structure 2 overaged). The dislocations in the extremely susceptible structure seemed to have sheared the precipitate since there was no evidence of dislocation loops and bowing between precipitates. This behavior is expected because the matrix precipitate in this structure appeared to have a high degree of coherency with the matrix. Since the slip plane and Burger's vector would be continuous in this structure, it would appear possible that dislocations would be able to move in a continuous manner.

In the absence of impenetrable barriers in the slip plane and under certain conditions of stress, it seems possible that the dislocations in this structure

would be able to glide large distances. This would increase the possibility of many dislocations in the slip band impinging on a grain boundary (Figures 13b and 14b).

In contrast, the dislocations in the least susceptible material could not deform the matrix precipitate and a much different situation obtained (Figure 14c). It is rather difficult to clearly observe the dislocations in this type structure since the scale of the matrix precipitate is very similar to the scale of the dislocation size and distribution. One can point out, however, that the vast majority of dislocations present in the overaged structure were in the form of loops around the matrix precipitate and that the lengths of the remaining dislocations were of the order of the precipitate spacing. Considering the relatively large size of the incoherent matrix precipitate as well as the large interparticle spacing, the dislocation arrangement observed in the overaged material was hardly unexpected. In the presence of potent barriers to dislocation motion in the slip plane, it seems that unlike the "freely" moving dislocations in material susceptible to stress-corrosion, the dislocation motion in overaged material would be very restricted (small slip distances between barriers). The result of this behavior would be to have either fewer dislocations acting on the grain boundary or a lower stress on the boundary due to a high friction stress. The dislocation-matrix precipitate interaction observed in moderately susceptible material (structure 1 - underaged) was between the above two extremes in intensity (Figures 14a). The dislocation lines seemed longer than those in the least

susceptible condition but much shorter than those in the most susceptible condition. In many instances evidence of strong dislocation - precipitate interactions was observed in the form of bowed dislocations and dislocation loops around precipitate particles. These results agree well with the reported finding of Holl<sup>(5)</sup> and Spiedel<sup>(6)</sup>.

Figures 13b and 14a show dislocations that are located within the P.F.Z. However, the density of dislocations in these regions is no greater than in the grain interior and in no sense can this be described as preferential slip within the P.F.Z.

Extensive amounts of plastic deformation accompanying a propagating stress-corrosion crack were observed (Figures 15 and 16). The large size of the plastic zone (up to 10 grain diameters) was probably due to the plane-stress conditions under which these specimens were tested. The slip lines which appeared on the side surfaces of structure 2 - underaged seemed very straight and had a mean slip step height of approximately  $0.2\mu$  (Figure 15), while the slip lines in the overaged structure appeared more wavy and were approximately  $0.05\mu$  high (Figure 16).

#### 4.5 Fractography

Fracture surface observations support the well documented fact that stress-corrosion cracking in this system is predominately intergranular in nature<sup>(63,72)</sup>. In general, all of the fracture surfaces exhibited regions of both brittle and ductile fracture. Only the brittle region is believed to be caused by

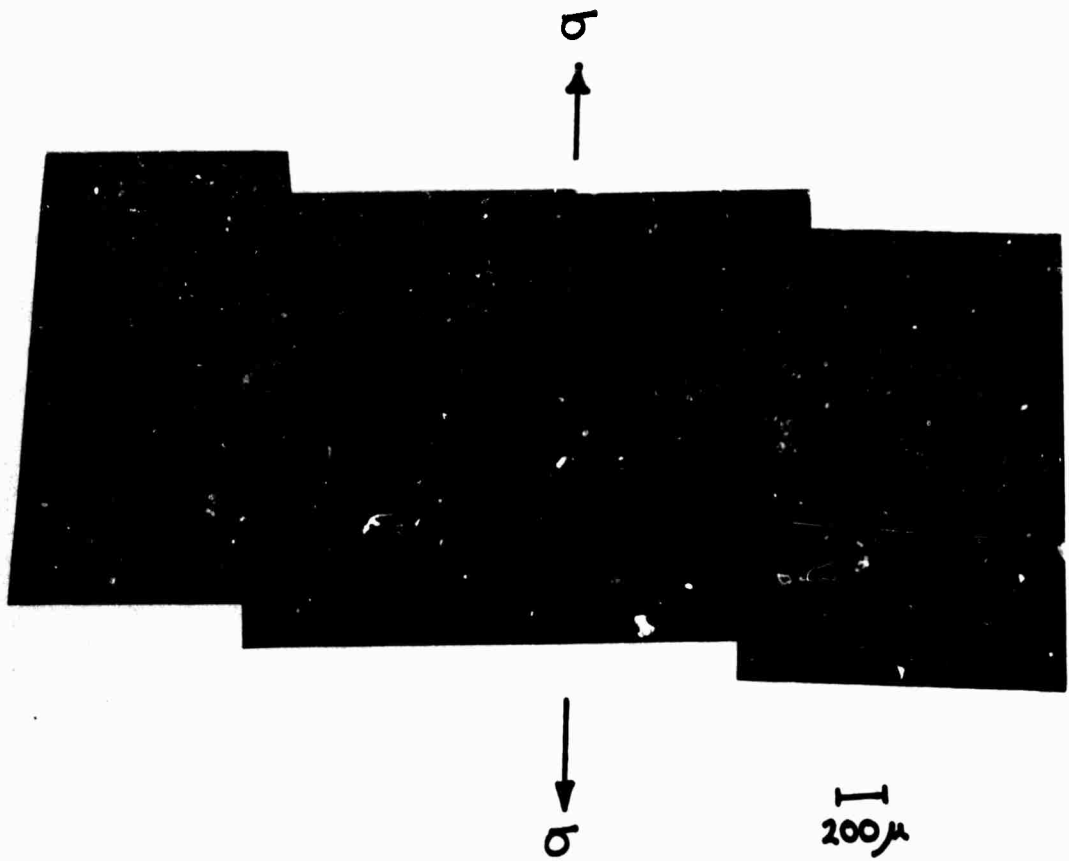


Figure 15. Optical micrograph illustrating the deformation accompanying a stress-corrosion crack in structure 2 - underaged.

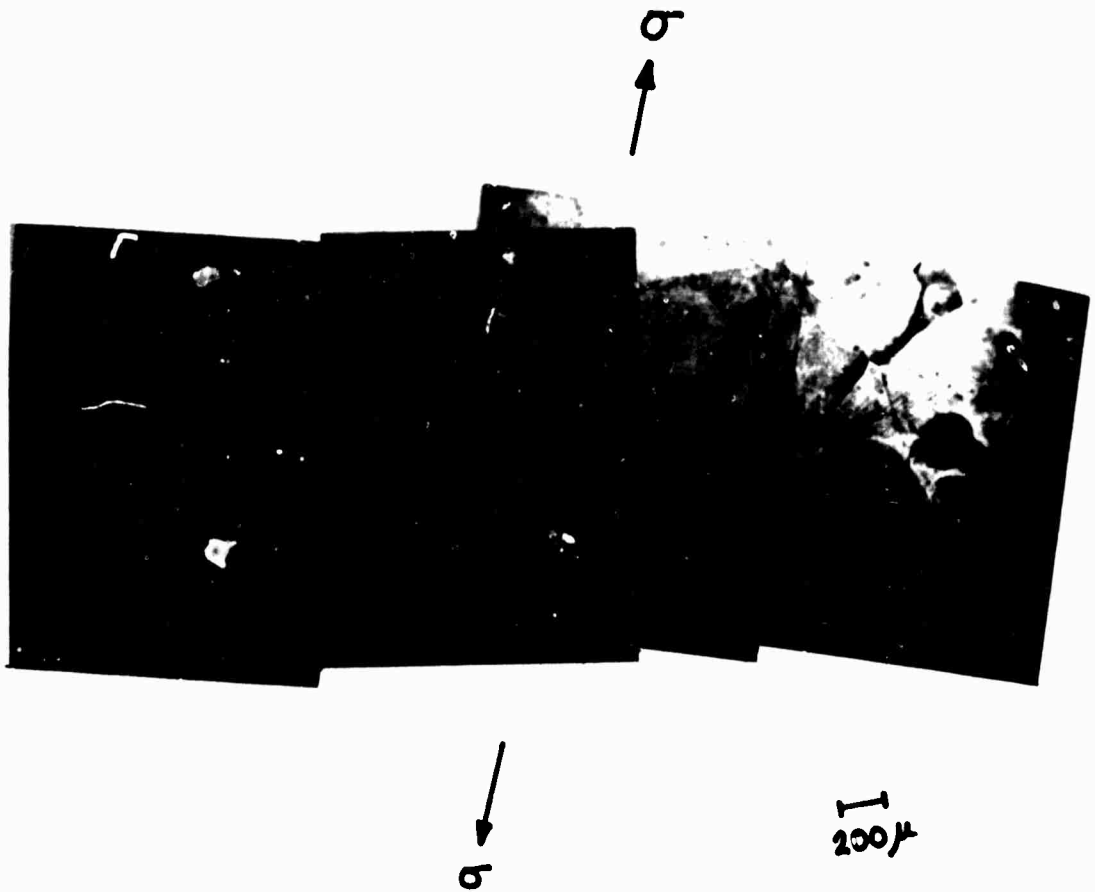


Figure 16. Optical micrograph illustrating the deformation accompanying a stress-corrosion crack in structure 2 - overaged.

stress-corrosion while the ductile region is believed to result from mechanical overload<sup>(72)</sup>. This seems reasonable since the brittle region followed an intergranular path while the ductile region transversed a transgranular path.

Figure 17 shows schematically the differences in fracture surfaces between extremely susceptible material (structure 2 - underaged) and unsusceptible material (structure 2 - overaged). The region of brittle fracture of structure 2 - underaged was planar with very light pitting and slip steps while the ductile region showed dimpling characteristic of this type of fracture. Figure 18a shows the flat region of brittle fracture with a shear lip at A, intersecting slip bands at B, large holes at C and striations at D. For clarification, area E is the side surface. Figure 18b shows the dimpled structure mentioned above. The fractographic observations revealed that structure 2 - underaged (extremely susceptible) suffered continuous brittle fracture over perhaps 60% of the grain boundary region and continuous ductile fracture over the remainder (Figure 17). The fracture surfaces of structures 1 - underaged and 2 - overaged were not so informative since the fractured boundaries had been exposed to the solution for very long times. Nevertheless, it was evident that structure 2 - overaged had what appeared to be both brittle and ductile regions. Figure 17 shows how these regions were located. There seemed to be a higher fraction of ductile region in the overaged than in the underaged condition of structure 2.

Extreme care as well as good judgement should be exercised when interpreting the fine detail appearing on stress-corrosion fracture surfaces. There are

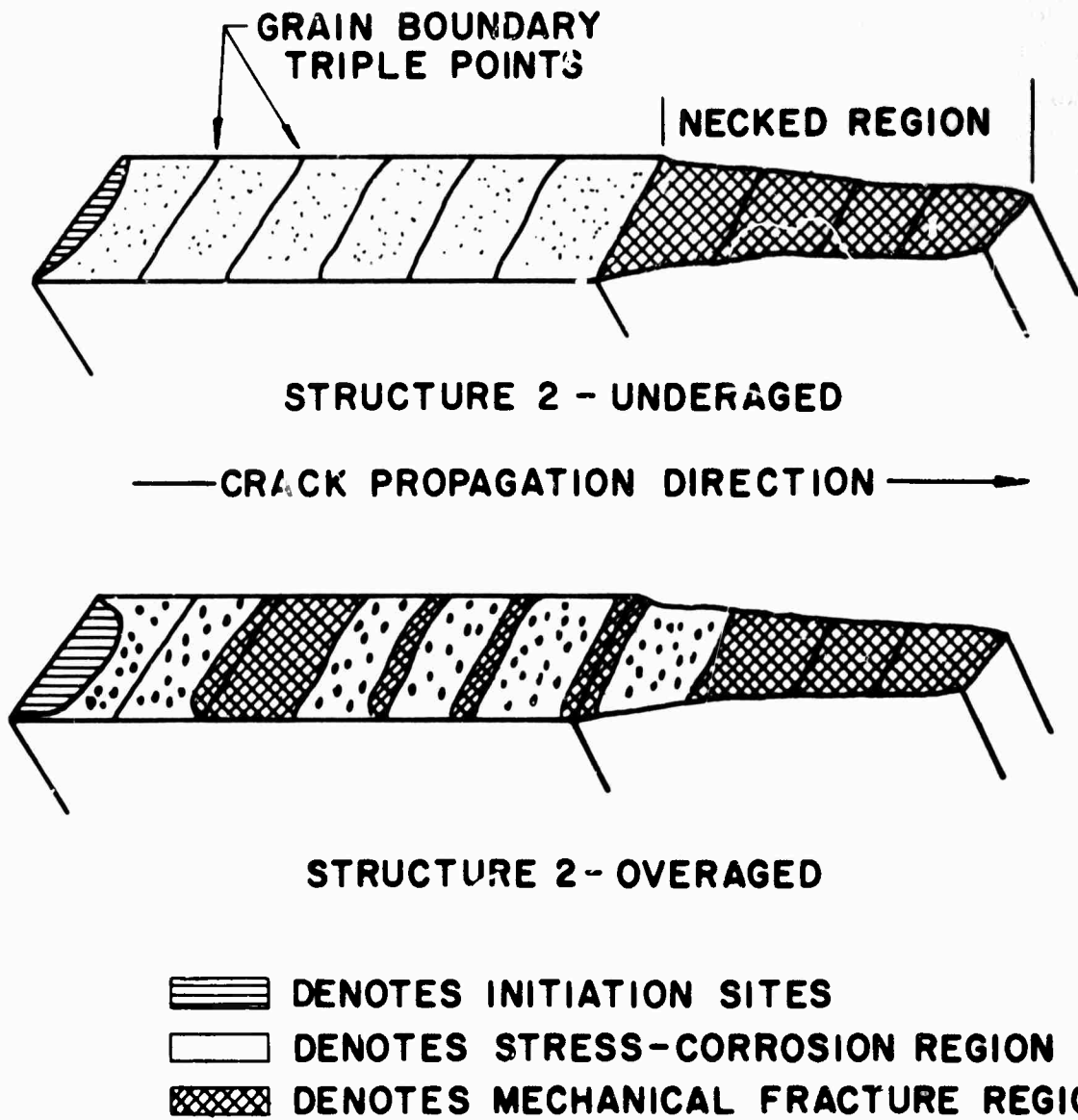


Figure 17. Schematic representation of fracture surface appearance.



18(a)



18(b)

**Figure 18.** Scanning electron micrographs of stress-corrosion fracture surface of structure 2 - underaged.

(a) Region of stress-corrosion fracture X300.

(b) Region of ductile fracture X1000.

two (at least) obvious reasons for caution. The first is that, in general, there were many fine features on all of the fracture surfaces examined and therefore one could find nearly anything one wished. A good example of this is Figure 18a where in one area of one grain boundary evidence can be found to support three different mechanisms proposed for stress-corrosion cracking, viz. large holes<sup>(67)</sup>, striations<sup>(3,68)</sup> and slip bands<sup>(5,6)</sup>. The other reason for caution is the after-the-fact corrosion of the fractured boundaries. Consider a portion of the grain boundary which suffers stress-corrosion cracking. This portion of the fractured boundary would be exposed to the environment for the remainder of the test after which it would be removed from the corrosion cell. It should be clear that the longer the life of the specimen, the less informative will be the fracture surface.

The conclusions arising from this fractography work have been made in light of the problems outlined above. Despite these shortcomings, a few valuable observations could be made. There was a distinct difference in fracture surface appearance between very susceptible and unsusceptible material. The susceptible material had a larger portion of brittle fracture than did unsusceptible material. The fine detail in the brittle region of the susceptible material forces one to assume that crack propagation is predominately mechanical in nature: (1) there is no evidence of heavy pitting in spite of the after-the-fact corrosion, (2) slip bands that, prior to cracking, had been pushing on the grain boundary are present giving a relief effect and (3) there is much evidence

(general lack of fine detail and constant-deflection test results) to support a mechanism whereby an entire grain boundary ruptures with a high crack velocity, in a manner similar to cleavage.

In the case of unsusceptible material, nothing can be said about the fine detail on the brittle fracture surfaces because of the large amount of intense pitting that has occurred.

#### 4.6 Correlation of Rate of Work Hardening with Stress-Corrosion Susceptibility

The relationship between stress-corrosion behavior and the tangent modulus of each of the six microstructures is shown in Table IV. These data indicate that as the rate of work hardening (tangent modulus) decreased, the susceptibility to stress-corrosion also decreased.

One interesting and surprising fact emerged from this work, viz. that the microstructure containing nearly coherent matrix precipitates had a higher rate of work hardening than microstructures containing large, incoherent matrix precipitates.

The correlation between susceptibility and rate of work hardening is not considered fortuitous. If the matrix precipitate were to control the susceptibility to stress-corrosion through its effect on the dislocation behavior, it appears plausible that the matrix precipitate might also effect the rate of work hardening, again, through its effect on the dislocation behavior.

TABLE IV

Correlation of Tangent Modulus (T) and Stress-Corrosion  
Susceptibility for Microstructures Investigated

<u>MICROSTRUCTURE</u>		<u>TANGENT MODULUS</u>	<u>SUSCEPTIBILITY</u>
<u>Heat Treatment</u>	<u>Aged State</u>	$\frac{T}{10^5}$ <u>(psi)</u>	$t_f$ <u>(minutes)</u>
H.T.1	Underaged	3.75	540
H.T.2	Underaged	4.41	48
H.T.3	Underaged	3.78	490
H.T.1	Overaged	2.97	2470
H.T.2	Overaged	2.66	2440
H.T.3	Overaged	2.38	2100

## Discussion

### 5.1 P.F.Z. Hypothesis in the Stress-Corrosion Cracking of Al-Zn-Mg Alloys

The P.F.Z. hypothesis began when Geisler<sup>(44)</sup> and later Varley et al.<sup>(89)</sup> postulated that the tensile brittleness frequently observed in relatively concentrated Al-Zn-Mg alloys was due to the presence of P.F.Z.s. This unconfirmed postulate was directly responsible for the P.F.Z. hypothesis in stress-corrosion. As described earlier, the P.F.Z. theory<sup>(1,2,4)</sup> is based on the following assumptions:

- (1) A susceptible microstructure (only) must have a P.F.Z.
- (2) Upon the application of a stress, preferential plastic deformation will occur in the P.F.Z. because it has a lower flow stress than does the matrix.
- (3) Preferential corrosive attack occurs in those regions where preferential plastic flow has taken place (viz. in the P.F.Z.).

There exists much experimental information, including that of the present investigation, which simply refutes these basic assumptions. For example, the overaged structures in the present investigation all proved relatively unsusceptible even though they had not only P.F.Z.s present but also P.F.Z.s of differing widths. It is strongly believed that if the overaged structures had been aged for even longer times, the susceptibility would have been further reduced regardless of the presence or width of the P.F.Z.

Regarding assumption (2) it should be noted that no one, including the

advocates of the P.F.Z., has ever shown conclusive, direct evidence of preferential slip in the P.F.Z.

Assumption (3) has been shown to be partially correct. Preferential corrosive attack did indeed occur in regions where preferential plastic deformation had taken place. These regions were the slip bands across the grains that intersected the free surface, however, and not along the boundary.

In light of the discrepancies mentioned above, a few remarks concerning the latest P.F.Z. work might be informative. As mentioned earlier, Sedriks et al.<sup>(4)</sup> have reported that a decrease in the P.F.Z. width caused an increase in susceptibility to stress-corrosion. These authors varied the P.F.Z. width by using different aging temperatures immediately after quenching to room temperature. They have also stated that the matrix precipitate appeared similar in all of their microstructures. However, due to the relationship existing between the P.F.Z. width and the matrix precipitate it is very unlikely that the matrix precipitate would be similar and this suspicion can be readily confirmed by observing their published and unpublished micrographs. It should be noted that with the type of heat treatment employed by these authors, in general, high temperature aging will result in both wide P.F.Z.s and coarse matrix precipitates while low temperature aging will result in both narrow P.F.Z.s and fine matrix precipitates. It appears very possible that the high degree of susceptibility noted for the specimens aged at the lowest temperature was not due to the narrow P.F.Z. but rather resulted from the details of the matrix precipitate.

Thomas<sup>(69)</sup> has performed experiments which, he contends, show that specimens with P.F.Z.s are more susceptible than specimens without these zones. He compared the susceptibilities of quenched and aged (type II) specimens and specimens that had plastic deformation introduced during an interruption of the age. The specimens that had been plastically deformed were less susceptible than the undeformed specimens and the susceptibility decreased with increasing amounts of plastic deformation. Thomas has suggested<sup>(69)</sup> that the decrease in susceptibility was probably due to the plastic deformation being concentrated in the P.F.Z. which would allow precipitation to take place and thereby eliminate the P.F.Z. McEvily et al.<sup>(3)</sup> later used a treatment similar to that of Thomas and showed that the plastic deformation introduced during interrupted aging caused a jogging of the grain boundaries probably due to partial recrystallization ( $T_{\text{melt}} \sim 870^{\circ}\text{K}$ ,  $T_{\text{age}} \sim 420^{\circ}\text{K}$  and 50% strain). The matrix precipitate in the specimens that had an interrupted age consisted of both  $\eta'$  and G.P. zones while only G.P. zones were present after the standard heat treatment. It is impossible to tell from the published micrographs whether or not the P.F.Z.s were eliminated by the interrupted aging treatment. One must note that although this treatment may have reduced or eliminated the P.F.Z., there were other microstructural changes also occurring and it is not at all clear that the increase in stress-corrosion resistance should be attributed only to the changes in the P.F.Z.

Another experimental observation which discredits the P.F.Z. hypothesis

is that P.F.Z.s have been shown to exist in single crystals (at low angle boundaries) but these crystals have an extremely high if not total resistance to stress-corrosion<sup>(22)</sup>.

It should be clear at this point that the whole P.F.Z. hypothesis is, at best, very questionable. There is little doubt that the P.F.Z. can (and probably does) take part in stress-corrosion but it seems very unlikely, in light of much negative experimental evidence, that either the P.F.Z. itself or variations in its width control the susceptibility to stress-corrosion.

#### 5.2 Grain Boundary Precipitate Hypothesis in the Stress Corrosion Cracking of Al-Zn-Mg Alloys

Another group of investigators<sup>(75,76,90)</sup> suggests that stress-corrosion is controlled by the grain boundary precipitates. As mentioned earlier, Kent<sup>(76)</sup> showed that microstructures with larger grain boundary precipitates proved less susceptible than those with finer grain boundary precipitates. These precipitates in Kent's experiments were varied by changing the quenching rate. These quenching treatments were followed by aging treatments which were designed to minimize differences in the matrix precipitate. Unfortunately, Kent's treatments did result in slight variations in the matrix precipitate and this variation can be seen in his published micrographs. The results of the present investigation support the contention that variations in grain boundary precipitates can possibly have an effect in stress-corrosion behavior. Microstructures having different sizes and spacings of grain boundary precipitates but similar matrix precipitate did have slightly different degrees of susceptibility. In agreement

with Kent's observations, the microstructure having the larger, more widely spaced grain boundary precipitate (structure 1 - underaged versus structure 3 - underaged) were the more resistant to stress-corrosion. This correlation between grain boundary precipitates and susceptibility does not appear to exist in the overaged microstructures. There are two possible explanations for this inconsistency:

(1) Perhaps there really isn't a relationship between susceptibility and grain boundary precipitates. This could be true since the matrix precipitate in the two structures (1 and 3 - underaged) are similar but not identical. Perhaps the almost insignificant difference in their susceptibility (540 versus 490 minutes) is merely a reflection of the very slight difference in the matrix precipitate rather than being due to a larger difference in grain boundary precipitate. If this were true, it would also indicate that Kent's results are due to differences in the matrix precipitate and not to differences in grain boundary precipitate.

(2) Susceptibility may depend on both the grain boundary and matrix precipitate. For example, both precipitates can, perhaps, contribute to susceptibility in the underaged condition while in the overaged condition the role of the matrix precipitate is dominant.

### 5.3 Matrix Precipitate Hypothesis in the Stress-Corrosion Cracking of Al-Zn-Mg Alloys

The third group of investigators favors the matrix precipitate as controlling susceptibility<sup>(5,6,78,79)</sup>. These investigators have shown that there is a strong correlation between susceptibility and the type, size and distribution of matrix precipitates. Some of these workers<sup>(5,6,80)</sup> have gone into more detail and explained that the correlation exists because of the effect of the matrix precipitate on dislocation behavior.

The results of the present investigation appear to clearly support the conclusion of this last group, viz. that the matrix precipitate seems to be the metallurgical feature which controls susceptibility. The microstructures tested in the present investigation exhibited three degrees of susceptibility; each degree corresponding to a different size, spacing and degree of coherency of the matrix precipitate. The deformation characteristics observed in the specimens of varying degrees of susceptibility were also different indicating that susceptibility does correlate with the details of the deformation process occurring within the matrix. This deformation is, of course, controlled by the matrix precipitate.

An understanding of the effect of microstructure on deformation is therefore necessary at this point. In particular, it would be advantageous to know how the matrix precipitate affects the heterogeneity of the deformation.

#### 5.4 Effect of Matrix Precipitate on Deformation

The response to aging of aluminum alloy single and polycrystals has been explained in terms of the matrix precipitates which are present in the various stages of aging. In general, the initial increase in strength from the as-quenched to just prior to maximum strength has been attributed to the formation and growth of G.P. zones. There is strong (both direct and indirect) evidence that these zones can be sheared by dislocations<sup>(22,91-94)</sup>. As these zones coarsen in underaged Al-Zn-Mg (type II microstructure), the barrier to dislocation motion also increases and there is an increase in strength. As the peak strength is approached,  $\eta'$  begins to form and this precipitate has been shown to be sheared by dislocations at least in the initial stages of its existence<sup>(22,94)</sup>. The transition phases in Al-Cu<sup>(94-96)</sup> and Al-Ag<sup>(97)</sup> have also been shown to be sheared by dislocations. Statham<sup>(22)</sup> has shown that the peak strength (type II microstructures) obtains in Al-Zn-Mg single crystals when the  $\eta'$  can no longer be sheared by dislocations. As aging progresses, the  $\eta'$  gives way to  $\eta$  and overaging begins. This  $\eta$  phase does not appear to be deformed by dislocations<sup>(22,94)</sup>. It seems clear that at and beyond peak strength, yielding occurs by the Orowan<sup>(98)</sup> mechanism and that the strength falls during overaging due to the larger size and spacing of precipitates<sup>(22)</sup>. These observations regarding dislocation-precipitate interactions have been confirmed in the present investigation.

The heterogeneous nature of the deformation similar to that observed in the present investigation (especially in the most susceptible material) was

investigated by Thomas and Nutting<sup>(99)</sup>. They studied the deformation characteristics of Al as well as solid solutions of Al-Cu, Al-Mg and Al-Ag. Their<sup>(99)</sup> results showed that in Al and Al-Ag deformation was accommodated by slip band broadening through the addition of slip lamellae to existing bands. With Al-Cu and Al-Mg, however, deformation was accommodated by the formation of new bands. These results indicate that the deformation in Al-Cu and Al-Mg is more heterogeneous than in Al and Al-Ag. Thomas and Nutting suggest that the explanation for this behavior lies in the fact that both Cu and Mg distort the Al matrix while Ag does not<sup>(100)</sup>. After reviewing the various mechanisms proposed by Brown<sup>(101)</sup>, Cottrell<sup>(102)</sup>, Fisher et al.<sup>(103)</sup>, Orowan<sup>(104)</sup>, Kuhlman-Wilsdorf et al.<sup>(105)</sup> and Diehl et al.<sup>(106)</sup> explaining the formation and spacing of slip bands, Thomas and Nutting<sup>(99)</sup> note that the mechanism proposed by Diehl et al.<sup>(106)</sup> appeared to be best able to explain their observations. This model<sup>(106)</sup> assumes that dislocations are produced at some source until an interaction stress is high enough to force one of the dislocations on the original slip plane to form a loop along another (intersecting) slip plane on which the resolved shear stress is low. This loop will eventually act as another source on a slip plane parallel to the original plane. This process would continue thereby producing laminated slip bands. This model, however, does not explain the well documented fact<sup>(104)</sup> that the slip bands themselves are so uniformly spaced. It appears as though the combination of the models of Diehl et al.<sup>(106)</sup> along with that of either Orowan<sup>(104)</sup> or Kuhlman-Wilsdorf et al.<sup>(105)</sup> is necessary to more completely

explain experimental observations. In principle, Orowan<sup>(104)</sup> and Kuhlman-Wilsdorf et al.<sup>(105)</sup> suggest the same model viz. that the operation of a source will preclude the operation of other sources within a certain distance of the original source by either stress cancelling<sup>(104)</sup> or dislocation annihilation<sup>(105)</sup>.

The deformation of a polycrystalline solid solution can now be outlined. Deformation begins by the activation of (say) one source. As deformation continues, the dislocations first emitted by the source eventually encounter an obstacle such as a grain boundary and a back stress on the slip plane builds up until the source can no longer operate. At this point, one of the dislocations leaves the slip plane by either duplex slip or cross slip. After this dislocation has moved a distance greater than required distance (as given by Orowan<sup>(104)</sup> or Kuhlman-Wilsdorf et al.<sup>(105)</sup>), it will act as a new source on a plane parallel to the original. This process would then continue accommodating all of the strain in these slip bands. Thomas and Nutting<sup>(99)</sup> have shown that these bands can be made up of few lamellae (Al-Mg and Al-Cu) or many lamellae (Al and Al-Ag) depending on the solute atom. The step heights were much higher for the Al-Mg and Al-Cu and increased with increasing solute concentration. For example, at the same total strain, the step height increased from 580 to 1350Å as the Mg content increased from 1 to 7% while the step height for Al-Ag was 70Å and was independent of Ag content<sup>(99)</sup>. Thomas and Nutting<sup>(99)</sup> also found that Mg and Cu also retarded duplex slip while Ag did not. These authors conclude<sup>(99)</sup> that solute atoms which distort the solvent lattice tend to keep dislocations on their

original slip plane. It should be clear at this point that in this case both the nature and concentration of solute atoms can have a strong effect on the degree of heterogeneity of the deformation process.

In summary, the deformation of polycrystalline aluminum alloy solid solutions can be roughly divided into two classifications. When cross slip or duplex slip is easy, the deformation will be accommodated by the lateral growth of slip bands (by the addition of slip lamellae). This situation will result in relatively fine slip band characteristics. When cross slip or duplex slip is impeded, the deformation will be accommodated by the formation of new slip bands well removed from the original and this type behavior will result in relatively coarse slip band characteristics.

Concerning the present investigation, it is entirely possible that variations in the matrix precipitate can also have a strong influence on the degree of heterogeneity of deformation. In order to explain the deformation occurring in both the microstructures used in the present investigation and those used to generate Figure 3, it will be assumed that microstructure 2 - underaged (G.P. zones) would be representative of a structure near the maximum of susceptibility in Figure 3, structures 1 and 3 - underaged would be representative of a slightly overaged structure in Figure 3 and the overaged structures (1, 2 and 3) would be representative of an overaged structure in Figure 3.

Statham<sup>(22)</sup> has observed the slip lines of screw dislocations at many points on the hardness curve of Figure 3. This work, performed using single

crystals of Al-Zn-Mg, has shown that as aging progresses from the as-quenched condition to just before peak strength is reached (in the region where G.P. zones are the major strengthening phase), the traces of screw dislocations change from being wavy to being very straight. It is interesting to note that these straight, intense slip lines (indicative of little cross slip) occur in microstructures very close to those where the maximum of susceptibility exists and also at the point where  $\eta'$  is about to form. As aging progresses, the slip lines stay relatively straight but become broader and much less intense. One possible explanation of these observations is that as aging progresses from the as-quenched condition to the point just before  $\eta'$  forms (or becomes significant) G.P. zones form and grow. It has been suggested<sup>(107)</sup> that one of the major strengthening effects of G.P. zones is stacking fault strengthening. Since this strengthening mechanism depends on both the size of the zone as well as the difference in stacking fault energy between the zone and the matrix, it is entirely possible that this could account for the noted increase in strength with increase in size of G.P. zones. The increase in strength resulting from the increase in G.P. zone size as aging progresses is likely due to two factors. The first is that Hirsch and Kelly<sup>(107)</sup> have shown that the flow stress should increase with the zone radius (1/2 power) and the second is that as aging progresses, it is very likely that the composition within the G.P. zone would become more concentrated with solute atoms. Hirsch and Kelly<sup>(107)</sup> note that the addition of solute to many close packed solid solutions lowers the stacking

fault energy. They<sup>(107)</sup> say that this has been verified for many aluminum alloys, viz. Al-Zn and Al-Ag. Hirsch and Kelly<sup>(107)</sup> further contend that if a partial dislocation transforms the fcc G.P. zone to an hcp structure on the slip plane, and if the hcp structure is thermodynamically more stable than the fcc structure, then one might expect the stacking fault energy within the G.P. zones to be negative. It can be concluded from these arguments that it is possible that the stacking fault energy within the G.P. zones decreases as aging progresses and thereby increases the difference in stacking fault energy between the solute depleted matrix and the G.P. zones.

Consider the deformation of two specimens, one having very small G.P. zones and the other having G.P. zones of maximum size. Each might begin to deform by having one source operating and as deformation continues the back stress on this slip plane would be increasing. The specimen with the smaller G.P. zones would have not only a lower yield stress but also a lower barrier to cross slip (smaller size of zone and difference in stacking fault energy). At some point it perhaps would be more energetically feasible for dislocations to cross slip in the specimen with the smaller zones than to resist the back stress on the original slip plane. Since the barriers to both cross and primary slip would be expected to be much higher in the specimen with the larger zones, the original source might be expected to operate for a longer time and thereby add more dislocations onto the original slip plane. Further deformation (once the source on the primary plane in each specimen has stopped operating) might be

expected to occur in different ways. First, the operation of a new source would be expected at different distances from the original plane. In general, the more dislocations on the original plane the greater the distance away from the original plane must be in order for a new source to become activated<sup>(104,105)</sup>. Sources would be expected to operate closer to the original in the specimen with the smaller G.P. zones. Second, the mechanism of accommodating additional deformation should be different in the two specimens. In the specimen with the smaller zones, the new source would probably be a screw dislocation that had cross slipped from the original plane. In the specimen with the larger zones some other pre-existing source located at the proper distance from the original plane would probably become activated. The final result of these processes would be fine, wavy slip lines of low intensity (resulting from slip band broadening as observed by Thomas and Nutting<sup>(99)</sup>) in the specimen with small G.P. zones and coarse, straight slip bands of high intensity (resulting from the formation of new bands) in the specimen having the larger G.P. zones. It should be emphasized again that this behavior has indeed been observed<sup>(22)</sup>.

It appears that the maximum susceptibility in Figure 3 occurs in microstructures just before  $\eta'$  begins to form. The deformation behavior between the maximum of susceptibility and the maximum of hardness can be explained on the basis that both G.P. zones and small  $\eta'$  precipitates are present in these microstructures and both phases appear to be deformed by dislocations<sup>(22)</sup>. However, as the  $\eta'$  is deformed, interface dislocations are produced around the  $\eta'$  because

of the difference in Burgers vectors in the solid solution and  $\eta'$ . This results in work hardening on the slip plane and when added to the effects of having fewer G.P. zones present because of the presence of the  $\eta'$  and having a lower solute content in the matrix, limited amounts of cross slip might be expected. One would then expect more cross slip and lower step heights as aging time increased from the maximum of susceptibility to the maximum of hardness.

At maximum strength and in the overaged region, the slip bands stay relatively straight but become less intense (lower slip step heights and more slip line broadening) as aging progressed<sup>(22)</sup>. The work of Nicholson et al.<sup>(94)</sup> has shown that since dislocations cannot shear incoherent precipitates, the dislocations must bypass them either by cross slip<sup>(108)</sup> or without cross slip<sup>(98, 109)</sup>. The deformation of microstructures strengthened with incoherent precipitates would start again by having one source operating. The dislocations from this source would encounter severe obstacles in the slip plane in the form of incoherent precipitates as well as the debris left behind by the first few dislocations and therefore would have to change their slip plane to accommodate the strain. Since there would be few dislocations expected on any plane, the barrier to the operation of other sources would not extend very far from the original slip plane and this would lead to what Thomas and Nutting observed in Al-Ag viz. the broadening of slip bands through the addition of slip lamellae. These bands would appear relatively straight since the distance of cross slip would be small due to lack of many dislocations on parallel planes and the step height

would also be small because there were few dislocations moving on any given slip plane.

In summary, it has been postulated that the matrix precipitate controls the details of the deformation process. The type of dislocation behavior exhibited by a microstructure depends on: (1) whether or not the precipitates can be sheared and (2) the strength of the barrier to cross (and duplex) slip. Microstructures having G.P. zones present can exhibit various degrees of heterogeneous deformation depending upon the barrier to cross slip while microstructures strengthened by non-deformable precipitates show a more homogeneous deformation pattern.

It is interesting at this point to interpret the results of Table IV in terms of the deformation model suggested above. The data in Table IV correlate the tangent modulus (work hardening rate) with both the microstructure and the stress-corrosion susceptibility. One very unexpected result emerged from this work, viz. that the specimens hardened by G.P. zones had a higher work hardening rate than did the overaged material. This observation can be explained by comparing the deformation characteristics of the various specimens. In structure 2 - underaged with the very heterogeneous deformation, all of the deformation was accommodated by slip in a few bands. In structures 1 and 3 - underaged the slip was more homogeneous while in all of the overaged structures the slip was very homogeneous. Consider the force necessary to accommodate an increment of strain in each of the three types of structures. It is not surprising

that more force (and therefore a higher  $T$ ) would be necessary to accommodate a certain amount of strain in a material that exhibits coarse slip (the absence of cross slip) since there would be a high back stress to be overcome on the slip planes. This back stress would not be so much of a problem in the other structures since cross slip could occur. Another thing to remember is that most work hardening rates (and theories) evolve from work performed on single crystals and so there would be no obstacle to the elimination of dislocations at free surfaces in material hardened by G.P. zones. In other words, single crystals simply do not have the impenetrable barriers such as grain boundaries that polycrystals have and one might correctly expect different behavior.

An effect similar to the one just described has been reported by Thomas (110). He reported that the macroscopic yield stress of  $\alpha$ -brasses is an inverse function of the stacking fault energy. When the stacking fault energy of the brasses was altered by heat treatment, the yield stress changed correspondingly. This has been interpreted by Stoloff et al. (111) in a manner similar to the explanation given above. The material with the low stacking fault energy would have the highest barrier to cross slip. This would force dislocations to stay on the original slip plane and in order to accommodate deformation, dislocations would have to overcome back stresses on these planes. This would result in higher flow stresses in materials with lower stacking fault energies.

### 5.5 Electrochemical Conditions at Grain Boundaries

Having gained some insight into the way the matrix precipitate controls the deformation process, the mechanism of stress-corrosion cracking can now be examined in terms of the results of the present investigation. However, before a model can be postulated involving the effect of deformation on susceptibility, the grain boundary region must be examined since this was the only metallurgical feature that was not controlled through heat treatment. Sprowls<sup>(112)</sup> has suggested that the heat treatments used in the present investigation might possibly have changed the solute concentrations in the grain boundary region in the various microstructures and this could partially be responsible for the changes in susceptibility. Sprowls<sup>(112)</sup> points out that the electrode potential of an Al-Zn-Mg solid solution is a function of the composition<sup>(113)</sup> and therefore variations in the solute concentration at the grain boundaries might be expected to produce variations in corrosion rates. As mentioned earlier, there is no strong correlation between the size and spacing of grain boundary precipitate and susceptibility (Tables I and II). However, there is one observation which could support Sprowls' contention and that is when specimens having similar matrix precipitates but different grain boundary precipitates were compared, the specimens having the smaller grain boundary precipitates were more susceptible. This can perhaps be explained by noting that if both specimens had a similar initial solute content present in the boundary, the solute concentration would be expected to be higher in the boundary which had the smaller grain boundary

precipitates. This would cause the potentials of both the precipitates as well as the remainder of the boundary to be highly anodic. In the case where the grain boundary precipitates were larger, the remainder of the boundary would be less anodic because of a lower solute concentration.

There are observations which tend to minimize the importance of the suggestion of Sprowls<sup>(112)</sup>. If the metallurgical features of the grain boundary (viz. size and spacing of the precipitates and solute content on boundary) were to control susceptibility through their relative effects on electrochemical relationships, then one would expect a much larger difference in susceptibilities between structures 1 and 3 - underaged. This was, however, not the case (Table II). Also, there simply is no correlation between susceptibility and the details of the grain boundary precipitates for the specimens in the overaged condition (Tables I and II). Finally, there was a large variation in susceptibility in specimens which had very similar grain boundary precipitates but different matrix precipitates.

One might be tempted to explain some of the results of the present investigation by assuming: (1) that stress-corrosion susceptibility depends upon the rate at which the grain boundary precipitates are attacked, (2) that the corrosion of these precipitates is under cathodic control and (3) that the cathode area stays relatively constant.

This hypothesis could explain why the underaged specimens (with the smaller grain boundary precipitates) were more susceptible than the overaged

specimens (with the larger grain boundary precipitates) for any given heat treatment. It could not explain, however, why specimens of treatments 1 and 3 - underaged had different susceptibilities and also why specimens of treatments 1 and 3 - underaged had similar susceptibilities.

It does not appear that susceptibility can be explained using electrode potential arguments. For example, it has been shown that although both  $MgZn_2$  and an Al-4% Zn solid solution have identical electrode potentials<sup>(113)</sup>, the  $MgZn_2$  phase is preferentially attacked in stress-corrosion experiments<sup>(77)</sup>. It seems that some work is required in the field of electrochemical kinetics in order to more adequately specify the role of electrochemistry during the stress-corrosion cracking process. In some recent work, Brown et al.<sup>(114)</sup> have shown that the pH at the tip of a stress-corrosion crack is very low ( $\sim 3.5$  max.) regardless of either the initial pH of the bulk environment or the alloy used. Other work<sup>(115)</sup> has investigated the effect of plastic strain on the electrode potential of pure Al in dilute NaCl solutions under a variety of conditions. Some of the results of this work are:

(1) At a pH of 5.5, the application of a plastic strain of 4.5% results in a shift of electrode potential of 0.92V (S.C.E.) in the anodic direction. This potential then decays to a value representing a steady state displacement of 0.5V (S.C.E.) in the anodic direction.

(2) This steady state shift of potential was independent of the initial pH of the environment within the range of 2.5 to 8.5.

(3) Dissolved oxygen assists in repairing the oxide film that was ruptured during straining.

It would appear that more experiments similar to the two described above should be performed since it seems that experiments of this type would enable investigators of stress-corrosion to better understand the complex nature of the interaction of stress, microstructure and environment occurring at the tip of a stress-corrosion crack.

#### 5.6 Effect of Matrix Precipitate on Stress-Corrosion Susceptibility of Al-Zn-Mg Alloys

As mentioned above, there is a strong correlation between the type, size and spacing of the matrix precipitate and the degree of susceptibility of a microstructure to stress-corrosion cracking. The matrix precipitate has also been shown to control the details of the dislocation motion during plastic deformation. It is believed here and elsewhere<sup>(5,6,80)</sup> that the details of the deformation process control the susceptibility of a microstructure. In principle, this behavior can be summarized by noting that the more heterogeneous the deformation, the more susceptible the microstructure is liable to be. The results of the present investigation strongly support this contention. Microstructures, each containing one of three types and distributions of matrix precipitates, exhibited three degrees of susceptibility as well as three degrees of heterogeneous deformation. The microstructure which showed the fine, coherent precipitates deformed in a very heterogeneous manner, viz. dislocations arranged in sharp bands and straight, intense slip lines on the free surface, and proved to be very

susceptible to stress corrosion. As the matrix precipitate changed in size, spacing and degree of coherency, the deformation became more homogeneous and the susceptibility decreased.

The role of microstructure in controlling stress-corrosion susceptibility can now be explained. In principle this relationship occurs because of the way in which the matrix precipitate controls the details concerning the intersection of slip bands and grain boundaries.

In the absence of a corrosive environment, it has been shown both theoretically<sup>(116-118)</sup> and experimentally<sup>(119,120)</sup> that slip bands can cause the formation of microcracks at grain boundaries when slip cannot be transferred across the boundary. Johnston and Parker<sup>(119)</sup> have shown that in MgO, where cross slip is difficult, there are regions of severe stress concentrations at the intersections of grain boundaries and sharp slip bands (Figure 19). Johnston and Parker<sup>(119)</sup> have also shown that in materials where cross slip is easy, viz. NaCl, the slip bands are ill-defined and the stress concentrations at the intersections of slip bands and grain boundaries are much lower (Figure 20). These authors<sup>(119)</sup> conclude that this effect is responsible for the ductility being higher in polycrystalline NaCl than in MgO. Johnston et al.<sup>(120)</sup> have shown that the misorientation across the grain boundary is important with respect to the nucleation of grain boundary cracks. They<sup>(120)</sup> discovered that slip bands could penetrate low angle boundaries and no cracking was observed. Grain boundary cracks were nucleated at high angle boundaries in MgO by slip bands

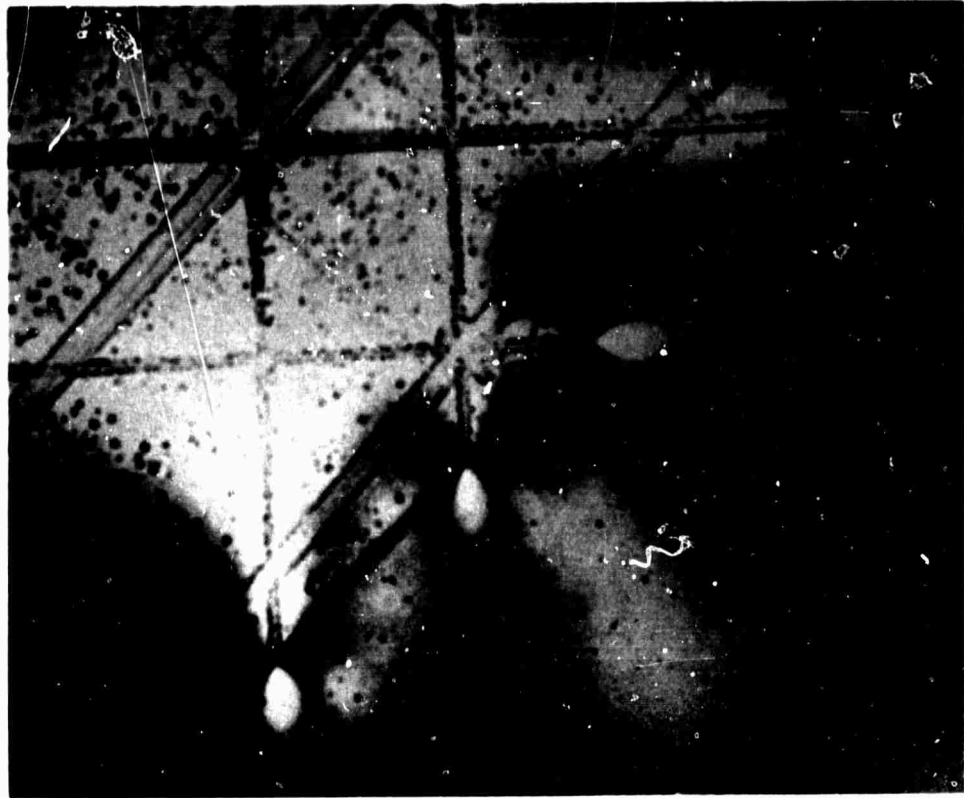


Figure 19. Stress concentrations at slip band-grain boundary intersections in MgO bicrystal. Polarized transmitted light photomicrograph. 120X. (119)

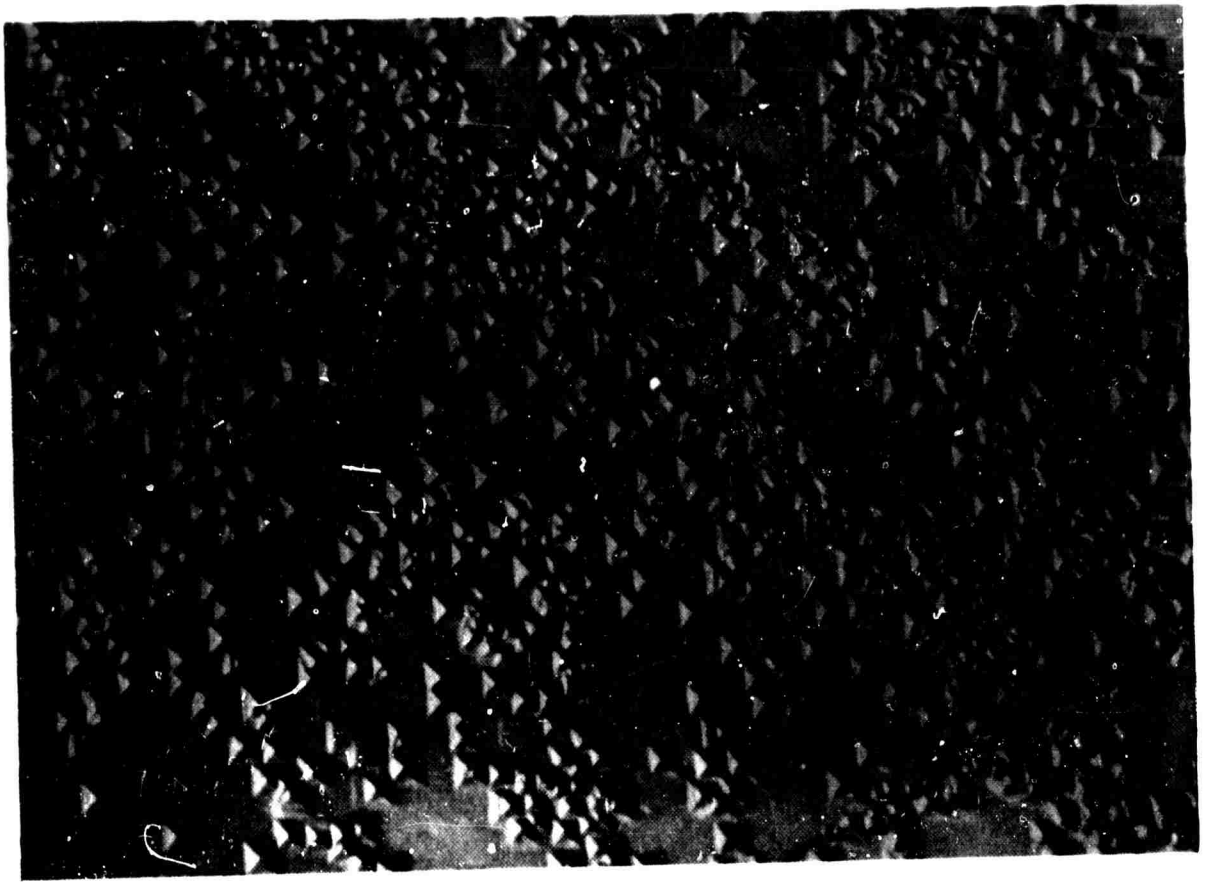


Figure 20. Broad slip band in NaCl deformed at room temperature, 330X. (119)

composed of edge dislocations (Figure 21).

After reviewing the fundamentals of fracture in many metallic systems, Low<sup>(121)</sup> has concluded that the nucleation of grain boundary fracture can result from localized plastic deformation. A necessary condition for this type of crack nucleation is that microscopically inhomogeneous deformation be blocked by grain boundaries.

It would appear that the results of the present investigation directly support the observations of Johnston et al.<sup>(119,120)</sup>. Figure 10 shows that the minimum ductility (near maximum yield strength) for the microstructure of heat treatment 2 was zero while the minimum ductility for microstructures of heat treatment 1 and 3 was 3%. This difference in behavior can be explained in a manner similar to that used by Johnston and Parker<sup>(119)</sup> to explain the difference in ductility of polycrystalline MgO and NaCl. It is postulated here that structure 2 and MgO would behave in a similar manner; the brittleness of these materials arising from the difficulty of cross slip and the resulting high stress concentrations at the slip band-grain boundary intersections. Structures 1 and 3 on the other hand would behave similarly to NaCl. These materials show easy cross slip and resulting low stress concentrations at slip band - grain boundary intersections. This situation results in higher ductility for these materials showing easy cross slip.

In the presence of a corrosive environment, crack nucleation has also been related to the details of the intersection of slip bands and grain

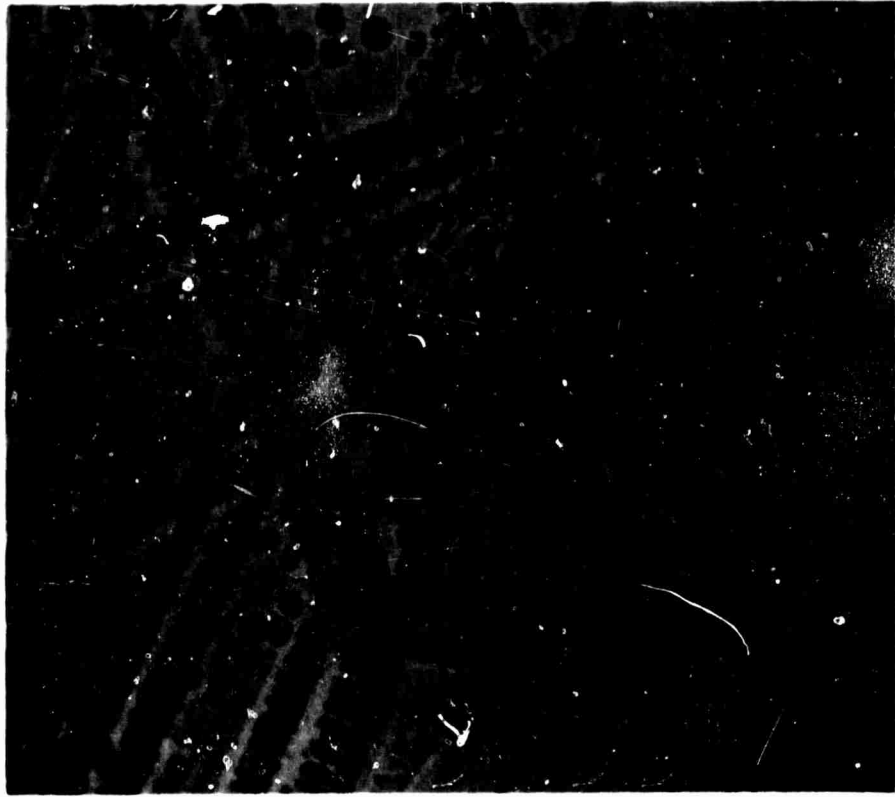


Figure 21. Microcracks at slip bands blocked by grain boundary in MgO bicrystal<sup>(120)</sup>.

boundaries. Westwood<sup>(122)</sup> has shown that when silver chloride is stressed in an embrittling environment of 6N sodium chloride, cracks are formed only where slip bands are arrested at a grain boundary and that these cracks propagate in a relatively brittle manner (Figure 22). Cracks were not observed when the slip bands pass through the boundary (Figure 22). Tromans and Nutting<sup>(123)</sup> have shown that cracks are formed at the intersection of dislocation pile-ups and grain boundaries. Thin foils of Cu-30 Zn were strained, corroded in ammonium hydroxide, cleaned and then observed in the electron microscope. Their results indicate that in many cases the initiation of cracking occurred at slip band - grain boundary intersections regardless of whether the propagation was intergranular or transgranular.

It is now possible to suggest that the details of the intersection of slip bands and grain boundaries control the susceptibility of a microstructure to stress-corrosion cracking. Consider a grain boundary that will not allow slip to be transferred across it. The susceptibility of this boundary will depend on the nature of the slip bands that impinge on it. The details of the slip bands will strongly depend on the type, size and spacing of the matrix precipitate. It has been shown here and elsewhere<sup>(5,6)</sup> that susceptible microstructures exhibit coarse, heterogeneous slip and that the degree of susceptibility depends on the degree of the heterogeneity of the slip.

The details of the deformation process can influence susceptibility in two ways. Slip bands which impinge on the grain boundary at the crack tip could



Figure 22. Polycrystalline silver chloride deformed in a 6N sodium chloride solution presaturated with  $\text{AgCl}_3^{-}$  complexes; strain increasing progressively from (a) to (e). (a) and (b): Note that cracks are initiated only where slip bands are arrested at the grain boundary (A through K). (c) - (e): Illustrating subsequent "brittle" growth of intercrystalline cracks. Transmitted light<sup>(122)</sup>.

result in accelerated anodic dissolution at that point. Hoar and Hines<sup>(124)</sup> and Hines<sup>(125)</sup> have postulated a model explaining yield assisted electrochemical dissolution. This model<sup>(125)</sup> suggests that there are numerous anodically active surface sites produced at the root of a yielding corrosion fissure. According to this model the density of such sites would be higher in materials exhibiting coarse slip. Holl<sup>(5)</sup> points out that this would be true if local rupture of an oxide film is involved in the formation of an anodic site. The experiments of Leidheiser et al.<sup>(115)</sup> indicate that this model could be valid. There is some experimental evidence that the slip step height and band spacing vary with microstructure in a way that is compatible with both the model of Hines<sup>(125)</sup> and stress-corrosion susceptibility.

Another possible way in which the characteristics of the slip bands could influence susceptibility arises if the bands impinge on the grain boundary ahead of the crack tip. These bands, if of the coarse type, could possibly nucleate microcracks along the grain boundary ahead of the main crack. This, of course, would be behavior similar to that already noted for MgO<sup>(119)</sup>. Bands of the fine type could possibly hinder crack propagation by plastic blunting. If the coarse bands do not cause microcrack formation, they could still aid crack propagation by not only stressing the grain boundary but also by possibly attracting solute atoms and thereby making the region of the grain boundary - slip band intersection more anodic. There is evidence that solute segregation of this type can be important in stress-corrosion cracking<sup>(123,126,127)</sup>.

It is interesting to note at this point that recent work by Stoloff et al.<sup>(111)</sup> on various fcc metals and alloys has established a correlation between slip characteristics and intergranular liquid metal embrittlement that is very similar to the correlation between slip characteristics and susceptibility found in the present investigation. These authors<sup>(111)</sup> have found that an increased resistance to cross slip increased the embrittlement of the materials tested. When copper based solid solutions of Al, Si and Ge, Zn and Ge were tested<sup>(111)</sup>, it was found that there was a linear decrease in the degree of embrittlement with increasing stacking fault energy. These authors<sup>(111)</sup> conclude that although different chemical species are present, all of the alloys were embrittled by the same fundamental mechanism and that specific chemical effects between the embrittling, liquid mercury and solute atoms at the grain boundaries must be of secondary importance. Stoloff et al.<sup>(111)</sup> explain these results by noting that cross slip would be difficult in the solid solutions having low stacking fault energies and this would result in higher stress concentration at slip band-grain boundary intersections.

#### 5.6.1 Initiation of Stress-Corrosion Cracks

The initiation of stress-corrosion cracks appears to occur at corrosion crevices located in the grain boundaries<sup>(67)</sup>. The site of initiation of a crack is a relatively small region of the fracture surface that shows severe pitting. The formation of these corrosion crevices seems to be stress assisted since:

- (1) loaded specimens show a greater concentration of attack in the grain

boundary regions prior to cracking than unloaded specimens exposed to the environment for equal times (Figure 12), (2) exposure of the unloaded specimens to the environment for times equal to the life of failed specimens causes no degradation of mechanical properties and (3) exposure to the environment prior to loading causes no significant decrease in the time to failure<sup>(4)</sup>.

It is possible that attack starts at the grain boundary precipitates ( $MgZn_2$ ) which are considered anodic with respect to the surrounding material<sup>(67,75)</sup>. The cathodic sites could be the solute depleted matrix surrounding the precipitate or surface oxide as suggested by Jacobs<sup>(75)</sup>. The regions of solute depletion are normally much smaller than the P.F.Z. width<sup>(33)</sup>. It does not appear that a correlation exists between the length of the initiation period ( $t_i$ ) and the size and spacing of grain boundary precipitates (Tables I and III). The experimental observations of the present investigation indicate that the initiation period is likely controlled by deformation assisted anodic dissolution of the grain boundary region, perhaps in a manner postulated by Hines<sup>(125)</sup>. This contention is fortified by both the observations noted above (1-3) and Figure 12. Recent work on the commercial 7075 alloy has shown that in the absence of stress, the T6 age (maximum strength) and the T73 age (overaged) exhibited the same depth of grain boundary corrosion penetration when exposed in chloride environments<sup>(77,128)</sup>. When these two microstructures are exposed under stress, the T6 age is very susceptible while the T73 is not susceptible to stress-corrosion. It is likely that in both the Al-Zn-Mg and the 7075 systems,

the variations in stress-corrosion susceptibilities are due to differences in microstructure and the concomitant changes in the deformation processes.

It was mentioned above that the model proposed by Hines<sup>(125)</sup> might apply to the initiation stage of stress-corrosion. There is one direct experimental observation which supports this possibility. In the present investigation, slip lines on the free surface were observed to suffer a limited amount of preferential attack. However, the electrochemical conditions at the base of a corrosion crevice are likely to be considerably different than at a free surface and this preferential attack of slip bands may be more intense there<sup>(114)</sup>.

Tables II and III show that most of the life of specimens tested under constant-load conditions was used to initiate stress-corrosion cracks. It follows then that the details of the initiation stage not only directly determines the length of  $t_1$  but also determines, to a large degree, the total life of the specimen under the experimental conditions of the present investigation.

There are two obvious ways in which the microstructure can control the length of  $t_1$  and both are related to the details of the deformation process. The first is the effect of slip step height (at the crack tip) on the rate of anodic dissolution and there is some evidence indicating that the more coarse the slip, the higher the corrosion rate<sup>(125)</sup>. On the basis of this model, one might expect material with coarse slip to have a higher rate of crack initiation. There is another way in which the deformation process might influence  $t_1$ . It is very possible that the duration of the initiation stage depends on the onset

of the propagation stage. It has been shown<sup>(129)</sup> that stress-corrosion cracks will probably not propagate when loaded to less than some critical K value (usually taken as  $K_{ISCC}$ ). Under constant-load conditions, this is the equivalent of saying that until the corrosion crevice has reached some critical value, propagation will not occur. Since the critical crack length in 7075-T73 is longer than in 7075-T6<sup>(112)</sup>, one might expect that this critical crack length is a function of the microstructure. If this were true, one might also expect that materials exhibiting coarse slip characteristics to have not only a higher rate of grain boundary penetration but also a shorter distance to be penetrated before entering the propagation stage.

#### 5.6.2 Propagation of Stress-Corrosion Cracks

Under the conditions of the constant-deflection test, crack propagation occurred at a much greater average rate than crack initiation. The cracking rate was non-uniform and this could be attributed to orientation effects. The most obvious effect on propagation rate was the orientation of the grain boundary. When the boundary was oriented normal to the tensile axis, cracking was generally rapid. Slower cracking occurred when the boundary was not normal to the tensile axis. This effect has been observed before<sup>(67)</sup>. The slower cracking associated with unfavorably oriented boundaries could be caused by either the need for other initiation stages or, more simply, to the lowering of the resolved normal stress on these boundaries. Another possible explanation of the variation in crack growth rates involves the orientations of the grains relative

to the boundary. Kovacs<sup>(130)</sup> has shown that crack velocity in Al-Zn bicrystals, tested in a NaCl solution, depends on these orientations. The striking similarity should be noted between the observations of Kovacs<sup>(130)</sup> and those of Johnston et al.<sup>(120)</sup> in MgO and Westwood<sup>(122)</sup> in silver chloride. In all three cases, when slip could be transferred across a grain boundary, the material would have a low propensity toward cracking, but when slip could not be transferred across the boundary, there was a high propensity toward cracking. This orientation effect, while explaining differences in cracking rates, implies that a model invoking slip band-grain boundary intersections might be valid.

The slip bands on the free surface of partially cracked specimens (Figures 15 and 16) indicate that a considerable amount of plastic deformation accompanies a propagating crack. This together with the appearance of the fracture surface (Figure 18a) indicates that crack propagation is predominately mechanical in nature. Other recent work supports this possibility<sup>(131)</sup>.

It is possible that the role of deformation in crack propagation can vary depending on the specific nature of the deformation. In materials exhibiting coarse slip bands, the deformation accompanying a propagating crack may actually help the cracking process by: (1) causing deformation-accelerated anodic dissolution at the crack tip, (2) causing brittle fracture at the boundary ahead of the crack tip due to stress concentration effects and (3) increasing the anodic potential of the slip band-grain boundary intersections by causing solute atoms to segregate to these regions. In materials exhibiting fine slip bands,

the deformation might either impede cracking due to plastic blunting or, perhaps, aid cracking as in the case of material exhibiting coarse slip, except to a much lesser extent.

#### • Summary and Conclusions

The effect of microstructure on the stress-corrosion susceptibility of an Al-Zn-Mg alloy in a NaCl solution has been investigated. The results of this investigation clearly indicate that the matrix precipitate controls susceptibility. In particular, the type, size and spacing of the matrix precipitate correlates very strongly with susceptibility. The width of the P.F.Z. does not appear to have any effect on susceptibility. The situation regarding the grain boundary precipitates is less clear although it does appear that in certain cases susceptibility can be influenced by the size and spacing of these precipitates.

The degree of susceptibility of a microstructure depends on the details of the deformation process which occurs in the microstructure. In general, the more heterogeneous the deformation, the more susceptible a microstructure is liable to be. The degree of heterogeneity of the deformation process appears to depend on whether or not the matrix precipitates can be deformed and whether or not cross or duplex slip can occur. The highest degree of susceptibility obtains when the precipitates can be sheared (G.P. zones) and cross slip is inhibited.

The details of the deformation process can affect susceptibility in many ways. Two important possibilities are deformation-assisted anodic dissolution

at the crack tip and the formation of microcracks along the grain boundary ahead of the crack tip.

The phenomenon of stress-corrosion has two stages: initiation and propagation with the initiation stage being rate controlling under the experimental conditions of this work. Both stages appear to proceed under the joint action of stress and corrosion with corrosion being dominant during initiation and stress during propagation.

Finally, it appears likely that the proposed model for susceptibility which entails the details of the deformation process as controlled by the matrix precipitate can adequately explain many experimental observations such as the effects of composition, trace elements, stress level and grain size on susceptibility.

Bibliography

1. G. Thomas and J. Nutting, *J. Inst. Met.* 88, 81 (1959-60).
2. E. N. Pugh and W. R. D. Jones, *Metallurgia* 63, 3 (1961).
3. A. J. McEvily, Jr., J. B. Clark and A. P. Bond, *Trans. A.S.M.* 60, 661 (1967).
4. A. J. Sedricks, P. W. Slattery and E. N. Pugh, "Precipitate-Free Zones and Stress-Corrosion Cracking in a Ternary Al-Zn-Mg Alloy," *Trans. A.S.M.* (1969) In Press.
5. H. A. Holl, *Corrosion* 23, 173 (1967).
6. M. O. Speidel, "Interaction of Dislocations with Precipitates in High Strength Aluminum Alloys and Susceptibility to Stress-Corrosion Cracking," paper presented at Ohio State Conference on Stress-Corrosion, Columbus, Ohio, September 1967.
7. V. I. Mikheyeva, "Chemical Nature of High-Strength Alloys of Aluminum and Magnesium with Zinc.", Edition of Academy of Sciences of U.S.S.R. (1947).
8. J. D. Embury and R. B. Nicholson, *Acta Met.* 13, 403 (1965).
9. K. Hirano and Y. Takagi, *J. Phys. Soc. Japan* 10, 187 (1955).
10. A. Taylor, "An Introduction to X-Ray Metallography," Chapman and Hall Publishers, London (1949).
11. F. Laves, J. Löhberg and H. Witte, *Metallwirtschaft* 14, 793 (1935).
12. H. Schmalzried and V. Gerold, *Z. Metallk.* 49, 291 (1958).
13. L. Mondolfo, N. A. Gjostein and D. W. Levinson, *Trans. A.I.M.E.* 206, 1378 (1956).
14. F. Laves and J. Löhberg, *Nach. Acad. Wiss. (Göttingen)* 1, 59 (1934).
15. R. Craf, *C. R. Acad. Sci (Paris)* 244, 337 (1957).
16. L. Tarschisch, A. T. Titov and F. K. Garjanov, *Phys. Z. U.S.S.R.* 5, 503 (1934).

17. P. A. Thackery, *J. Inst. Met.* 96, 228 (1968).
18. A. T. Thomas, *J. Inst. Met.* 95, 92 (1967) Discussion.
19. A. J. Cornish and M. K. B. Day, *J. Inst. Met.* 97, 44 (1969).
20. W. B. Pearson, "Handbook of Lattice Spacings", Pergamon Press, London (1958).
21. R. Graf, *Compt. rend.* 242, 1311 (1956).
22. C. D. Statham, Carnegie-Mellon University (1969) Unpublished work.
23. A. Guinier, *Solid State Physics; Advances in Research and Applications* 9, 294, Academic Press, 1959.
24. R. Graf, *J. Inst. Met.* 86, 534 (1957-58) Discussion.
25. V. Gerold and H. Haberkorn, *Z. Metallk.* 50, 568 (1959).
26. G. W. Lorimer and R. B. Nicholson, *Acta Met.* 14, 1009 (1966) Letter.
27. C. Panseri and T. Federighi, *Acta Met.* 8, 217 (1960).
28. C. Panseri and T. Federighi, *Acta Met.* 11, 575 (1963).
29. D. Turnbull and H. N. Treafitis, *Acta Met.* 5, 534 (1957).
30. T. Federighi and L. Passari, *Acta Met.* 7, 422 (1959).
31. W. DeSorbo, H. N. Treafitis and D. Turnbull, *Acta Met.* 6, 401 (1958).
32. H. Jogodzinski and F. Laves, *Z. Metallk.* 40, 296 (1949).
33. A. Kelly and R. B. Nicholson, *Prog. Mat. Sci.* 10, 151 (1963).
34. C. Zener, *Proceedings of the International Conference on the Physics of Metals*, Amsterdam, 117 (1948).
35. T. Federighi, *Acta Met.* 6, 379 (1958).
36. I. J. Polmear, *J. Inst. Met.* 86, 113 (1957).
37. R. D. Townsend and R. A. Osiecki, Carnegie-Mellon University (1959) Unpublished work.

38. H. K. Hardy, *J. Inst. Met.* 79, 321 (1951).
39. G. W. Lorimer and R. B. Nicholson, *Conference on Mechanisms of Phase Transformations in Crystalline Solids*, Manchester, July (1968).
40. J. D. Embury and R. B. Nicholson, *J. Australian Inst. Met.* 8, 76 (1963).
41. A. H. Geisler, "Phase Transformations In Solids", J. Wiley, New York 387 (1951).
42. R. E. Smaliman, "Modern Physical Metallurgy", Butterworths, London, 293 (1963).
43. J. L. Taylor, *J. Inst. Met.* 92, 301 (1963-64) Letter.
44. A. H. Geisler, *Trans. A.I.M.E.* 180, 245 (1949).
45. I. J. Polmear, *J. Inst. Met.* 89, 193 (1960).
46. J. T. Vietz, K. R. Sargant and I. J. Polmear, *J. Inst. Met.* 92, 327 (1963).
47. R. B. Nicholson, *J. Inst. Met.* 90, 185 (1961).
48. N. Ryum, *Acta Met.* 16, 327 (1968).
49. H. A. Holl, *J. Inst. Met.* 93, 364 (1963-64).
50. M. Kiritani and S. Yoshida, *J. Phys. Soc. Japan* 18, 915 (1963).
51. S. Yoshida, M. Kiritani and Y. Shimomura, *J. Phys. Soc. Japan* 18, 175 (1963).
52. P. B. Hirsch, J. Silcox, R. E. Smallman and K. H. Westmacott, *Phil. Mag.* 3, 897 (1958).
53. W. Rosenhain, S. L. Archbutt and D. Hanson, "Eleventh Report to the Alloys Research Committee on Some Alloys of Aluminum", London (Institution of Mechanical Engineers), 1921.
54. W. Sanders and K. L. Mussner, *Z. Anorg. Chem.* 154, 144 (1926).

55. D. O. Sprowls and R. H. Brown, "Stress-Corrosion Mechanisms for Aluminum Alloys", paper presented at Ohio State Conference on Stress-Corrosion, Columbus, Ohio September (1967).
56. M. Hansen, A. Muhlenbruch and H. J. Seemann, *Metallwirt.* 19, 535 (1940).
57. A. Muhlenbruch and H. J. Seemann, *Luftfahrtforsch* 19, 337 (1943).
58. G. Siebel and H. Vosskühler, *Metallwirt.* 19, 1167 (1940).
59. H. G. Petri, G. Siebel and H. Vosskühler, *Aluminum* 26, 2 (1944).
60. R. Chadwick, N. B. Muir and H. B. Grainger, *J. Inst. Met.* 85, 161 (1956-57).
61. I. J. Polmear, *Nature* 186, 303 (1960).
62. R. W. Elkington and A. N. Turner, *J. Inst. Met.* 95, 294 (1967).
63. E. H. Dix, Jr., Edward de Mille Memorial Lecture - 1949, *Trans. A.S.M.* 42, 1057 (1950).
64. G. Wassermann, *Z. Metallk.* 35, 79 (1943).
65. W. Gruhl, *Z. Metallk.* 53, 670 (1962).
66. R. B. Mears, R. H. Brown and E. H. Dix, Jr., "Symposium on Stress-Corrosion Cracking of Metals", published jointly by A.S.T.M. and A.I.M.E., 329 (1944).
67. E. H. Dix, Jr., Institute of Metals Lecture, *Trans. A.I.M.E.* 132, 11 (1940).
68. A. J. McEvily and A. P. Bond, "On Film Rupture and Stress-Corrosion Cracking", *Environment-Sensitive Mechanical Behavior*, eds. A.R.C. Westwood and N. S. Stoloff, Metallurgical Society (AIME) Conferences 35, 421, Gordon and Breach, New York, 1966.
69. G. Thomas, *J. Inst. Met.* 89, 287 (1960-61).
70. G. Meikle, *J. Inst. Met.* 85, 540 (1956-57).
71. E. N. Pugh, "On the Mechanisms of Stress-Corrosion Cracking", *Environment-Sensitive Mechanical Behavior*, eds. A.R.C. Westwood and N. S. Stoloff, Metallurgical Society (AIME) Conferences 35, 351, Gordon and Breach, New York, 1966.

72. P. J. E. Forsyth and D. A. Ryder, *Metallurgia* 63, 117 (1961).
73. J. J. Howard, *Corrosion* 6, 249 (1950).
74. F. D. Coffin and S. L. Simon, *J. Appl. Phys.* 24, 1333 (1953).
75. A. J. Jacobs and N. J. Hoffman, "A New Model for Stress-Corrosion Cracking in the 7075 Aluminum Alloy", Rocketdyne Research Report (1966).
76. K. G. Kent, *J. Inst. Met.* 97, 127 (1969).
77. A. J. Jacobs, *A.S.M. Trans. Quart.* 58, 579 (1965).
78. W. Gruhl, *Alumin* 38, 775 (1962).
79. W. Gruhl and H. Cordier, *Z. Metallk.* 55, 577 (1964).
80. M. O. Speidel, *Phys. Stat. Sol.* 22, K71 (1967).
81. *Metals Handbook*, ed. T. Lyman, P.1247, A.S.M., Metals Park, Ohio, 1948.
82. H. A. Holl, *Met. Sci. Journal* 1, 111 (1967).
83. R. B. Nicholson, G. Thomas and J. Nutting, *Brit. J. Appl. Phys.* 9, 25 (1958).
84. G. Blankenburgs and M. J. Wheeler, *J. Inst. Met.* 92, 337 (1963-64).
85. D. Moon, Ph.D. Thesis, Carnegie-Mellon University, 1967.
86. R. L. Bisplingoff, J. W. Mar and T. H. H. Fian, *Statics of Deformable Solids*, Adison Wesley, Reading, Massachusetts (1965).
87. N. Ryum, B. Haegland and T. Lindtveit, *Z. Metallk.* 58, 28 (1967).
88. E. Hornbogen, *Z. Metallk* 58, 31 (1967).
89. P. C. Varley, M. K. B. Day and A. Sendorek, *J. Inst. Met.* 86, 337 (1957-58).
90. I. Taylor, *Met. Prog.* 84, (6), 96 (1963).
91. A. Kelly, A. Lassila and S. Sato, *Phil. Mag.* (8), 4, 1260 (1959).

92. J. R. Price and A. Kelly, *Acta Met.* 10, 980 (1962).
93. S. Sato and A. Kelly, *Acta Met.* 9, 59 (1961).
94. R. B. Nicholson, G. Thomas and J. Nutting, *Acta Met.* 8, 172 (1960).
95. G. Thomas and J. Nutting, *J. Inst. Met.* 86, 7 (1957-58).
96. S. Koda and T. Takeyama, *J. Inst. Met.* 86, 277 (1957-58).
97. R. B. Nicholson and J. Nutting, *Acta Met.* 9, 332 (1961).
98. E. Orowan, "Symposium on Internal Stresses in Metals and Alloys", P.451, Institute of Metals, London (1948).
99. G. Thomas and J. Nutting, *J. Inst. Met.* 85, 1 (1956-57).
100. H. J. Axon and W. Hume-Rothery, *Proc. Roy. Soc. (A)* 193, 1 (1948).
101. A. F. Brown, *J. Inst. Met.* 82, 610 (1953) Discussion.
102. A. H. Cottrell, "Dislocations and Plastic Flow In Crystals", Clarendon Press, 1953.
103. J. C. Fisher, E. W. Hart and R. H. Pry, *Phys. Rev.* 87, 958 (1952).
104. E. Orowan, *Nature* 147, 452 (1941) Letter.
105. D. Kuhlman-Wilsdorf, J. H. van der Merwe and H. Wilsdorf, *Phil. Mag.* 43, 632 (1952).
106. J. Diehl, S. Mader and A. Seeger, *Z. Metallk.* 46, 650 (1955).
107. P. B. Hirsch and A. Kelly, *Phil. Mag.* (8), 12, 831 (1965).
108. P. B. Hirsch, *J. Inst. Met.* 86, 13 (1957).
109. J. C. Fisher, E. W. Hart and R. H. Pry, *Acta Met.* 1, 336 (1953).
110. G. Thomas, *Aust. Inst. Met.* 8, 80 (1963).
111. N. S. Stoloff, R. C. Davies and T. L. Johnston, "Slip Character and Liquid Metal Embrittlement", *Environment-Sensitive Mechanical Behavior*, eds. A. R. C. Westwood and N. S. Stoloff, Metallurgical Society (AIME) Conferences 35, 613, Gordon and Breach, 1965.

112. D. O. Sprowls, Alcoa Research Laboratory, 1969, Private communication.
113. W. W. Binger, E. H. Hollingworth and D. O. Sprowls, *Aluminum* 1, 290 (1967) A.S.M.
114. B. F. Brown, C. T. Fugii and E. P. Dahlberg, *J. Electrochem. Soc.* 116, 218 (1969).
115. H. Leidheiser, Jr., E. Kellerman and V. V. Subba Rao, "Electrochemical Studies of Stress-Corrosion Cracking of Aluminum Alloys Utilizing Strain Electrometry and Synthetic Cracks", N.A.C.E. Symposium on Fundamental Corrosion Research in Progress, Houston, 1969.
116. W. D. Robertson and A. S. Tetelman, *Strengthening Mechanisms in Solids*, A.S.M. Seminar, Metals Park, Ohio, 1962.
117. A. N. Stroh, *Proc. Roy. Soc. (A)* 223, 404 (1954).
118. E. Smith and J. T. Barnby, *Met. Sci. Journal* 1, 56 (1967).
119. T. L. Johnston and E. R. Parker, "Fracture of Nonmetallic Crystals", *Fracture of Solids*, eds. D. C. Drucker and J. J. Gilman, Metallurgical Society (AIME) Conferences 20, 267, Interscience, 1962.
120. T. L. Johnston, R. J. Stokes and C. H. Li, 12th and 13th Tech. Reports O.N.R. Proj., Nonr 2456 (00) NR-032-451, 1961.
121. J. R. Low, Jr., "Microstructural Aspects of Fracture", *Fracture of Solids*, eds. D. C. Drucker and J. J. Gilman, Metallurgical Society (AIME) Conferences 20, 197, Interscience, 1962.
122. A. R. C. Westwood, "Environment-Sensitive Mechanical Behavior-Status and Problems", *Environment-Sensitive Mechanical Behavior*, eds. A. R. C. Westwood and N. S. Stoloff, Metallurgical Society (AIME) Conferences 35, 1, Gordon and Breach, 1965.
123. D. Tromans and J. Nutting, *Corrosion* 21, 143 (1965).
124. T. P. Hoar and J. G. Hines, *J. Iron and Steel Inst.* 182, 124 (1956).
125. J. G. Hines, *Corr. Sci.* 1, 21 (1961).
126. P. R. Swann, *Corrosion* 19, 102t (1963).

127. N. Ohtari and R. A. Dodd, *Corrosion* 21, 161 (1965).
128. M. S. Hunter, W. G. Fricke, Jr., D. O. Spricwls, J. M. Walsh and D. L. McLaughlin, "Study of Crack Initiation Phenomena Associated with Stress-Corrosion of Aluminum Alloys", Third Quarterly Report, Contract NAS 8-20396, Alcoa Research Laboratory, April 1967.
129. B. F. Brown, *Metals and Materials* 2, 171 (1968).
130. W. J. Kovacs, Ph.D. Thesis, Carnegie-Mellon University, 1969.
131. B. F. Brown, U.S. Naval Research Laboratory, Private communication, 1969.

## DOCUMENT CONTROL DATA - R&amp;D

(Security classification of title, body of abstract and indexing annotation must be entered when the overall report is classified)

1. ORIGINATING ACTIVITY (Corporate author) Dept. of Metallurgy and Materials Science Carnegie-Mellon University Pittsburgh, Pa. 15213		2a. REPORT SECURITY CLASSIFICATION Unclassified	
		2b. GROUP	
3. REPORT TITLE The Effect of Microstructure on the Stress-Corrosion Susceptibility of an Al-Zn-Mg Alloy			
4. DESCRIPTIVE NOTES (Type of report and inclusive dates) Technical Report			
5. AUTHOR(S) (Last name, first name, initial) DeArdo, A. J., Jr. and Townsend, R. D.			
6. REPORT DATE February 1970	7a. TOTAL NO. OF PAGES 97	7b. NO. OF REFS 131	
8a. CONTRACT OR GRANT NO. Nonr-760(31)	9a. ORIGINATOR'S REPORT NUMBER(S)		
b. PROJECT NO. C-6	9b. OTHER REPORT NO(S) (Any other numbers that may be assigned this report)		
10. AVAILABILITY/LIMITATION NOTICES Distribution of this document is unlimited and reproduction in whole or in part is permitted for any purpose of the U. S. Government			
11. SUPPLEMENTARY NOTES		12. SPONSORING MILITARY ACTIVITY Advanced Research Projects Agency Washington, D. C.	
13. ABSTRACT The effect of microstructure on the susceptibility of a high purity Al-6.8% Zn-2.3% Mg alloy to stress-corrosion cracking in an aqueous salt solution (3.5 wt % NaCl) has been studied. The results of testing a series of specimens having controlled microstructures and the same yield strength of 40,000 psi indicate that the susceptibility to stress-corrosion is controlled by the type, size, and spacing of the matrix precipitate through the effect of these precipitates on the deformation process. Although the width of the precipitate free zone appears to have no effect on susceptibility, the grain boundary precipitate seems to influence susceptibility in certain cases. Supporting evidence for these observations has been obtained by light and electron microscopic examinations of deformed specimens and by fractographic studies. A model is proposed which explains many experimental observations.			

14. KEY WORDS	LINK A		LINK B		LINK C	
	ROLE	WT	ROLE	WT	ROLE	WT
Al-Zn-Mg Alloy Stress-Corrosion Heat Treatment Microstructure Precipitates Precipitate Free Zone Deformation						

INSTRUCTIONS

1. **ORIGINATING ACTIVITY:** Enter the name and address of the contractor, subcontractor, grantee, Department of Defense activity or other organization (*corporate author*) issuing the report.

2a. **REPORT SECURITY CLASSIFICATION:** Enter the overall security classification of the report. Indicate whether "Restricted Data" is included. Marking is to be in accordance with appropriate security regulations.

2b. **GROUP:** Automatic downgrading is specified in DoD Directive 5200.10 and Armed Forces Industrial Manual. Enter the group number. Also, when applicable, show that optional markings have been used for Group 3 and Group 4 as authorized.

3. **REPORT TITLE:** Enter the complete report title in all capital letters. Titles in all cases should be unclassified. If a meaningful title cannot be selected without classification, show title classification in all capitals in parenthesis immediately following the title.

4. **DESCRIPTIVE NOTES:** If appropriate, enter the type of report, e.g., interim, progress, summary, annual, or final. Give the inclusive dates when a specific reporting period is covered.

5. **AUTHOR(S):** Enter the name(s) of author(s) as shown on or in the report. Enter last name, first name, middle initial. If military, show rank and branch of service. The name of the principal author is an absolute minimum requirement.

6. **REPORT DATE:** Enter the date of the report as day, month, year, or month, year. If more than one date appears on the report, use date of publication.

7a. **TOTAL NUMBER OF PAGES:** The total page count should follow normal pagination procedures, but enter the number of pages containing information.

7b. **NUMBER OF REFERENCES:** Enter the total number of references cited in the report.

8a. **CONTRACT OR GRANT NUMBER:** If appropriate, enter the applicable number of the contract or grant under which the report was written.

8b, 8c, & 8d. **PROJECT NUMBER:** Enter the appropriate military department identification, such as project number, subproject number, system numbers, task number, etc.

9a. **ORIGINATOR'S REPORT NUMBER(S):** Enter the official report number by which the document will be identified and controlled by the originating activity. This number must be unique to this report.

9b. **OTHER REPORT NUMBER(S):** If the report has been assigned any other report numbers (*either by the originator or by the sponsor*), also enter this number(s).

10. **AVAILABILITY/LIMITATION NOTICES:** Enter any limitations on further dissemination of the report, other than those

imposed by security classification, using standard statements such as:

- (1) "Qualified requesters may obtain copies of this report from DDC."
- (2) "Foreign announcement and dissemination of this report by DDC is not authorized."
- (3) "U. S. Government agencies may obtain copies of this report directly from DDC. Other qualified DDC users shall request through \_\_\_\_\_."
- (4) "U. S. military agencies may obtain copies of this report directly from DDC. Other qualified users shall request through \_\_\_\_\_."
- (5) "All distribution of this report is controlled. Qualified DDC users shall request through \_\_\_\_\_."

If the report has been furnished to the Office of Technical Services, Department of Commerce, for sale to the public, indicate this fact and enter the price, if known.

11. **SUPPLEMENTARY NOTES:** Use for additional explanatory notes.

12. **SPONSORING MILITARY ACTIVITY:** Enter the name of the departmental project office or laboratory sponsoring (*paying for*) the research and development. Include address.

13. **ABSTRACT:** Enter an abstract giving a brief and factual summary of the document indicative of the report, even though it may also appear elsewhere in the body of the technical report. If additional space is required, a continuation sheet shall be attached.

It is highly desirable that the abstract of classified reports be unclassified. Each paragraph of the abstract shall end with an indication of the military security classification of the information in the paragraph, represented as (TS), (S), (C), or (U).

There is no limitation on the length of the abstract. However, the suggested length is from 150 to 225 words.

14. **KEY WORDS:** Key words are technically meaningful terms or short phrases that characterize a report and may be used as index entries for cataloging the report. Key words must be selected so that no security classification is required. Identifiers, such as equipment model designation, trade name, military project code name, geographic location, may be used as key words but will be followed by an indication of technical context. The assignment of links, roles, and weights is optional.